MICRO-PATTERNED LIGAND SURFACES PROVIDE NEW INSIGHTS INTO SPATIAL REGULATION OF EGF RECEPTOR SIGNALING AND IGE RECEPTOR ENDOCYTOSIS

A Dissertation

Presented to the Faculty of the Graduate School

of Cornell University

in Partial Fulfillment of the Requirements for the Degree of

Doctor of Philosophy

by

Amit Singhai

January 2013

MICRO-PATTERNED LIGAND SURFACES PROVIDE NEW INSIGHTS INTO SPATIAL REGULATION OF EGF RECEPTOR SIGNALING AND IGE RECEPTOR ENDOCYTOSIS

Amit Singhai, Ph.D.

Cornell University 2013

FcεRI, the high affinity receptor for immunoglobulin E (IgE), is primarily found on the surface of mast cells and basophils. FcεRI signaling is triggered by the crosslinking of receptor-bound IgE by a multivalent antigen (Ag). This initiates a series of intracellular signaling events that eventually lead to secretion of mediators such as histamines and cytokines, which are responsible for allergic reactions. In addition, Ag-crosslinked IgE-FcεRI complexes are internalized. Although the sequelae of signaling events leading to release of preformed mediators has been extensively studied, much less is known about the FcεRI internalization pathway.

Recent investigations of our laboratory have focused on the roles that the plasma membrane and the actin cytoskeleton play in FcεRI-mediated signaling leading to secretory events. However, the tools available to study spatial regulation of cellular responses were limited. Towards overcoming this limitation, we previously developed micro/nanofabricated surfaces with patterned arrays of ligand to spatially control the stimuli provided to cells. This enabled us to visualize the formation of signaling complexes at the plasma membrane of the cells.

My research has now extended the application of these micro-patterned surfaces to study the assembly of FcεRI endocytic machinery, in conjunction with fluorimetry, flow cytometry, and confocal microscopy. I found that inhibitors of F-actin cycling cause

crosslinked IgE-FcεRI complexes too localize in membrane invaginations that are not cleaved from the plasma membrane. I provided evidence that FcεRI internalization is sensitive to cholesterol, phosphoinositide synthesis at the plasma membrane, and the tyrosine kinase Syk. My experiments with micro-patterned ligand surfaces showed that recruitment of F-actin to the FcεRI signaling complexes is diminished in the presence of inhibitors of phosphoinositide synthesis.

I have further extended the application of micro-patterned ligand surfaces to study the spatial regulation of epidermal growth factor (EGF) receptor (EGFR) signaling by developing a scheme to covalently immobilize micron-sized patches of functionally active EGF. I utilized NIH-3T3 cells stably over-expressing EGFR to detect the formation of EGFR signaling complexes via fluorescence confocal microscopy. I detected actin cytoskeleton-dependent recruitment of EGFR signaling partners H-Ras, MEK, and phosphorylated Erk to the EGFR signaling complexes on the plasma membrane of cells. In addition, I observed recruitment of F-actin and the adaptor protein paxillin, including phosphorylated paxillin, to regions where EGFR is clustered at the EGF patches. I also found that recruitment of F-actin and Erk to EGFR signaling complexes is diminished in the presence of inhibitors of phosphoinositide synthesis. Integrin α-5, the most abundant integrin in NIH-3T3 cells, is excluded from these EGFR signaling complexes. These results demonstrate that micro-patterned EGF surfaces are valuable for investigation of spatially orchestrated interactions of signaling proteins with EGFR at the plasma membrane.

BIOGRAPHICAL SKETCH

Amit Singhai was born on 28th May 1985 in Indore, Madhya Pradesh, India to parents Sunil and Indra. His father, Sunil, is Vice-President at Dr. Reddy's Laboratories Ltd., one of the biggest biopharmaceutical industries in India, and his mother, Indra is a housewife. He also had an amazing sibling in his sister Aditi, with whom he spent a lot of exciting times. During his childhood, which was mostly spent at Indore, he was known to be a very shy, and innovative at avoiding homework from school. He was madly in love with the sport of Cricket, and spent countless hours playing, watching, analyzing, and memorizing a lot of facts about Cricket. At one point of time, he considered a career in Cricket, but he decided to continue his education. His childhood sketch would be incomplete without the mention of the summers that he spent at Guna with all of his cousins. After completing his grade 10th education from Indore, he moved to Kota to prepare for the Joint Entrance Examination for the prestigious Indian Institute of Technology (IIT). During his stay at Kota, in the able tutelage of some exemplary teachers, Drs. Rao and Shishir Mittal, he developed a passion for the subject of Chemistry. After ranking in top 1.5% in the nationwide entrance examination for IITs, he had no hesitation in selecting to study Chemistry at the prestigious IIT Kanpur.

During his stay at IIT Kanpur, he received basic training in organic, physical, and inorganic chemistry. However, after taking some introductory classes in Biology, he got really interested in learning more about the subject. Apart from academics, he spent a lot of time in organizing events like cultural and technical festivals and in the process he developed his teamwork and leadership skills. He also made some incredible friendships along with his fellow students at IIT Kanpur. He did a couple of summer projects at a pharmaceutical industry where he worked on synthesizing organic molecules for inhibiting the enzyme activity and really enjoyed them. He

also spent a couple of summers at McMaster University, Ontario, Canada, where he worked in the area of bioanalytical chemistry under the guidance of Dr. John D. Brennan, which helped in further advancing his budding interest in the subject of chemical biology.

He decided to continue his learning in the field of chemical biology upon completion of his Bachelor's and Master's in Chemistry from IIT Kanpur. Upon receiving encouragement from his professors, fellow students and especially his father, he applied to PhD programs in the United States. He got accepted at University of Illinois – Urbana Champaign, John's Hopkins University, McMaster University and Cornell University. He got interviewed, and accepted in the prestigious Tri-Institutional Program in Chemistry and Chemical Biology, which involved Cornell University, Rockefeller University, and Memorial Sloan-Kettering Cancer Research Centre. After doing rotation projects in all these three prestigious institutes, he decided to join the laboratory of Drs. Barbara Baird and David Holowka, and focus his efforts to understand the biophysical aspects of immune cell signaling. During his stay in lab, he worked on a variety of projects, including assembling an optical set-up for sub-optical resolution fluorescence microscopy, collaborated with Kan group in Electrical Engineering Department to develop low-cost, high throughput biosensors. His thesis projects focused on developing functionalized, nanofabricated, micro-patterned ligand arrays to study cellular signaling, and developing fluorimetric, microscopy based assays to study receptor internalization.

During his stay at Cornell University, he got a chance to attend some classes at Cornell Law School in the areas of Intellectual Property (IP) and Patent Law. He realized the role that IP protection plays in maintaining a balance between incentive for scientific research and availability of economic commodities for the consumers. After completing his PhD, he got

offered a job at a law firm based in New Jersey, where he will employ his skills in the exciting area of intellectual property.

This biographical sketch will be incomplete without the mention of another significant event his personal life. He met his life partner, Shruti and got married to her on 9th December 2011. This beginning of a new phase of his life was an important catalyst in keeping his focus, and timely completion of his thesis.

Dedicated to my wife, parents, and family

ACKNOWLEDGEMENTS

The work presented in this thesis would not have been possible without the tutelage of my advisors, Drs. Barbara Baird and David Holowka. The constant encouragement and guidance they provided, especially in stressful times, cannot be described in words. When I first joined the group, my experience in cell biology research was very limited, and I am very thankful for the faith they posed in my abilities. Barbara always helped in maintaining focus on the 'bigger picture' and Dave always helped me to pay attention to detail in experimental observations. Their guidance and support in the development of my analytical thinking, personality and writing skills can't be described in words. A special thanks to my committee members, Drs. Frederick Maxfield and Richard Cerione for their contributions and helpful insights in my projects.

I have been very fortunate to enjoy an excellent working atmosphere in our lab. Special thanks must go to Alexis J. Torres, who has always been very empathetic in stressful times, provided excellent platform for bouncing scientific ideas and was very helpful in training me at the clean room. Special note of thanks should go to Kari M. Midthun, who has been an invaluable friend, lab-mate during my academic journey at Cornell. She also introduced me to fascinating world of baking and letterboxing. I will also like to acknowledge the tremendous amount of effort that Kirsten Bryant put in supplying me cells and helping me plan all the experiments. Apart from that, I will like to thank all the Baird-Holowka lab members including Lavanya, Norah, Alice, Stephanie, Ethan, Sarah V, Sarah S, Roy, Jinmin, Deepti, Nat, Kate, Josh, Marek, Marcus, John, Tristan, Devin, Chris and Dwaipayan. I had several lively discussions with them over diverse range of topics ranging from sports and travel to academic careers. I will also remember the races that I took part in as a member of Team Balowka! I am also thankful to my collaborators, Krishna from Kan Lab; JB Lee, Songming from the Luo lab; and Dr. Stepehen Hammes.

Life outside the bounds of laboratory was made memorable by some special friends. I would specially like to mention and thank Anand Vaidya, my housemate for 4 consecutive years, who has always been there to celebrate triumphs and disasters. Suresh, Vivek, Rajendran and Anand for sharing cooking turns and keeping me well fed along with the lively dinner discussions, ranging from abstract mathematics and philosophy to the latest development in the sports world. I learnt a lot of about life in Ithaca and in graduate school from Shridhar, who was a mentor in my first year of graduate school. Kaushik, Aritro, Anand and Debashree were excellent batch-mates, and we spent some good times together. I will also like to extend my thanks to all my friends, Kalyan, Abhinav, Lekha, Jaya, Debamita, Siddharth, Deepti, Hari, Amit Halder, Rachna, and Parag, who have made living away from home more bearable. This acknowledgement will be incomplete without special mention of Samanvaya, who was tremendously helpful in my last month of stay in Ithaca. My stay in Ithaca would not have been this memorable without the companionship and support they provided.

I will never forget the contributions made by my parents, their constant efforts in instilling the value of hard work, patience, and perseverance at a very early age. The numerous sacrifices they have made in their life in lieu of my studies have been immense, without their constant guidance, support, and blessings; I would not have been able to embark on my academic journey. My sister, Aditi, has been an amazing sibling and friend, and the childhood memories we shared together, will always be cherished. They have always been a constant source of motivation, and have always encouraged me to follow my heart and give more than 100% in whatever task I pursue. I will also like to extend my thanks to my extended family, my father-in-law, mother-in-law, Shishir, Shreya, Somil, Deepika, Sarthak and Mahak, for welcoming me in their family and celebrating some special moments with me.

Most importantly, I will like to thank my beloved wife, Shruti, who has provided constant and unwavering support during the last year of my graduate school. I will forever be indebted for the countless sacrifices she has made during the compilation of this dissertation. In the past 6 months she has made each and every day in Ithaca truly memorable and wonderful.

This section of acknowledgements will never be complete without mentioning the contributions of some of the excellent teachers that I have had during my schooling years and during my undergraduate education at IIT Kanpur. They helped me to develop sound understanding in all the subjects and piqued my curiosity in Chemistry. We stand on shoulders of giants to have an understanding of science that we have right now, and without their efforts, this work would not have been possible. In addition to all the names that I have mentioned in this section, I will like to thank a lot of known and unknown people who have helped me reach me where I am. To all of you – thank you. Lastly, I will thank god for providing me such a wonderful wife, family, in-laws, friends and mentors. I close this section, with the hope that my modest attempts at making contributions for the advancement of science will be one day useful to answer the fundamental questions in life.

TABLE OF CONTENTS

LIST OF FIGURES

LIST OF ABBREVIATIONS

A488	alexa fluor 488
A568	alexa fluor 568
A647	alexa fluor 647
ADP	adenosine-diphosphate
agLDL	aggregated low density lipoproteins
Ag	Antigen
APC	antigen presenting cells
Arf	ADP ribosylation factor
Arp2/3	actin related protein 2/3
BMMC	bone marrow-derived mast cells
BSA	bovine serum albumin
BSS	buffered saline solution
CY3	cyanine 3
Cy5	cyanine 5
DAG	diacylglycerol
DMEM	d-minimum essenial medium
DNP	dinitrophenyl
DNP-CAP-PE	1,2-dipalmitoyl-sn-glycero-3 phosphatidylethanolamine-N-(6-(2,4-dinitrophenyl)amino)hexanoyl)
DRM	detergent resistance membrane
ECM	extracellular matrix
EGF	epidermal growth factor

EGFR	epidermal growth factor receptor
ER	endoplastic reticulum
ERK	extracellular regulated kinase
FAK	focal adhesion kinase
FITC	fluorescein isothiocyanate
FRAP	fluorescence recovery after photobleaching
GEF	guanine nucleotide exchange factor
GFP	green fluorescent protein
GMBS	N-(γ-maleimidobutyryloxy) succinimide
GPCR	G-protein coupled receptors
HB-EGF	heparin binding EGF
ICAM-1	intercellular adhesion molecule-1
IgE	immunogobulin E
IgG	immunogobulin G
IP	immunoprecipitation
IP_3	inositol 1,4,5 trisphosphate
IS	immunological synapse
ITAMS	immunoreceptor tyrosine-based activation motifs
LAT	linker for the activation T-cells
MβCD	methyl-β-cyclodextrin
MFI	mean fluorescence intensity
MHC	major histocompatibility complex
MPTS	3 -mercaptopropyltrimethyoxy silane

PALM	photo-activated localization microscopy
PAO	phenylarsine oxide
PBS	phosphate buffered saline
PDB	phorbol dibutyrate
pERK	phosphorylated extracellular regulated kinase
PH	pleckstrin homology
PI	phosphoinositides
PI(4)K	phosphatidylinositol 4- kinase
PI(4)P	phosphatidylinositol 5-phosphate
$PI(4,5)P_2$	phosphatidylinositol 4,5 bisphosphate
PI3K	phosphatidylinositol 3- kinase
PKC	protein kinase C
PLC	phosphorlates phospholipase
PM	palmitate/myristate
POPC	palmitoyl-2-oleoyl-sn-glycero-3-phosphocholine
PP2	4-amino-5-(4-chlorophenyl)-7-(dimethylethyl)pyrazolo[3,4-d]pyrimidine
RBL	rat basophilic leukemia
RTK	receptor tyrosine kinase
siRNA	small interfering RNA
SOS	son of sevenless
STAT	signal transducers and activators of transcription
STO RM	stochastic optical reconstruction microscopy
TCR	T-cell receptor

TGFα	transforming growth factor-α
WASP	Wiskott-Aldrich syndrome protein

Chapter 1

Introduction

1.1 Receptor mediated signaling in cell biology:

One of the criteria that defines life is that all living organisms are responsive to changes in their external environment and certain type of stimuli (1). The smallest single unit of life in mammals, a cell, is no exception to that rule. Over the decades, research has demonstrated that cells are responsive to changes in extracellular environment and to chemical or physical stimuli. Chemical stimuli can be caused by several kinds of molecules including proteins, peptides, amino acids, nucleotides, small molecules such as nitric oxide and carbon monoxide. In some cases, these molecules might be freely diffusing in the extracellular milieu or might be tightly bound to the plasma membrane of a stimulating cell. Since the inside of the cell is separated from the extracellular environment by plasma membrane, which is impermeable to most molecules, the mechanism of how changes in extracellular environment affect the cells on the inside has been a central topic of research. Although some molecules can easily diffuse across the plasma membrane of the cell, most cannot. Cells are particularly responsive to a specific class of molecules that act by binding to their high affinity receptors on the plasma membrane of the cell. Cell surface receptors are a class of transmembrane proteins that are expressed on the plasma membrane of the cells. They become activated upon ligand-binding and the cell initiates a signaling cascade eventually leading to cellular responses (5). Depending on the specific receptor, these may lead to a range of responses in varying cell types including migration, proliferation, morphological changes, gene transcription and apoptosis. A wide array of signaling

molecules, along with their specific, receptors on the plasma membrane of the cells, lead to diversity in the responses (6).

Since receptor mediated signaling is known to regulate so many important processes in the cells, misregulation of these pathways has been implicated in many physiological diseases, including diabetes, allergic reactions to harmless substances, and cancer. Molecular understanding of the signaling pathway will open more avenues for exploring new drug targets in the effort to cure these diseases. In this dissertation, I concentrate specifically on studying two types of receptor mediated signaling systems: 1) FcεRI, a high affinity receptor for immunoglobulin E (IgE) on the surface of mast cells, which is involved in allergic responses (7), 2) epidermal growth factor (EGF) receptor (EGFR) on the surface of fibroblasts (8), which has been known to be misregulated in different kinds of cancer.

1.2 FcεRI receptor mediated signaling

FcεRI, expressed on the plasma membrane of mast cells and basophils, is a high affinity receptor for immunoglobulin E (IgE), which binds to IgE in a 1:1 ratio. For review, see (9). FcεRI receptor expressed on rat basophilic leukemia (RBL) cells has proved to be a useful model system to study receptor mediated signaling in hematopoietic cells. Physiologically, signaling by IgE bound to FcεRI is initiated by an oligovalent antigen (allergen), which causes aggregation of IgE-FcεRI. This results in association of aggregated FcεRI receptors with ordered membrane domains (also referred to as 'lipid rafts'). As depicted in Figure 1.1, crosslinking of IgE by a multivalent antigen leads to formation of receptor signaling complexes, which facilitates the recruitment of signaling partners including Src family kinase, Lyn (10), which is known to

Figure 1.1: Schematic demonstration of FcεRI signaling pathway: The FcεRI signaling pathway is initiated upon the crosslinking of IgE bound receptors on the surface of cells. This is followed by FcεRI receptor phosphorylation by Lyn and subsequent activation of Syk kinase, LAT, and PLC. $PI(4,5)P_2$ is hydrolyzed by PLC to generate IP_3 and DAG. IP_3 binds to its receptor on the ER to initiate calcium mobilization, plasma membrane bound DAG activates PKC. This leads to further downstream signaling events eventually resulting in exocytosis of secretory vesicles, in a process known as degranulation.

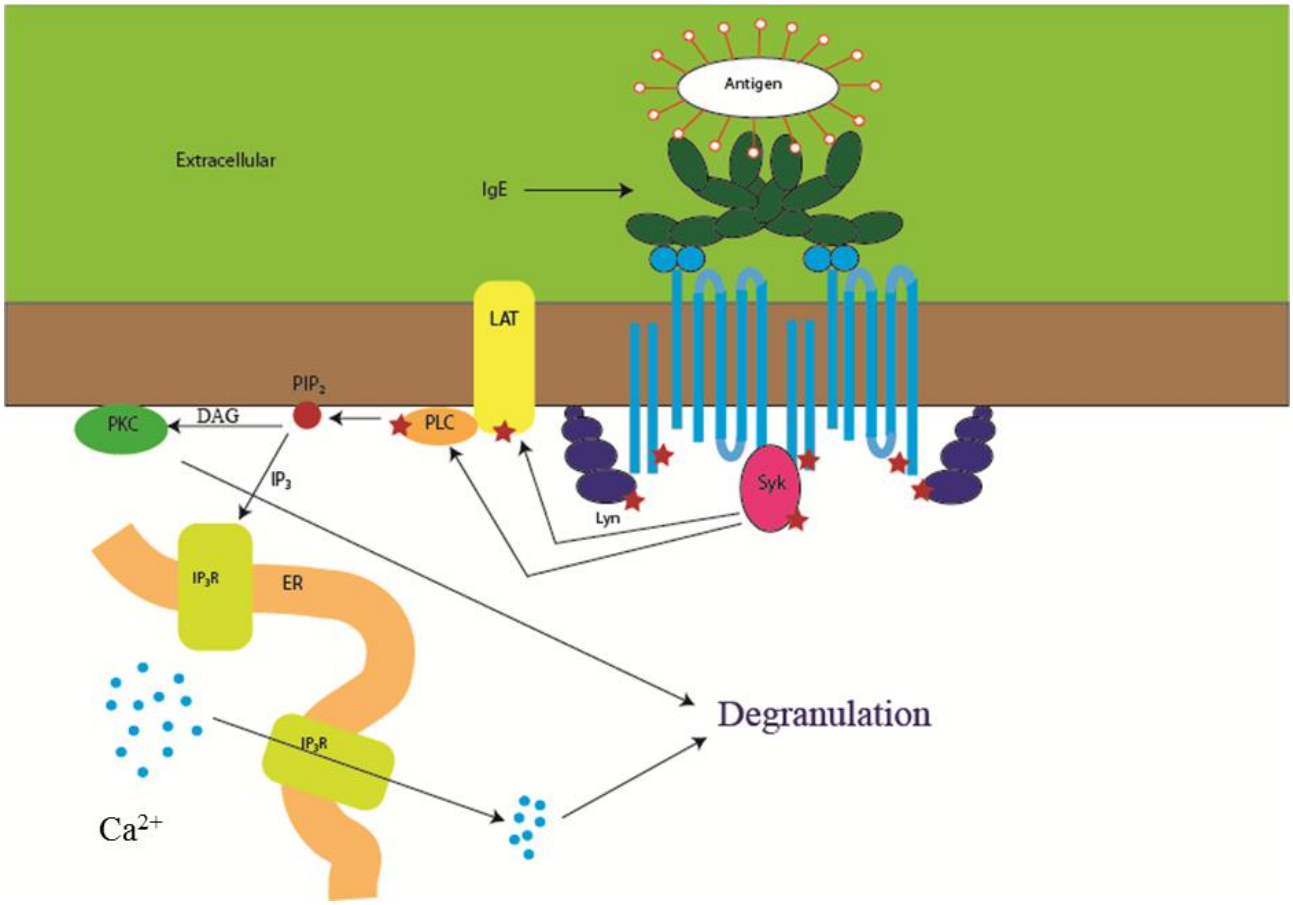
Antigen
Extracellular
IgE
LAT
PIP2
PKC
DAG
PLC
IP3
Syk
Lyn
IP3R
ER
IP3R
Degranulation
Ca2+

phosphorylate tyrosine residues located in the immunoreceptor tyrosine-based activation motifs (ITAMs) of FcεRI β and γ subunits (11). Tyrosine phosphorylation of ITAMs results in the recruitment and phosphorylation of Syk, a tyrosine kinase of the Syk/ZAP-70 family and Lyn through their Src homology-2 (SH2) domain, which in turn phosphorylates phospholipase C (PLC) and linker for the activation of T-cells (LAT) amongst other signaling partners. Activated PLC, recruited to the plasma membrane by binding to phosphorylated LAT, hydrolyzes phosphoinsositide 4,5 bisphosphate ($PI(4,5)P_2$), leading to generation of inositol triphosphate (IP_3) and membrane bound diacylglycerol (DAG). IP_3 plays a critical role in Ca^{2+} mobilization by causing release of Ca^{2+} from the intracellular stores in endoplasmic reticulum (ER) to cytoplasm, whereas DAG is involved in the activation of protein kinase C (PKC). Together, Ca^{2+} mobilization and PKC activation, coupled with further downstream signaling events lead to exocytosis of secretory vesicles, which is also known as degranulation. These secretory vesicles contain chemical mediators, such as histamine that are responsible for causing allergic reactions such as sneezing and itching (11). It has been observed that degranulation occurs within minutes after FcεRI bound IgE is crosslinked with the multivalent antigen (12). Although the sequelae of biochemical signaling events that take after IgE-FcεRI are aggregated are well characterized, until recently not much was known about the interaction of the signaling partners such as Lyn with the FcεRI signaling complexes at the plasma membrane.

1.3 Micro-patterned ligands to study spatial regulation of receptor mediated signaling:

Recently, much interest has focused on understanding the spatiotemporal regulation of cell signal transduction. Once the receptor is activated by binding to its ligand, ligand-bound receptor interacts with its signaling partners, which may lead to formation of supramolecular

complexes of activated receptor with proteins participating in the signaling pathway. One of the most important tools to study the localization of proteins is fluorescence microscopy, where localization of different proteins may be detected through labeling them with different fluorescent dyes. Advances in fluorescent imaging after the development of genetically encoded green fluorescent protein (GFP) (13) and the advent of confocal fluorescence microscopy (14) allow us to study the sub-cellular localization of proteins. It should be noted, however, that fluorescence microscopy was limited by the optical resolution, which is diffraction limited (~250 nm). With recent advances in the development of sub-optical resolution microscopy techniques – stochastic optical reconstruction microscopy (STORM) (15, 16) and photoactivated localization microscopy (PALM) (17, 18), the optical resolution has increased significantly (~20 - 40 nm). However, morphological heterogeneities and cellular autofluorescence as well as appropriate image analysis continue to present challenges.

The advent of photolithography and modern nanofabrication technology have enabled us to manipulate surfaces and substrates at micron and nano scale with high accuracy, a realm that was previously inaccessible (19). Together these technologies provide a unique methodology to create surfaces for spatially controlled interactions with cells that can be visualized. Features that can be generated using photolithography, range from a few nanometers to several micrometers in size. For a long time, due to the harsh conditions in the nanofabrication technology, these techniques were not very appealing for making biologically-relevant, functionalized surfaces. Recent advances, focused on finding biological applications for nanofabricated surfaces (reviewed in (3, 20)) led to development of micro/nano-patterned ligand surfaces. These fabrication methods utilize a number of techniques including nanocontact printing (21),

Figure 1.2: Preparation of micro-patterned surfaces using parylene lift-off method: A) Silicon/glass substrates are coated with ~ 1 μm layer of parylene and followed by a 1 μm thick layer of photoresist. Photolithography is then carried out with an appropriate mask followed by developing and etching to obtain a micro-patterned parylene layer on the silicon/glass substrate. Biomaterial (ligand) of interest is then incubated on these substrates prior to mechanical lift-off of parylene to obtain a micropatterned ligand surface. B) A representative fluorescent image of a micropatterned surface with covalently attached Cy3-DNP_{22}-BSA. Scale bar: 10 μm.

A

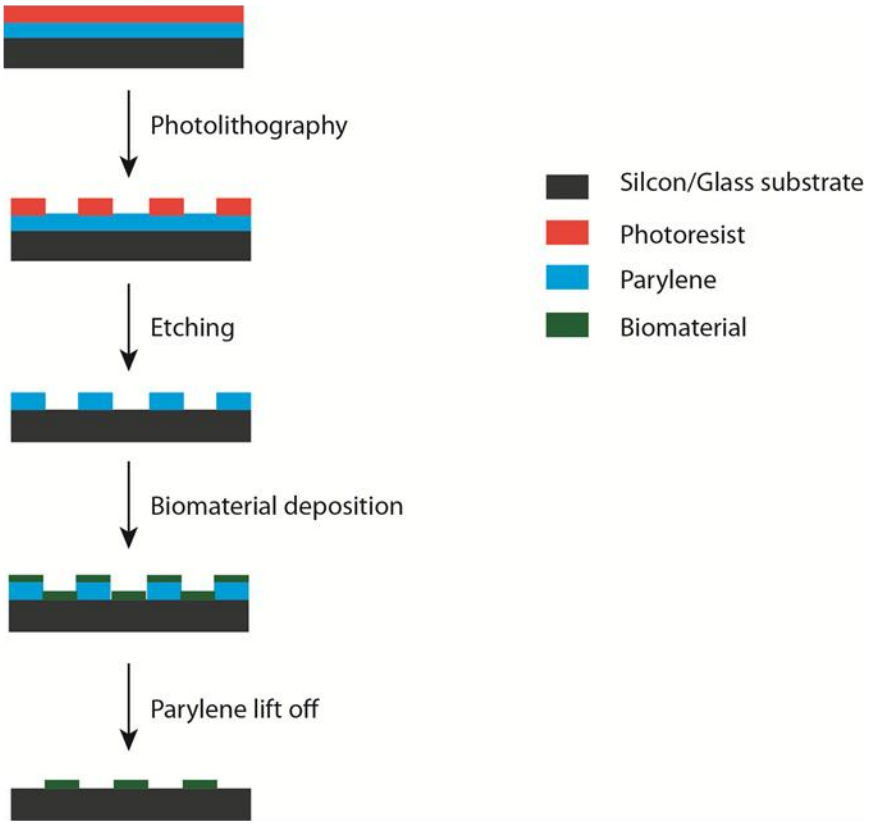
Photolithography
Etching
Biomaterial deposition
Parylene lift off
Silcon/Glass substrate
Photoresist
Parylene
Biomaterial

B

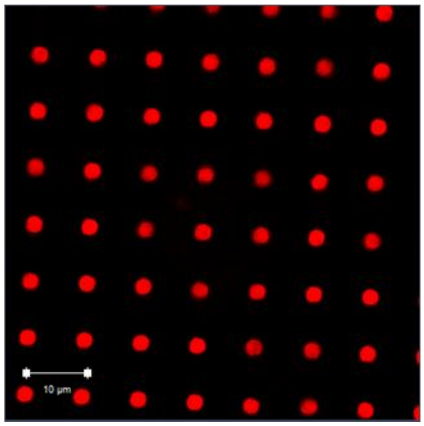
10 µm

nanoimprint lithography (22), scanning probe lithography (23), microcontact printing (24) and polymer lift-off method (25). All of these techniques offer diversity and control over different parameters such as the size of features, compatibility with the biomaterial in question, high through-put manufacturing and cost effectiveness. Therefore, the choice of technique to be used primarily depends on the feature size required and the biomaterial to be utilized.

The substrates generated using these techniques have been implemented to answer previously unsolved biological questions. An interesting example is using these micro-patterned surfaces to study cell adhesion mechanisms. Cell adhesion is mediated by the binding of integrins, present in the plasma membrane of cells, to proteins in the extracellular matrix (ECM). This interaction of cells with the ECM is known to play an important role in cellular processes such as cell cycle regulation (26). A pioneering study utilized the micro-patterned fibronectin, an ECM protein, to study cell attachment and spreading. The authors found that they could vary the extent of cell spreading by varying the size of ECM features, which, in turn, controls important cellular processes such as cell growth, proliferation and apoptosis (27).

Another interesting example involved utilization of micro-patterned substrates to study T-cell signaling, which is known to operate in immune responses. T cells are activated by association with APC (antigen presenting cells) and recognition of foreign peptides displayed by major histocompatibility complex (MHC) on the surface of the APC. This interaction of T-cell receptor (TCR) with these complexes, along with integrin-mediated interactions, leads to the formation of a microscale structure known as the immunological synapse (IS) (28). In one particular study, E-beam lithography was used to generate 100 nm wide x 5 nm high chromium strips separated by 1 μm spacing on silica substrates (29). Lipid bilayers, containing intercellular adhesion molecule 1 (ICAM1) and major histocompatibility complex (MHC) peptides for the

activation of TCR, were prepared on these substrates. The authors found that TCR clusters are formed within the grid space with distinct orientation towards the center. They also found that the phosphorylation state of the TCR, visualized by labeling with anti-phosphotyrosine antibodies, depends on the geometrical location of TCR.

In a separate study, micro-patterned ligands were also utilized to study the interactions of aggregated low density lipoproteins (agLDL) with macrophages. Amongst the various functions of macrophages in the human body, one of the most medically important functions is their interaction with agLDL in the walls of blood vessels. This interaction results in the massive uptake of cholesterol and conversion of macrophages to foam cells, which serve as an early step in the development of atherosclerosis (30). In this particular study, the authors utilized substrates with covalently attached, micro-patterned agLDL. Upon incubating the macrophages on these surfaces, they observed regions of low pH at the contact sites. Since the agLDL was covalently attached to the substrate, it was concluded that these regions of low pH are extracellular, in regions known as the lysosomal synapse (31).

As illustrated in Figure 1.2, we previously utilized the prepared patterned lipid bilayers, consisting of fluorescent lipids for visualization and dinitrophenyl (DNP) conjugated phospholipids for binding with anti-DNP-IgE on the surface of RBL-2H3 cells. These micro-patterned surfaces were prepared using polymer lift-off method described previously (3, 32, 33). Figure 1.3A shows the schematic of the RBL-2H3 cells incubated over patterned lipid bilayers containing specific ligand. Figure 1.3B demonstrates that Alexa Fluor 488 (A488) tagged IgE co-localizes with DNP liganded fluorescent patches within a few (~ 5 min) after incubating the cells on the patterned surfaces. FcεRI localized over the DNP containing lipid bilayers is tyrosine phosphorylated, as detected by anti-phosphotyrosine antibodies (32). Spatial localization of Lyn,

was investigated using these micro-patterned ligand surfaces. It was observed that transiently transfected Lyn-GFP co-redistributes with the IgE receptor signaling complex on the plasma membrane 15 minutes after incubation of the cells (Figure 1.3B). GFP tagged palmitate/myristate (PM) acylated region of Lyn, responsible for anchoring of the kinase to plasma membrane, is also observed to co-redistribute with patterned ligand patches at the somewhat longer time scale (~45 min). However, co-localization of $PI(4,5)P_2$ bound to a specific GFP construct (PH domain of PLCδ), or GFP tagged PKC, is not observed with liganded patterned bilayers under similar time scales (Wu, Holowka, unpublished results). Fluorescence recovery after photobleaching (FRAP) experiments revealed that signaling complexes formed by stimulation with patterned lipid bilayers are dynamic in nature (32).

The role of actin cytoskeleton in FcεRI was also investigated using these micro-patterned ligand surfaces. Transiently transfected actin-GFP in RBL-2H3 also co-redistributes over the micron sized ligand patches. To further investigate the role of actin cytoskeleton in receptor mediated signaling, RBL cells were pretreated with cyotochalasin-D, an inhibitor of actin polymerization. This pretreatment with cytochalasin-D prevented the observed accumulation of Lyn-GFP, actin-GFP and PM-EGFP (32). In contrast, the same treatment did not reduce the accumulation of FcεRI or its tyrosine phosphorylation over the micron sized patches of liganded lipid bilayers. This demonstrates that the actin cytoskeleton in stabilizes the macromolecular FcεRI signaling complexes formed on the plasma membrane.

The actin cytoskeleton and other actin binding proteins are known to participate in integrin-mediated signaling upon formation of focal adhesions in adherent cells. RBL-2H3 cells show enhanced stimulated degranulation when they are adherent to ECM (34), which indicates a possibility of crosstalk between the FcεRI and integrin mediated signaling pathways (35).

Figure 1.3: Micro-patterned ligands to study FcεRI receptor signaling: A) A schematic representing RBL cells with clustered IgE-FcεRI and downstream signaling partners on the surface of patterned DNP lipid bilayers. B) A confocal micrograph demonstrating the clustering of fluorescently labeled proteins on top of DNP containing lipid bilayers. The clustering of A488-IgE, along with localized tyrosine phosphorylation, is observed within 5 minutes of plating the cells on patterned ligand surfaces, which is significantly faster than the clustering Lyn and actin. (Adapted from reference (3))

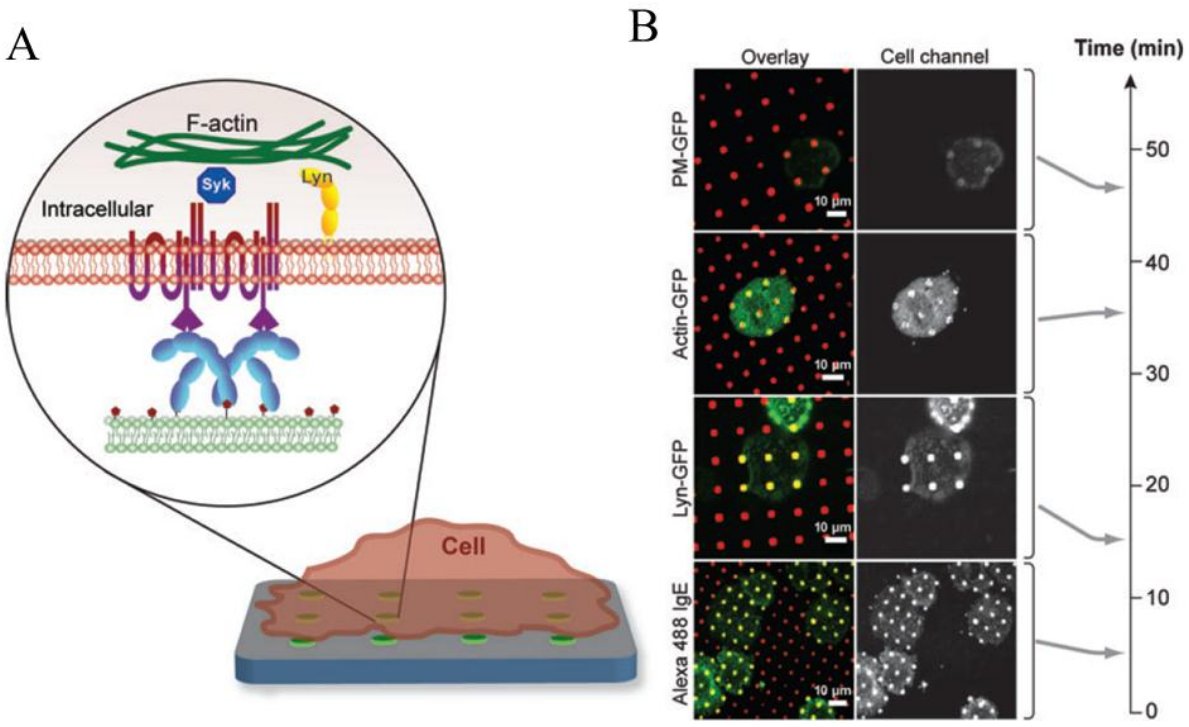
A
F-actin
Syk
Lyn
Intracellular
Cell
B
Overlay
Cell channel
Time (min)
PM-GFP
Actin-GFP
Lyn-GFP
Alexa 488 IgE
10 µm
50
40
30
20
10
0

Studies with patterned ligands have revealed that, in addition to actin-GFP, other cytoskeleton interacting proteins such as vinculin, paxillin and talin also co-redistribute with anti-DNP-IgE sensitized FcεRI at DNP containing lipid bilayers. However, the GFP construct of integrin α-5, one of the most prominent integrins present in RBL-2H3 cells, was found to be excluded from the regions of antigen containing lipid bilayers (33). Together, these results demonstrate that actin, paxillin, vinculin and talin associate with IgE receptor signaling complexes on the plasma membrane independently of integrin association. Biochemical investigations show that paxillin knock down alters Ca^{2+} responses in RBL-2H3 cells (32, 33). These studies provided new insights regarding the spatial interaction of FcεRI with its signaling partners and the actin cytoskeleton.

1.4 FcεRI receptor endocytosis

Endocytosis is an ubiquitous process utilized by cells to internalize a variety of molecules. It is becoming evident that endocytosis plays a key role in regulating important cellular processes such as antigen presentation, cell migration and mitosis (36). In addition to regulation by phosphatases and kinases, endocytosis is one of the most important pathways that lead to down-regulation of receptor mediated signaling responses in immune cells. Internalization also leads to degradation of receptors and thereby inhibition of their interactions with ligands (37, 38). Interestingly, it has also been determined that receptors in endosomes can signal intracellularly, which is different from the signals initiated from the receptors at the plasma membrane (39, 40). As schematically depicted in Figure 1.4, receptors can be endocytosed by a variety of mechanisms (36, 41, 42). Of the pathways available for receptor endocytosis, clathrin mediated pathway has been the most widely studied (42-45), and the

clathrin, protein has been known to be involved many intracellular cargo transport processes (46). The pathways of endocytosis can be constitutive or can be triggered by a specific signal, as in the case of receptor mediated endocytosis, or even hijacked by virus as-to gain entry into the cell (47). While a lot of endocytic processes have been traditionally thought of as a clathrin dependent processes, recently several clathrin independent endocytic pathways have been identified (4, 48).

Another important component of the endocytic machinery known to play a role in several internalization pathways is the GTPase dynamin 2. In model systems this enzyme binds to liposomes, and, upon GTP hydrolysis, can stretch and tubulate these liposomes (49). Dynamin 2 has been implicated in a wide array of internalization processes and is primarily responsible for the scission of newly formed vesicles (50). Although clathrin and dynamin are very well characterized for their role in endocytosis, there are other players such as adaptor protein 2 (AP2) (42), BAR-domain containing proteins (51, 52), ADP-ribosylation factor (Arf) (53) and the Rho subfamilies (54) of proteins, that also play important roles in endocytosis. In addition to the role of proteins, other components of plasma membrane, such as the phospholipids $PI(4,5)P_2$ (55) and cholesterol (56), have been shown to participate in various clathrin-dependent and clathrin-independent endocytic pathways. The role of the actin cytoskeleton in endocytic pathways has been a subject of investigations and it appears that, some, but not all, endocytic pathways depend on the actin cytoskeleton. (36, 57). The sensitivity of endocytosis to actin cytoskeleton disruption depends on the cell type, identity of endocytic cargo and the endocytic machinery involved.
In RBL-2H3 cells, the sequelae of signaling events after FcεRI receptor activation via crosslinking of IgE has been well established, but less is known about the mechanism of

Figure 1.4: Internalization pathways: The schematic represents the various routes adopted by a cell for the uptake of different particles. Big particles are engulfed by phagocytosis while the fluid uptake is completed in a process known as macropinocytosis. Endocytosis for smaller particles (typically < 1 μm) goes primarily through two different pathways: clathrin-dependent and clathrin-independent. These endocytic pathways may rely on dynamin and/or the actin cytoskeleton depending on the internalization mechanism used. (Reproduced from reference (4))

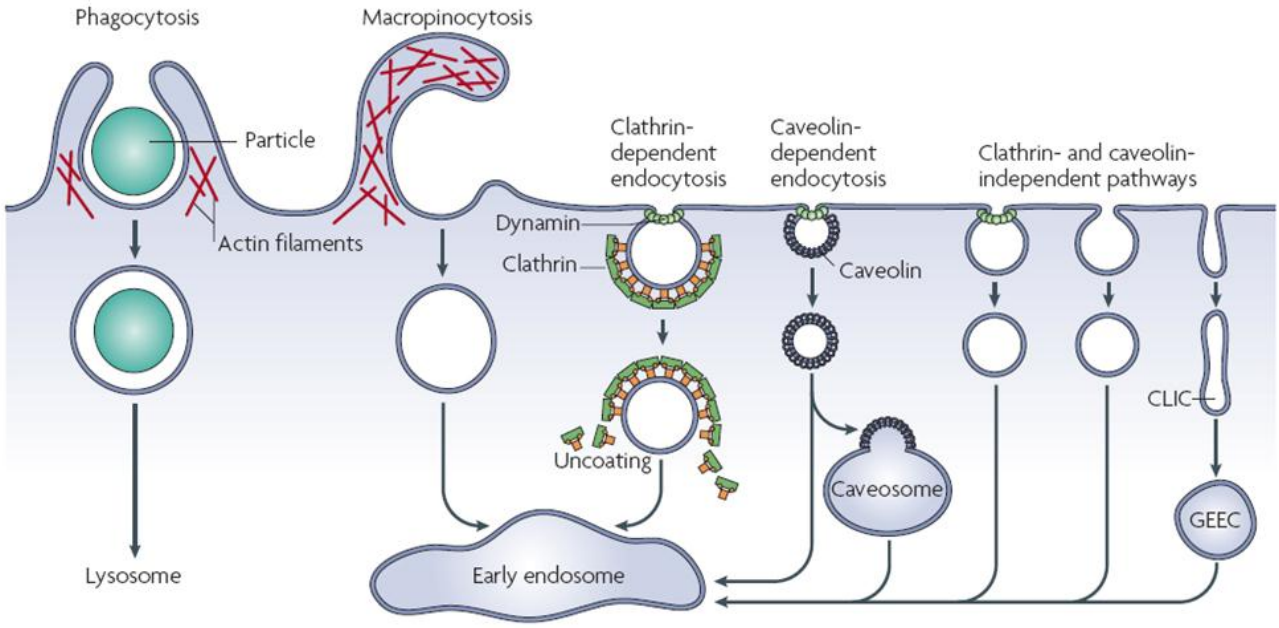
Phagocytosis
Macropinocytosis
Particle
Actin filaments
Clathrin-dependent endocytosis
Caveolin-dependent endocytosis
Clathrin- and caveolin-independent pathways
Dynamin
Clathrin
Caveolin
Uncoating
CLIC
Caveosome
GEEC
Lysosome
Early endosome

internalization of the FcεRI receptor. Initial evidence demonstrated that RBL-2H3 cells expressing FcεRI treated with oligomeric IgE led to internalization of the IgE-FcεRI complexes (58), whereas monomeric IgE tended to stay on the plasma membrane for prolonged periods of time. Subsequently, it was demonstrated that FcεRI, sensitized with monomeric IgE, were internalized upon crosslinking of IgE with a specific antigen (12). It was further determined that crosslinked, endocytosed IgE is then trafficked to the lysosomes for degradation (59). These authors also demonstrated that internalization of IgE, following its crosslinking, occurred rapidly with a $t_{1/2}$ of 13-19 minutes and, unlike degranulation, it is independent of the presence of extracellular Ca^{2+}. This indicates that crosslinking of FcεRI bound IgE initiates two distinct signaling cascades, leading to degranulation and internalization of crosslinked IgE-FcεRI complexes, although the relationship between these two signaling pathways is not well understood.

Some studies have investigated the mechanism of FcεRI internalization. Prior evidence utilizing flow cytometry and Lyn knock-out mice, demonstrated that FcεRI internalization is dependent on Lyn (60), however, the role of Syk kinase in FcεRI internalization has not been clearly deliniated. One set of experiments via flow cytometry report robust FcεRI receptor internalization in Syk-/- cells (60, 61), whereas others using the same technique have concluded that FcεRI receptor internalization is inhibited in Syk-/- cells (62). Previous studies utilizing flow cytometry to assess surface accessible IgE have shown that FcεRI internalization is clathrin independent (63). However, other studies via electron microscopy showed that clathrin-coated pits are colocalized with aggregated FcεRI receptor, suggesting, FcεRI is internalized via clathrin mediated endocytosis (64, 65). Over-expression of catalytically inactive dynamin 2 mutant (K44A) reduces FcεRI internalization substantially, pointing towards a dependence on dynamin

2 for FcεRI internalization (63). Another study has demonstrated that IgE receptor internalization is sensitive to cholesterol depletion (62). The role of the actin cytoskeleton in FcεRI endocytosis has been elusive, with some studies showing that it is insensitive to disruptions of the actin cytoskeleton (66), whereas some studies have shown that it is independent of actin cytoskeleton (67).

In this work, we have utilized fluorescence spectroscopic techniques, flow cytometry and confocal microscopy to probe the role of cholesterol, Syk kinase, actin cytoskeleton and dynamin 2 in FcεRI receptor endocytosis after its crosslinking. We utilize the micro-patterned ligand surfaces to study the interplay between dynamin 2 and the actin cytoskeleton at the activated FcεRI receptor complexes on the plasma membrane.

1.5 EGFR mediated signaling

EGFR is part of a broader family of receptor tyrosine kinases (RTKs), that are highly conserved in evolution and play an important role in the regulation of cellular processes, such as proliferation, migration, differentiation, metabolism and survival (68). Mutations or dysregulations in this pathway have been linked to several disorders including cancer, diabetes and angiogenesis (69). EGF was first isolated and identified as a growth factor in the 1960's from a serum that accelerated the growth of new born mice (8, 70). Sequence analysis of EGF revealed that it is a small peptide with 53 amino acids and 6 cysteine residues, known to form three disulfide bonds, which are critical for EGF activity (71). EGFR was later identified to be a transmembrane glycoprotein, which possesses intrinsic tyrosine kinase activity, stimulated by binding to EGF. The EGFR consists of an extracellular ligand binding domain, a single

Figure 1.5: Schematic of signaling pathway activated by EGFR: The EGFR signaling pathway is initiated upon binding of EGF to EGFR on the surface of the cells, leading to dimerization of EGFR and activation of its tyrosine kinase activity. The tyrosine phosphorylated residues on the cytoplasmic tail of EGFR act as docking sites for its signaling partners. EGFR activation leads to activation of Erk via the Ras, Raf, MEK pathway and the activation of mTor via the PI3K-Akt pathway. These pathways are critical in controlling cellular responses such as growth, proliferation, and apoptosis. (Reproduced from reference (2))

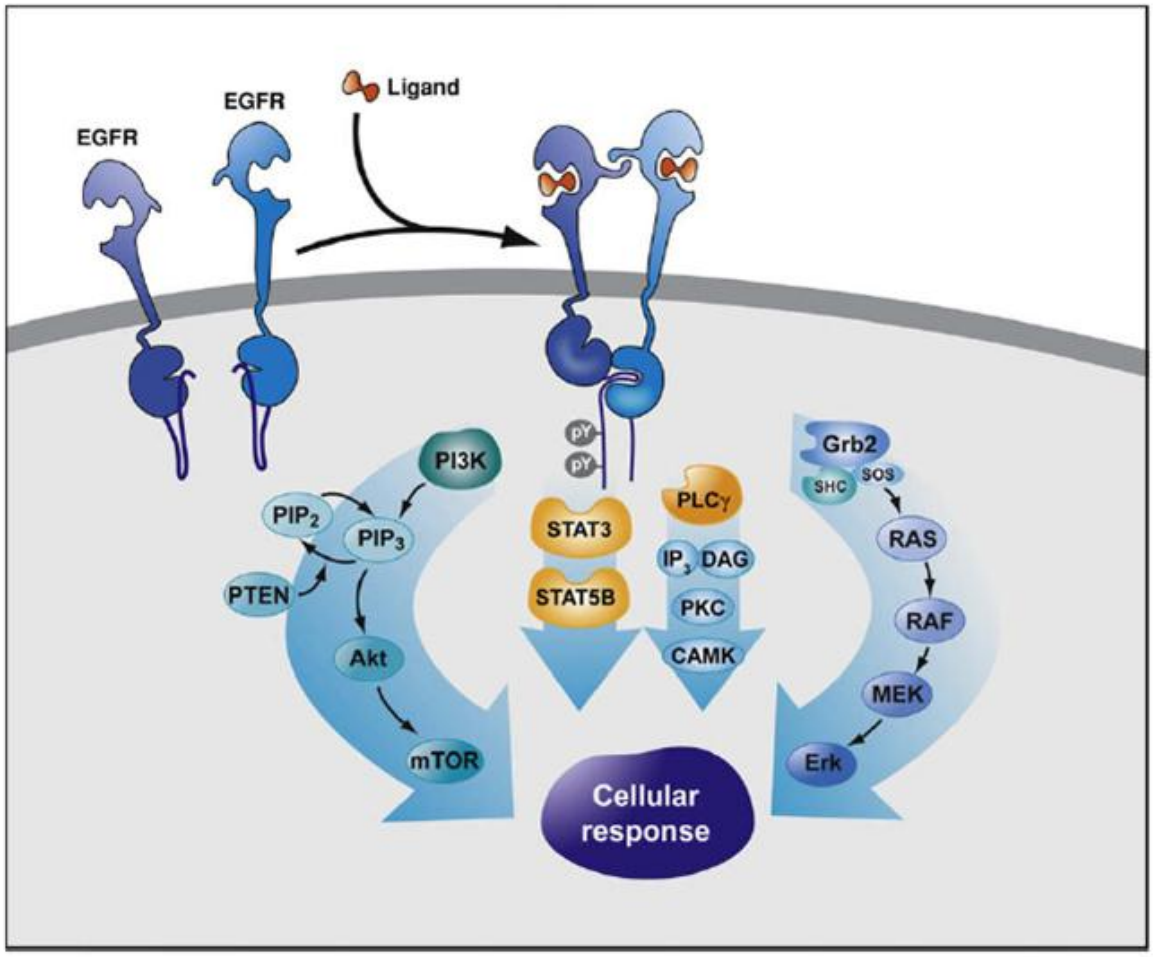
Ligand
EGFR
EGFR
pY
pY
PI3K
PIP2
PIP3
PTEN
Akt
mTOR
STAT3
STAT5B
PLCγ
IP3
DAG
PKC
CAMK
Grb2
SHC
SOS
RAS
RAF
MEK
Erk
Cellular response

transmembrane domain and a cytoplasmic domain (72, 73). EGF binding to the extracellular domain of EGFR (ErbB1), causes a conformational change, leading to the exposure of the dimerization arm in the cytoplasmic domain (74, 75). This leads to the formation of EGFR homodimers and/or heterodimers with other members of EGFR family, ErbB2, ErbB3 and ErbB4 (76). The intracellular portion of the EGFR includes a polybasic juxtamembrane region, the tyrosine kinase domain, and a carboxy terminal regulatory region. Tyrosine kinase residues in the carboxy terminal region are not phosphorylated in the monomeric state of EGFR (77). EGF-induced dimerization of EGFR, causes the transphosphorylation of tyrosine residues which act as docking sites for several SH2 domain-containing proteins (78). Additionally, the tyrosine kinase domain of the EGFR can phosphorylate tyrosine residues on other signaling partners, such as phospholipase Cγ (PLCγ) (79) and cytoskeleton-associated proteins such as α-actinin (80). Apart from tyrosine residues phosphorylated by EGFR kinase, other residues on the EGF receptor intracellular segments can be phosphorylated by other kinases, which are activated as result of EGFR activation. Examples of residues that are phosphorylated by a non EGFR kinase include the phosphorylation of Tyr-845 by tyrosine kinase Src (81) and Thr-654 by protein kinase C (PKC) (82).

EGFR tyrosine phosphorylated residues act as sites for the recruitment of adaptor protein 2 (Grb2), which binds to the son of sevenless (SOS) protein (83). SOS is the guanine nucleotide exchange factor (GEF) that is required for the activation of Ras, a GTPase and a potent oncoprotein (84, 85). GTP-bound Ras then activates and phosphorylates its effector kinase, Raf. Activated Raf is responsible for the activation of mitogen-extracellular activated protein kinase kinase-I (MEK), which in turn phosphorylates extracellular regulated kinase (ERK) (86). ERK has numerous downstream and upstream substrates, which further explains how dysregulation of

ERK signaling pathway has such profound effects on cell growth (87). In addition to the activation of the Ras/Raf/MEK/Erk pathway, as described in Figure 1.5, EGFR also activates several other critical signaling pathways including the phosphatidylinositol 3-kinase (PI3K)/Akt pathway (88) and the signal transducers and activators of transcription (STAT) pathway (89). Altogether, these pathways are responsible for key cellular processes like migration, division and proliferation. Dysregulation of any one of these pathways has often been implicated in causing cancer (69, 90).

Although much work has been done to study the series of signaling events that take place upon the EGFR activation, not much is known about the spatial regulation of signaling partners like Ras, MEK and ERK with EGFR in the cells. Previous results have shown the association of signaling partners such as Grb2 and PLCγ with the EGFR via immunoprecipitations (IP) (79, 83). However, visualization of the signaling complexes formed with the EGF receptor is governed by the limitations in fluorescence microscopy and receptor internalization.

In this work, we utilize silicon substrates patterned with immobilized, covalently attached micron sized EGF patches to stimulate the EGFR. This stimulation results in the formation of macromolecular signaling complexes of EGF receptor, which are localized at the plasma membrane. We then study the recruitment of the EGFR signaling partners utilizing confocal fluorescent microscope.

1.6 Role of $PI(4,5)P_2$ in cell signaling

Phosphoinositides (PI) comprise some of the most functionally important lipids of the inner leaflet of the plasma membrane. $PI(4,5)P_2$ is one of the most widely studied phospholipids due to the role it plays in cellular signaling (91). Initially, $PI(4,5)P_2$ was considered to be an

important precursor in signaling because it led to the formation of secondary messengers IP_3 and DAG upon hydrolysis by PLC (92). Subsequently, it was discovered that $PI(4,5)P_2$ can directly affect signaling by interacting with signaling proteins and actin cytoskeleton-regulating proteins such as profilactin (93). $PI(4,5)P_2$ can also be phosphorylated by phosphatidylinositol 3-kinase (PI3K) leading to the formation of $PI(3,4,5)P_3$, which is important for a variety of cellular processes including proliferation, migration, differentiation and phagocytosis (94). In addition, $PI(4,5)P_2$ has also been implicated in controlling important cellular processes such as endocytosis, vesicular trafficking, membrane dynamics and activation of ion channels (91, 94).

Together, $PI(4,5)P_2$ and $PI(3,4,5)P_3$ comprise 1% of total plasma membrane lipid content and they require constant replenishment. $PI(4,5)P_2$ may be synthesized by phosphorylation of phosphatidylinositol 4-phosphate (PI(4)P) via phosphatidylinositol 5-kinase (PI5K), or by phosphorylation of phosphatidylinositol 5-phosphate (PI(5)P) via phosphatidylinositol 4-kinase (PI4K). Since PI(4)P is much more concentrated in cells in comparison to PI(5)P, it has been generally accepted that the majority of $PI(4,5)P_2$ is derived from the phosphorylation of PI(4)P by PI5K (91). Interfering with $PI(4,5)P_2$ concentrations by pharmacological treatments or by expression of dominant negative versions of PI4K/PI5K has profound effects on cellular physiology (94).

Hydrolysis of $PI(4,5)P_2$ by PLC into IP_3 and DAG has already been implicated in Ca^{2+} mobilization and activation of PKC respectively. Ca^{2+} mobilization and activation of PKC are both essential for the stimulated exocytosis in RBL cells. Previous studies done by inhibition of PI4K by the pharmacological inhibitors phenylarsinoxide (PAO) and quercetin in RBL-2H3 cells have shown that they affect Ca^{2+} mobilization and inhibit degranulation (95). Although, the role of $PI(4,5)P_2$ in degranulation has been widely studied, its role in FcεRI endocytosis has not been

very well understood. Some previous experiments, utilizing acid stripping method in RBL cells have demonstrated that interfering with $PI(4,5)P_2$ synthesis by treatment with quercetin does not inhibit crosslinked IgE internalization (66). Given the role of $P(4,5)P_2$ in endocytosis and the regulation of endocytic proteins such as AP-2, epsin and dynamin 2, it is of considerable interest to study the effects of $PI(4,5)P_2$ on FcεRI internalization (96).

The role of $PI(4,5)P_2$ in EGFR signaling, leading to the activation of downstream targets such as ERK, as well as EGFR endocytosis, has not been established. EGFR has a polybasic juxtamembrane domain, and it is predicted that negatively charged $PI(4,5)P_2$ binds to the positively charged residues in the juxtamembrane domain to maintain the EGFR kinase in an inactive state (97). Consistent with this, it has been shown that up-regulation of $PI(4,5)P_2$ levels results in lower EGF stimulated tyrosine phosphorylation of EGFR, whereas down-regulation of $PI(4,5)P_2$ leads to enhanced tyrosine phosphorylation of EGFR upon stimulation with EGF (98). This evidence indicates that EGFR activation is tightly regulated by the $PI(4,5)P_2$ levels in the inner leaflet of the plasma membrane. $PI(4,5)P_2$ turnover is also critical in EGF receptor signaling, as the hydrolysis of $PI(4,5)P_2$ by PLC leads to formation of IP_3 and DAG, which are important in calcium mobilization and PKC activation and further mediate downstream responses. PI3K phosphorylation of $PI(4,5)P_2$ to generate $PI(3,4,5)P_3$, which is responsible for regulation of various signaling pathways including the activation of Akt/mTor. $PI(3,4,5)P_3$ also interacts with GEFs that are responsible for regulation of cellular processes such as proliferation, migration and differentiation (99).

EGFR is thought to be endocytosed by both clathrin-dependent and clathrin-independent pathways (100). As previously mentioned, $PI(4,5)P_2$ plays an important role in these pathways by regulation of endocytic proteins, and thus may play an important role in EGFR endocytosis.

Despite the significance of $PI(4,5)P_2$ in the regulation of EGFR signaling and EGFR endocytosis, not much is known about the spatial localization of $PI(4,5)P_2$ with respect to the EGFR signaling complex on the plasma membrane.

1.7 Scope of thesis:

As described in this dissertation, I have used a myriad of cell biological approaches to study the spatial regulation of cell signaling following receptor activation. In Chapter 2, I have examined endocytosis utilizing flow cytometry, fluorescence spectroscopy and confocal microscopy to determine the localization of crosslinked FcεRI bound to IgE. I determined that in the presence of inhibitors of F-actin cycling, crosslinked IgE is in membrane invaginations which are not cleaved from the plasma membrane. Utilization of micro-patterned ligands demonstrated that dynamin 2 plays a role in the organization of the actin cytoskeleton at the sites of clustered IgE-FcεRI. Both internalization of FcεRI and recruitment of F-actin to micro-patterned surfaces are inhibited in presence of pharmacological inhibitors of $PI(4,5)P_2$ synthesis.

In Chapter 3, I demonstrate that micro-patterned arrays of covalently conjugated EGF can activate EGFR on the surface of NIH-3T3 cells. I utilized these micro-patterned EGF surfaces to observe that EGFR signaling partners including PLCγ, Ras, MEK and ERK co-redistribute with EGFR signaling complexes on the plasma membrane in a ligand and cytoskeleton dependent manner. F-actin and paxillin are also recruited to the EGFR signaling complexes on the plasma membrane. This recruitment of signaling partners to the micron sized patches of EGF via EGFR is independent of integrin α-5, the most abundant integrin expressed in NIH-3T3 cells. Moreover, this recruitment of signaling partners such as Ras and Erk, F-actin depends on $PI(4,5)P_2$ synthesis.

Collectively, these results demonstrate that fluorescence confocal microscopy and micro-patterned ligand arrays can be utilized to study the spatial localization of signaling partners in ligand activated receptor mediated signaling pathways. These immobilized ligands on the surfaces activate the receptor signaling, but prevent their internalization without pharmacological inhibition. These techniques provide a novel opportunity to study the orchestrated accumulation of biomolecules involved in cell signaling and endocytosis.

References:

1. Luisi PL. About various definitions of life. Origins of Life and Evolution of Biospheres.1998;28:613-622.
2. Pines G, Köstler WJ, Yarden Y. Oncogenic mutant forms of EGFR: Lessons in signal transduction and targets for cancer therapy. FEBS letters.2010;584:2699-2706.
3. Torres AJ, Wu M, Holowka D, Baird B. Nanobiotechnology and cell biology: micro- and nanofabricated surfaces to investigate receptor-mediated signaling. Annu Rev Biophys.2008;37:265-288.
4. Mayor S, Pagano RE. Pathways of clathrin-independent endocytosis. Nat Rev Mol Cell Biol.2007;8:603-612.
5. Lodish H, Berk A, Zipursky SL, Matsudaira P, Baltimore D, Darnell J. Molecular cell biology. New York.1995.
6. Hardie DG. Biochemical messengers: hormones, neurotransmitters, and growth factors. Springer, 1991.
7. Beaven MA. Our perception of the mast cell from Paul Ehrlich to now. European journal of immunology.2009;39:11-25.
8. Edwin F, et al. A historical perspective of the EGF receptor and related systems. METHODS IN MOLECULAR BIOLOGY-CLIFTON THEN TOTOWA-.2006;327:1.
9. Holowka D, Baird B. Antigen-mediated IgE receptor aggregation and signaling: a window on cell surface structure and dynamics. Annual review of biophysics and biomolecular structure.1996;25:79-112.
10. Young RM, Holowka D, Baird B. A lipid raft environment enhances Lyn kinase activity by protecting the active site tyrosine from dephosphorylation. Journal of Biological Chemistry.2003;278:20746-20752.
11. Kinet JP. The high-affinity IgE receptor (FcεRI): from physiology to pathology. Annual review of immunology.1999;17:931-972.
12. Furuichi K, Rivera J, Isersky C. The fate of IgE bound to rat basophilic leukemia cells. III. Relationship between antigen-induced endocytosis and serotonin release. The Journal of Immunology.1984;133:1513-1520.

13. Shimomura O, Johnson FH, Saiga Y. Extraction, purification and properties of aequorin, a bioluminescent protein from the luminous hydromedusan, Aequorea. Journal of cellular and comparative physiology.1962;59:223-239.
14. White J, Amos W, Fordham M. An evaluation of confocal versus conventional imaging of biological structures by fluorescence light microscopy. The Journal of cell biology.1987;105:41-48.
15. Rust MJ, Bates M, Zhuang X. Sub-diffraction-limit imaging by stochastic optical reconstruction microscopy (STORM). Nature methods.2006;3:793-796.
16. Huang B, Wang W, Bates M, Zhuang X. Three-dimensional super-resolution imaging by stochastic optical reconstruction microscopy. Science.2008;319:810-813.
17. Betzig E, et al. Imaging intracellular fluorescent proteins at nanometer resolution. Science.2006;313:1642-1645.
18. Hess ST, Girirajan TPK, Mason MD. Ultra-high resolution imaging by fluorescence photoactivation localization microscopy. Biophysical journal.2006;91:4258-4272.
19. Campbell SA. The science and engineering of microelectronic fabrication. Oxford University Press Oxford, UK, 1996.
20. Voldman J, Gray ML, Schmidt MA. Microfabrication in biology and medicine. Annual review of biomedical engineering.1999;1:401-425.
21. Odom TW, Thalladi VR, Love JC, Whitesides GM. Generation of 30-50 nm structures using easily fabricated, composite PDMS masks. Journal of the American Chemical Society.2002;124:12112-12113.
22. Falconnet D, et al. A novel approach to produce protein nanopatterns by combining nanoimprint lithography and molecular self-assembly. Nano Letters.2004;4:1909-1914.
23. Agarwal G, Naik RR, Stone MO. Immobilization of histidine-tagged proteins on nickel by electrochemical dip pen nanolithography. Journal of the American Chemical Society.2003;125:7408-7412.
24. Quist AP, Pavlovic E, Oscarsson S. Recent advances in microcontact printing. Analytical and bioanalytical chemistry.2005;381:591-600.
25. Ilic B, Craighead H. Topographical patterning of chemically sensitive biological materials using a polymer-based dry lift off. Biomedical Microdevices.2000;2:317-322.

26. Bijian K, Takano T, Papillon J, Khadir A, Cybulsky AV. Extracellular matrix regulates glomerular epithelial cell survival and proliferation. American Journal of Physiology-Renal Physiology.2004;286:F255-F266.
27. Chen CS, Mrksich M, Huang S, Whitesides GM, Ingber DE. Geometric control of cell life and death. Science.1997;276:1425-1428.
28. Bromley SK, et al. The immunological synapse. Annual review of immunology.2001;19:375-396.
29. Mossman KD, Campi G, Groves JT, Dustin ML. Altered TCR signaling from geometrically repatterned immunological synapses. Science's STKE.2005;310:1191.
30. Maxfield FR, Tabas I. Role of cholesterol and lipid organization in disease. Nature.2005;438:612-621.
31. Haka AS, et al. Macrophages create an acidic extracellular hydrolytic compartment to digest aggregated lipoproteins. Molecular biology of the cell.2009;20:4932-4940.
32. Wu M, Holowka D, Craighead HG, Baird B. Visualization of plasma membrane compartmentalization with patterned lipid bilayers. Proc Natl Acad Sci U S A.2004;101:13798-13803.
33. Torres AJ, Vasudevan L, Holowka D, Baird BA. Focal adhesion proteins connect IgE receptors to the cytoskeleton as revealed by micropatterned ligand arrays. Proc Natl Acad Sci U S A.2008;105:17238-17244.
34. Hamawy MM, Oliver C, Mergenhagen SE, Siraganian RP. Adherence of rat basophilic leukemia (RBL-2H3) cells to fibronectin-coated surfaces enhances secretion. The Journal of Immunology.1992;149:615-621.
35. Ra C, Yasuda M, Yagita H, Okumura K. Fibronectin receptor integrins are involved in mast cell activation. Journal of allergy and clinical immunology.1994;94:625-628.
36. Doherty GJ, McMahon HT. Mechanisms of endocytosis. Annual review of biochemistry.2009;78:857-902.
37. Cheng PC, Steele CR, Gu L, Song W, Pierce SK. MHC class II antigen processing in B cells: accelerated intracellular targeting of antigens. The Journal of Immunology.1999;162:7171.
38. Liu H, Rhodes M, Wiest DL, Vignali DAA. On the dynamics of TCR: CD3 complex cell surface expression and downmodulation. Immunity.2000;13:665-675.

39. McPherson PS, Kay BK, Hussain NK. Signaling on the endocytic pathway. Traffic.2001;2:375-384.
40. Hoeller D, Volarevic S, Dikic I. Compartmentalization of growth factor receptor signalling. Current opinion in cell biology.2005;17:107-111.
41. Conner SD, Schmid SL. Regulated portals of entry into the cell. Nature.2003;422:37-44.
42. Sorkin A. Cargo recognition during clathrin-mediated endocytosis: a team effort. Current opinion in cell biology.2004;16:392-399.
43. Robinson MS. The role of clathrin, adaptors and dynamin in endocytosis. Current opinion in cell biology.1994;6:538-544.
44. Schmid EM, McMahon HT. Integrating molecular and network biology to decode endocytosis. Nature.2007;448:883-888.
45. Mousavi SA, Malerød L, Berg T, Kjeken R. Clathrin-dependent endocytosis. Biochemical Journal.2004;377:1.
46. Kirchhausen T. Clathrin. Annual review of biochemistry.2000;69:699-727.
47. Marsh M, Helenius A. Virus entry: open sesame. Cell.2006;124:729-740.
48. Kirkham M, Parton RG. Clathrin-independent endocytosis: new insights into caveolae and non-caveolar lipid raft carriers. Biochimica et Biophysica Acta (BBA)-Molecular Cell Research.2005;1745:273-286.
49. Stowell M, Marks B, Wigge P, McMahon HT. Nucleotide-dependent conformational changes in dynamin: evidence for a mechanochemical molecular spring. Nat Cell Biol.1999;1:27-32.
50. Hinshaw J. Dynamin and Its Role in Membrane Fission 1. Annual review of cell and developmental biology.2000;16:483-519.
51. David C, McPherson PS, Mundigl O, De Camilli P. A role of amphiphysin in synaptic vesicle endocytosis suggested by its binding to dynamin in nerve terminals. Proceedings of the National Academy of Sciences.1996;93:331.
52. McPherson VA, et al. Contributions of F-BAR and SH2 Domains of Fes Protein Tyrosine Kinase for Coupling to the FcεRI Pathway in Mast Cells. Molecular and cellular biology.2009;29:389-401.
53. Donaldson JG, Klausner RD. ARF: a key regulatory switch in membrane traffic and organelle structure. Current opinion in cell biology.1994;6:527-532.

54. Ellis S, Mellor H. Regulation of endocytic traffic by rho family GTPases. Trends in cell biology.2000;10:85-88.
55. Haucke V. Phosphoinositide regulation of clathrin-mediated endocytosis. Biochemical Society Transactions.2005;33:1285.
56. Nabi IR, Le PU. Caveolae/raft-dependent endocytosis. The Journal of cell biology.2003;161:673-677.
57. Fujimoto LM, Roth R, Heuser JE, Schmid SL. Actin assembly plays a variable, but not obligatory role in receptor-mediated endocytosis in mammalian cells. Traffic.2000;1:161-171.
58. Isersky C, Rivera J, Segal D, Triche T. The fate of IgE bound to rat basophilic leukemia cells. II. Endocytosis of IgE oligomers and effect on receptor turnover. The Journal of Immunology.1983;131:388-396.
59. Furuichi K, Rivera J, Buonocore LM, Isersky C. Recycling of receptor-bound IgE by rat basophilic leukemia cells. The Journal of Immunology.1986;136:1015-1022.
60. Kitaura J, Xiao W, Maeda-Yamamoto M, Kawakami Y, Lowell CA, Kawakami T. Early divergence of Fc epsilon receptor I signals for receptor up-regulation and internalization from degranulation, cytokine production, and survival. J Immunol.2004;173:4317-4323.
61. Fattakhova GV, et al. Endosomal trafficking of the ligated FcvarepsilonRI receptor. Mol Immunol.2009;46:793-802.
62. Molfetta R, et al. Lipid raft-dependent FcepsilonRI ubiquitination regulates receptor endocytosis through the action of ubiquitin binding adaptors. PLoS One.2009;4:e5604.
63. Fattakhova G, Masilamani M, Borrego F, Gilfillan AM, Metcalfe DD, Coligan JE. The high-affinity immunoglobulin-E receptor (FcepsilonRI) is endocytosed by an AP-2/clathrin-independent, dynamin-dependent mechanism. Traffic.2006;7:673-685.
64. Wilson BS, Pfeiffer JR, Oliver JM. Observing FcεRI signaling from the inside of the mast cell membrane. The Journal of cell biology.2000;149:1131-1142.
65. Burns AR, Oliver JM, Pfeiffer JR, Wilson BS. Visualizing Clathrin-Mediated IgE Receptor Internalization by Electron and Atomic Force Microscopy. METHODS IN MOLECULAR BIOLOGY-CLIFTON THEN TOTOWA-.2008;440:235.
66. Furuichi K, Ra C, Isersky C, Rivera J. Comparative evaluation of the effect of pharmacological agents on endocytosis and coendocytosis of IgE by rat basophilic leukaemia cells. Immunology.1986;58:105-110.

67. Ra C, Furuichi K, Rivera J, Mullins JM, Isersky C, White KN. Internalization of IgE receptors on rat basophilic leukemic cells by phorbol ester. Comparison with endocytosis induced by receptor aggregation. Eur J Immunol.1989;19:1771-1777.
68. Lemmon MA, Schlessinger J. Cell signaling by receptor tyrosine kinases. Cell.2010;141:1117-1134.
69. Gschwind A, Fischer OM, Ullrich A. The discovery of receptor tyrosine kinases: targets for cancer therapy. Nature Reviews Cancer.2004;4:361-370.
70. Cohen S. The stimulation of epidermal proliferation by a specific protein (EGF). Developmental biology.1965;12:394-407.
71. Savage Jr CR, Inagami T, Cohen S. The primary structure of epidermal growth factor. Journal of Biological Chemistry.1972;247:7612-7621.
72. Carpenter G, Lembach KJ, Morrison M, Cohen S. Characterization of the binding of 125-I-labeled epidermal growth factor to human fibroblasts. Journal of Biological Chemistry.1975;250:4297-4304.
73. Cohen S, Ushiro H, Stoscheck C, Chinkers M. A native 170,000 epidermal growth factor receptor-kinase complex from shed plasma membrane vesicles. Journal of Biological Chemistry.1982;257:1523.
74. Burgess AW, et al. An open-and-shut case? Recent insights into the activation of EGF/ErbB receptors. Molecular cell.2003;12:541-552.
75. Bouyain S, Longo PA, Li S, Ferguson KM, Leahy DJ. The extracellular region of ErbB4 adopts a tethered conformation in the absence of ligand. Proceedings of the National Academy of Sciences of the United States of America.2005;102:15024.
76. Leahy DJ. Structure and Function of the Epidermal Growth Factor (EGF⁄ErbB) Family of Receptors. Advances in protein chemistry.2004;68:1-27.
77. Stamos J, Sliwkowski MX, Eigenbrot C. Structure of the epidermal growth factor receptor kinase domain alone and in complex with a 4-anilinoquinazoline inhibitor. Journal of Biological Chemistry.2002;277:46265.
78. Yarden Y, Sliwkowski MX. Untangling the ErbB signalling network. Nat Rev Mol Cell Biol.2001;2:127-137.
79. Margolis B, et al. EGF induces tyrosine phosphorylation of phospholipase C-II: a potential mechanism for EGF receptor signaling. Cell.1989;57:1101.

80. Akiyama T, et al. Substrate specificities of tyrosine-specific protein kinases toward cytoskeletal proteins in vitro. Journal of Biological Chemistry.1986;261:14797-14803.
81. Sato KI, Sato A, Aoto M, Fukami Y. c-Src phosphorylates epidermal growth factor receptor on tyrosine 845. Biochemical and biophysical research communications.1995;215:1078-1087.
82. Hunter T, Ling N, Cooper JA. Protein kinase C phosphorylation of the EGF receptor at a threonine residue close to the cytoplasmic face of the plasma membrane. Nature.1984;311:480-483.
83. Rozakis-Adcock M, Fernley R, Wade J, Pawson T, Bowtell D. The SH2 and SH3 domains of mammalian Grb2 couple the EGF receptor to the Ras activator mSos1.1993.
84. Wolfman A, Macara IG. A cytosolic protein catalyzes the release of GDP from p21ras. Science.1990;248:67-69.
85. Downward J, Riehl R, Wu L, Weinberg RA. Identification of a nucleotide exchange-promoting activity for p21ras. Proceedings of the National Academy of Sciences.1990;87:5998.
86. Marshall C. Specificity of receptor tyrosine kinase signaling: transient versus sustained extracellular signal-regulated kinase activation. Cell.1995;80:179.
87. Ramos JW. The regulation of extracellular signal-regulated kinase (ERK) in mammalian cells. The international journal of biochemistry & cell biology.2008;40:2707-2719.
88. Vivanco I, Sawyers CL. The phosphatidylinositol 3-kinase–AKT pathway in human cancer. Nature Reviews Cancer.2002;2:489-501.
89. Bromberg J. Stat proteins and oncogenesis. Journal of Clinical Investigation.2002;109:1139-1142.
90. Ullrich A, Schlessinger J. Signal transduction by receptors with tyrosine kinase activity. Cell.1990;61:203-212.
91. Di Paolo G, De Camilli P. Phosphoinositides in cell regulation and membrane dynamics. Nature.2006;443:651-657.
92. Berridge MJ, Irvine RF. Inositol phosphates and cell signalling.1989.
93. Yin HL, Janmey PA. Phosphoinositide regulation of the actin cytoskeleton. Annual review of physiology.2003;65:761-789.
94. Czech MP. PIP2 and PIP3: Complex Roles Minireview at the Cell Surface. Cell.2000;100:603-606.

95. Marcela de Souza Santos RMZGN, David Holowka and Barbara Baird. Inhibitors of PI(4,5)P2 Synthesis Reveal Dynamic Regulation of IgE Receptor Signaling by Phosphoinositides in Mast Cells. Journal of cell science.2012;Submitted.
96. Wenk MR, De Camilli P. Protein-lipid interactions and phosphoinositide metabolism in membrane traffic: insights from vesicle recycling in nerve terminals. Proceedings of the National Academy of Sciences of the United States of America.2004;101:8262.
97. McLaughlin S, Smith SO, Hayman MJ, Murray D. An electrostatic engine model for autoinhibition and activation of the epidermal growth factor receptor (EGFR/ErbB) family. The Journal of general physiology.2005;126:41-53.
98. Michailidis IE, et al. Phosphatidylinositol-4, 5-bisphosphate regulates epidermal growth factor receptor activation. Pflügers Archiv European Journal of Physiology.2011;461:387-397.
99. Cantley LC. The phosphoinositide 3-kinase pathway. Science's STKE.2002;296:1655.
100. Sorkin A, Goh LK. Endocytosis and intracellular trafficking of ErbBs. Experimental cell research.2009;315:683-696.

Chapter 2[1]

Investigating the interplay of dynamin and the actin cytoskeleton in FcεRI receptor internalization

2.1 Introduction

FcεRI, the high affinity receptor for immunoglobulin E (IgE), is a member of the cell surface family of multichain immune receptors that are activated by receptor aggregation and thereby induce phosphorylation of immunoreceptor tyrosine-based activation motifs (ITAMs) by Src family kinases (3, 4). FcεRI is mostly found on the surface of mast cells and basophils and is sensitized to stimulation by specific antigens by binding of IgE. Upon crosslinking by multivalent ligands (antigen), IgE-FcεRI mediate signaling events that lead to release of chemical mediators that cause inflammatory responses in allergic reactions (6, 7). Clustering of IgE-FcεRI complexes on the surface of the mast cells initiates a cascade of signaling events leading to multiple cellular responses including, but not limited to, cell spreading, ruffling, cytokine production and secretion, as well as exocytosis of chemical mediators (degranulation), and endocytosis of the aggregated IgE-FcεRI complexes. Although signaling steps leading to release of chemical mediators have been extensively characterized (4, 8), less is known about the role of signaling in receptor internalization after crosslinking by antigen.

Signaling responses in mast cells are regulated not only by kinases and phosphatases, but also by cell surface receptor expression and internalization that occurs after receptor aggregation (9, 10). Although there is some evidence for early divergence of pathways leading to IgE-FcεRI internalization and degranulation (11), the relationship between these two pathways is incompletely understood. Some recent investigations have focused on FcεRI internalization (11-

[1] Alexis J. Torres performed the protein knockdown experiments and dynamin localization to micro-patterned ligand surfaces. Part of this work is presented in his PhD thesis 1. Torres AJ. Investigating cytoskeletal regulation of

13), but the mechanism of the endocytosis of antigen crosslinked IgE-FcεRI complexes is not completely understood. Cell surface receptors can be endocytosed by a variety of mechanisms, and redundancy can exist such that endocytosis can be regulated by more than one signaling pathway (14).

Of all the available pathways for receptor internalization, clathrin mediated endocytosis has been best characterized. Recently, it has become more evident that many types of receptors can be endocytosed by clathrin-independent mechanisms (15). Cytokine receptors have been shown to be internalized via a clathrin-independent, cortactin/dynamin-dependent mechanism (16). Previous studies have provided evidence that FcεRI internalization is clathrin-dependent by virtue of colocalization of IgE-FcεRI complexes with clathrin-coated pits using electron microscopy (17, 18). In contrast, other studies using siRNA to knock down clathrin have shown that IgE receptor internalization is clathrin/AP-2 independent (12). These studies also demonstrated that IgE internalization is dynamin 2-dependent, as the over-expression of dominant negative, catalytically inactive dynamin 2 substantially reduced the IgE internalization. Furthermore, the role of the actin cytoskeleton in internalization of FcεRI remains to be defined, as there are some pathways that are actin-independent (19) and some that are actin-dependent (20). Dynamin 2 has been implicated in clathrin-independent, as well as clathrin-dependent receptor internalization (16, 21). PI(4,5)P_2, a phospholipid that is implicated in a variety of signaling processes, has been known to play a role in targeting the actin cytoskeleton to the sites of endocytosis on the plasma membrane (20, 22).

FcεRI-IgE complexes upon crosslinking are known to be stabilized in specialized ordered membrane domains enriched in cholesterol and sphingolipid, commonly called lipid rafts, where they couple with a Src family kinase, Lyn, to initiate signal transduction (23-25). Some evidence

shows that glycosyl-phosphatidylinositol (GPI) anchored proteins can be internalized by a clathrin-independent, lipid raft-dependent mechanism (26). Prior results have shown that crosslinked FcεRI internalization is sensitive to cholesterol depletion by methyl-β-cyclodextrin (MβCD) pretreatment (27). In addition, it has been demonstrated that IgE-sensitized RBL cells show different degranulation and signaling responses when stimulated by bivalent and trivalent ligands with different geometrical constraints (28). Prior experiments have shown that stimulating the cells with anti-FcεRI antibodies can cause internalization of IgE receptors (29). However, not much is known about the relationship between internalization and degree of crosslinking of IgE receptors.

Previous studies have utilized flow cytometry as a method to measure the extent of IgE receptor internalization (12, 27), but the method can be ambiguous. Here, we monitor the fluorescence quenching of FITC-IgE due to acidification of internalized FITC-IgE and also flow cytometry to assess the surface accessibility of IgE-FcεRI complexes. We find that in presence of inhibitors of F-actin polymerization, crosslinked IgE-FcεRI complexes are in membrane invaginations that are not detected via surface-accessible antibody labeling by flow cytometry, but are not pinched off from the plasma membrane to become internalized, as revealed by sensitivity to extracellular pH. We also demonstrate that the internalization of IgE receptors is sensitive to mild cholesterol depletion. Using siRNA to selectively knock down clathrin, dynamin, and cortactin, we find that IgE internalization does not depend on clathrin or cortactin, but depends on dynamin 2. We further utilize micropatterned ligand surfaces to show that dynamin-2 is recruited to clustered, activated FcεRI and plays a role in the consequent organization of the actin cytoskeleton. We also provide evidence that in $PI(4,5)P_2$ synthesis is

important for recruitment of F-actin to the activated FcεRI receptors and their subsequent internalization.

2.2 Materials and Methods

2.2.1 Materials:

1-Palmitoyl-2-oleoyl-sn-glycero-3-phosphocholine (POPC) and 1,2-dipalmitoyl-sn-glycero-3-phosphoethanolamine-N-[6-[(2,4-dinitrophenyl)amino]hexanoyl] (DNP-cap-PE) were purchased from Avanti Polar Lipids. Mouse monoclonal anti-DNP IgE was purified as described elsewhere (30) and conjugated to Alexa Fluor 488 (Invitrogen) or fluorescein isothiocyanate (FITC) as described previously (31). Alexa 568-labeled goat anti-mouse IgG_1, Alexa 568-labeled goat anti-rabbit (H+L), Alexa 568-labeled phalloidin, anti-Alexa 488 rabbit IgG, and Alexa 647-labeled goat anti rabbit IgG were purchased from Invitrogen. Mouse anti-dynamin 1 (clone 41) and mouse anti-clathrin heavy chain (clone 23) were purchased from BD Biosciences. Polyclonal anti-dynamin 2 (raised against a synthetic peptide corresponding to residues 760-779 from human dynamin 2) was purchased from Abcam. Mouse anti-cortactin (clone 4F11) was purchased from Millipore, rabbit anti-HS1 (rodent specific) was from Cell Signaling Technologies, monoclonal anti-α-tubulin (clone N.593) was from U.S. Biologicals, and human IgG was from Jackson Immunoresearch. Mouse anti-clathrin heavy chain (X-22) was a gift from Dr. Frances Brodsky (University of California, San Francisco). Dynamin 2-EGFP (32) and Dynamin 2 K44A –EGFP (32) cDNA were gifts from Dr. Mark McNiven (Mayo Clinic). Cytochalasin D was purchased from Calbiochem (EMD Chemicals). 3-methacryloxypropyl tris(trimethylsiloxy)silane (MPTS) was purchased from Fluka.

2.2.2 Cell Culture and Transfection :

RBL-2H3 cells were maintained in monolayer cultures and harvested with trypsin-EDTA (Invitrogen) 3–5 days after passage, as described previously (30). For internalization experiments by measuring IgE acidification, cells were sensitized for 1 h at 37°C with FITC-IgE prior to fluorescence measurements, and excess IgE was removed by three consecutive steps of centrifugation and resuspension in buffered saline solution (BSS: 135 mM NaCl, 5.0 mM KCl, 1.8 mM $CaCl_2$, 1.0 mM $MgCl_2$, 5.6 mM glucose and 20 mM Hepes, pH 7.4). In other experiments, cells were sensitized overnight with unlabeled or Alexa 488-labeled IgE. In experiments involving chemical inhibitors, cells were incubated with specified agents at 37°C for 2-5 min before and during the time of the measurement. Cells were transfected with specified EGFP constructs in a Gene Pulser Xcell electroporator system (Bio-Rad) as follows: Cells (10^7/ml) resuspended in buffer [137 mM NaCl, 2.7 mM KCl, 1 mM $MgCl_2$, 5.6 mM glucose, 20 mM Hepes (pH 7.4)] were electroporated in the presence of ~25 μg/mL of the appropriate DNA construct in a 4-mm cuvette with an exponential pulse of 280 V from a 950 μF capacitor. After electroporation, cells were cultured in medium for 24 h. Chemical transfection was carried out by mixing 2 μg DNA construct with 8 μL Fugene-HD (Promega) in 100μL Opti-MEM (Life Technologies), and this mixture was added to plated cells in 1 mL Opti-MEM in a MatTek culture dish. After 1 h incubation, phorbol dibutyrate (0.1 μg/mL) was added to the cells for an additional 3 h, then cells were washed into medium for overnight incubation.

2.2.3 Flow cytometry sample preparation:

RBL-2H3 cells were harvested, suspended in medium at a concentration of 5 x 10^6 cells/mL, then sensitized with 4 μg/mL Alexa 488-IgE for 1 h at 37°C. They were then washed by sedimentation and resuspension in BSS containing BSA (1mg/mL; BSS-BSA). Cells were treated with specified drugs for 2 min at 37°C prior to incubation with antigen for 20 min at 37°C. Samples were then chilled on ice, followed by addition of 5 μg/mL rabbit anti Alexa 488 IgG and 25 μg/mL human IgG (to block non-specific binding to Fcγ receptors) in BSS-BSA for 30 min at 4°C. After washing by centrifugation at 4°C, cells were incubated with 10 μg/mL Alexa 647-conjugated goat anti rabbit IgG and 25 μg/mL human IgG for 30 min at 4°C. Cells were then washed, and fixed with 4% paraformaldehyde and 0.1% glutaraldehyde for 10 min at room temperature, followed by washing with PBS containing BSA (10 mg/mL) and storage in PBS-BSA (1mg/mL) with 0.01% sodium azide at 4°C. Fluorescent antibody labeling of the cells was measured by flow cytometry (BD Biosciences LSR II) using the 488nm argon and 633 nm HeNe lasers, and >50,000 cells per sample were evaluated in each experiment. Control samples with only Alexa488-IgE or Alexa647-IgE were used to determine the settings to eliminate crosstalk between green and far red channels. The percentage of surface-accessible IgE was calculated by normalizing far red (Alexa 647 or Cy5) fluorescence for each sample by the far red fluorescence value obtained for the cells that were not treated with antigen in each experiment. The same samples prepared for flow cytometry were imaged by confocal microscopy, as described below.

2.2.4 Microfabrication of patterned ligands by polymer lift-off.

Surfaces of silicon wafers were patterned with 1.5 to 4 μm features that were functionalized with supported lipid bilayers containing 2,4-dinitrophenyl (DNP) ligands as

described previously (33, 34). In brief, small unilamellar vesicles were prepared by sonication. The lipid composition was 10 mol% DNP-cap-PE and 90 mol% POPC. For control experiments, DNP-cap-PE was not included in the samples. 10 μL of the vesicle suspension (1 mM lipids) was added to an 8 by 8 mm patterned parylene substrate at room temperature for 10 min. The samples were rinsed thoroughly with filtered water, and parylene was mechanically peeled away in solution to yield the patterned lipid bilayers. These functionalized surfaces were incubated with IgE-sensitized RBL cells as described below. In some experiments, Alexa 488-IgE was used to mark IgE-FcεRI that clustered over the liganded features.

In some experiments the surfaces were patterned with Cy3-conjugated DNP_{22}-BSA. These were prepared by functionalizing the patterned parylene with 3-methacryloxypropyl tris(trimethylsiloxy)silane (MPTS), followed by washing with ethanol and incubation with protein crosslinker, N-[γ-maleimidobutyryloxy] succinimide (GMBS), for 1 h at room temperature to generate amine reacting groups. The surfaces are then washed with PBS and incubated with 50 μg/mL DNP_{22}-BSA for 1 hour at room temperature, followed by rinsing with PBS before peeling off the parylene (35).

2.2.5 Confocal Fluorescence Microscopy

Suspended cell samples were imaged in a Zeiss LSM 710 inverted microscope with a motorized stage using a 63x Oil Plan-Apochromat lens. Both a 488 nm laser and a 633 nm laser were used for excitation of fluorophores. The images were collected sequentially in green and red channels. In separate experiments to study colocalization of dynamin 2-GFP with A647-IgE, the cells were plated overnight on a MatTek dish at a concentration of 0.2×10^6 cells/dish, transfected the following day, and incubated overnight before sensitization with 2 μg/mL with Alexa 647-IgE at room temperature. They were then treated with rabbit anti-IgE serum (1:200

dilution) for 15 min at 37°C in presence or absence of cytochalasin D, fixed with 4% paraformaldehyde for 20 minutes at room temperature, and then stored in PBS at 4°C. Pearson's correlation coefficients were calculated for each of the samples using a Matlab code[2] (also described elsewhere (36)). The equation used to calculate Pearson's crosscorrelation coefficient is:

$$\rho = \frac{\sum(x_i - x)(y_i - y)}{\sqrt{\sum(x_i - x)^2 \sum(y_i - y)^2}}$$

Where, x_i and y_i are the pixel intensity values for green and red channel, respectively, and x, y are the average values of x_i and y_i in the image. A mask is drawn around the cell of interest using a Matlab script, and ρ values are calculated for each individual cell. Statistical analyses were carried out by calculating the p values using Student's t-test, and a value of $p \leq 0.05$ was considered to be statistically significant.

For experiments involving patterned surfaces, cells ($0.5x10^6$/ml) suspended in BSS-BSA were added to the functionalized silicon substrate (8 × 8 mm) in the center of a 35-mm Petri dish with coverglass bottom (0.16–0.19 mm; MatTek). After the specified incubation time at 37°C, cells were fixed with 3.7% formaldehyde in PBS for 10 min followed by quenching with 10 mg/ml BSA in PBS. For immunofluorescence after fixation, cells were labeled with primary antibody at room temperature for 1 h in PBS-BSA (1 mg/mL) containing 0.1% Triton-X. After washing, the Alexa 568-labeled secondary antibody was added to samples at room temperature for 1 h in continued presence of 0.1% Triton-X. 2mL of PBS was added into the dish before inverting the silicon chip for imaging. Cells were imaged in a Bio-Rad-MRC600-confocal head coupled with a Zeiss Axiovert 10 inverted microscope. A 522/DF35 filter set was used for

[22] The Matlab code used for image analysis and calculation of Pearson's coefficient was written by Dr. Christopher V Kelly

simultaneous or sequential dual-color image acquisition with an oil-immersion 63x/1.4NA objective. Cells scored as positive showed fluorescent patterns that matched the patterned substrate with intensity in the overlapping patches at least three times greater than the background level.

2.2.6 Knock-down of proteins with siRNA

siRNA was electroporated into cells using the same conditions as those described above for DNA transfection. For optimal knock down, siRNA concentrations and the number of electroporations were varied depending on the siRNA used. For clathrin knock-down two different siRNAs with sequences, UAAUCCGAUUCGAAGACCAAU and AAUGGAUCUCUCUGAAUACGG, were pooled and delivered into the cells with three successive electroporations of 1μM siRNA every 24 h. Experiments were performed 24 h after the final electroporation. For simultaneous knock-down of cortactin and its homolog, HS1, siRNA for cortactin with sequence CCGAGAGAGCUCAGCGGAU and for HS1 with sequence UAGAAGAGCCAGUGUACGA (both from ON-TARGETplus, Dharmacon) were pooled and delivered into the cells with two consecutive electroporations of 2.5 μM siRNA separated by 24 h. Experiments with these cells were carried out 24 h after the final electroporation. The sequence used for dynamin 2 knock-down was GACAUGAUCCUGCAGUUUA, and optimal knock-down was achieved by two consecutive electroporations of 1.5 μM siRNA separated by a 24 h interval. Experiments were performed 48 h after the final electroporation. An siRNA with the sequence UUAACCUUACCGAGGGUCGAA was used as a control in all experiments. Protein knock-down was confirmed by immunoblotting with appropriate antibodies.

2.2.7 Immunoblotting

Whole-cell lysates were prepared on ice by suspending cells (~$3.5x10^5$/mL) in lysis buffer [5 mM *N*-ethylmaleimide, 5 mM EDTA, 0.5% (vol/vol) Triton X-100, 50 mM NaCl, 50 mM Tris, 1X Halt Protease Inhibitor Cocktail (Pierce, Thermo Fisher) and 1X Halt Phosphatase Inhibitor Cocktail (Pierce, Thermo Fisher), pH 7.6]. Lysates were centrifuged at 15,000 x g for 10 min at 4°C. The supernatant was mixed with 5X Tris-glycine SDS buffer (Pierce, Thermo Fisher) and boiled for 5 min. Samples were resolved on a 12% Tris-glycine polyacrylamide gels and transferred to an Immobilon-P membrane with a pore size of 0.45 μm (Millipore) by semidry transfer. Immunoblots were visualized with Enhanced Chemiluminescence after probing with specified antibodies as described previously (37).

2.2.8 FITC-IgE acidification assay

For each experiment, 1.8 mL of FITC-IgE-labeled cells (10^6/mL) were placed in a 10x10x40 mm acrylic cuvette and stirred continuously in a thermostatic sample chamber at 37°C. Cells were equilibrated for 5 min in the chamber at 37°C before being stimulated with 500 ng/mL DNP-BSA or 1:200 dilution of rabbit anti-IgE serum. In some experiments, inhibitors were added prior to the stimulation, and cells were equilibrated for 5 min at 37°C. Samples with added inhibitors were compared to a control sample measured on the same day. Fluorescence measurements were made with an SLM 8000 fluorescence spectrofluorometer operated in ratio mode. FITC was excited at 490 nm, and emission was monitored at 520 nm. When the cells are stimulated with DNP-BSA, fluorescence quenching of FITC-IgE occurs in two phases, the first phase (~ 120 sec) is due to rapid occupancy of DNP in IgE binding sites proximal to FITC (38). The second slower phase is due to acidification of endosomes containing crosslinked, internalized FITC-IgE (Figure 2.1A; (39)). Only the slower phase of the fluorescence quenching

currve, corresponding to endosomal acidification, is observed with stimulation by anti-IgE. The percentage quenching due to acidification was calculated with Eqn 1:

$$\% \text{ quenching} = [(F(i) - F(f))/(F(i) - F(b))] \times 100$$

F(i) is the steady-state FITC fluorescence prior to the slow phase quenching due to endosomal acidification: For stimulation by anti-IgE this corresponds to fluorescence just after its addition; for stimulation by DNP-BSA this corresponds to fluorescence after the rapid binding/quenching phase (~120 sec after addition). F(f) is the FITC fluorescence 20 minutes after the addition of DNP-BSA/anti-IgE. F(b) is the background fluorescence, measured in cells not sensitized with FITC-IgE (typically 2-3% of FITC intensity).

2.2.9 Measurements of FITC-IgE fluorescence sensitivity to extracellular pH

RBL-2H3 cells were harvested and sensitized with FITC-IgE as described above, then washed and stimulated with anti-IgE for 20 min at 37°C in presence or absence of specified drugs. After chilling on ice for 5 min, each sample was divided in two parts and pelleted via centrifugation at 4°C. One aliquot was resuspended in BSS-MES-BSA (BSS with 20mM 2-(N-morpholino) ethanesulfonic acid, pH 5.5, replacing HEPES; 1 mg/mL BSA) at 4°C, and the other aliquot was resuspended in BSS-BSA at pH 7.4. These samples (10^6 cells/mL) were warmed to 37°C just before measuring in the fluorescence spectrofluorometer operated at settings similar to those described for the FITC-IgE acidification assay. The fluorescence was measured for > 100 sec for each sample. For samples at pH 5.5, a small amount of NaOH (1M) was then added to the cuvette to raise the pH to 7.4, and fluorescence was again measured. After these fluorescence measurements, 0.1% Triton-X was added to all samples, and this resulting fluorescence was used for normalization. Error bars were calculated from the data obtained for at least 3 individual experiments.

Results:

2.3.1 FITC-IgE acidification assay in combination with flow cytometry to evaluate internalization

Crosslinking of FITC-IgE bound to FcεRI on the surface of RBL-2H3 cells by antigen or anti-IgE leads to clustering of these receptor complexes that is followed by their internalization into endosomes (40, 41), which become acidified by vacuolar pumps as they mature into lysosomes (42). As we have characterized previously, the fluorescence of FITC-labeled IgE is quenched by DNP occupancy of the IgE binding site (38, 39) and by a decrease in pH due to endosomal acidification after FITC-IgE internalization (43). When FITC-IgE on surface of cells is crosslinked with DNP_{22}-BSA, a biphasic change in fluorescence occurs. The first phase comprises rapid quenching of fluorescence due to the binding of DNP_{22}-BSA to FITC-IgE (38, 39) and lasts about ~ 120 seconds (Figure 2.1 A). This is followed by a slower quenching of FITC fluorescence, due to the acidification of endosomes. The magnitude of the slower phase of FITC fluorescence quenching is calculated using Eqn 1 and is inhibited in presence of 100 nM bafilomycin, which is an inhibitor of vacuolar proton pumps (Figure 2.1B). When the cells are treated with anti-IgE, only the slower fluorescence quenching due to endosomal acidification is observed, and this is inhibited upon pre-treatment with 100 nM bafilomycin (Figure 2.1 A). We quantify the extent of acidification by calculating the percentage quenching of FITC-IgE fluorescence after 20 minutes of crosslinking by addition of DNP_{22}-BSA or anti-IgE and find ~40% quenching of FITC-IgE fluorescence due to endosomal acidification (Figure 2.1B). In presence of bafilomycin, we see minimal (<5%) decrease in FITC-IgE fluorescence beyond that caused by DNP binding.

In addition to this endosomal acidification-based assay, we also employed a method to monitor the accessibility of IgE-FcεRI to labeling antibodies. Cells sensitized with A488-IgE were treated, or not, with DNP_{22}-BSA then incubated with anti-Alexa 488 primary antibody and a Cy5 or A647-labeled secondary antibody. The far-red (Cy5 or A647) fluorescence is an indicator of the amount of surface-accessible A488-IgE. We can qualitatively assess localization of crosslinked IgE by confocal imaging of these samples. The images in Figure (2.2A) show that, in absence of antigen, most of the A488-IgE (green channel) is on the plasma membrane and is labeled by Cy5/anti-Alexa 488 Ab (red channel). Note that binding of anti-Alexa 488 rabbit IgG substantially quenches the Alexa 488 fluorescence. In the cells incubated with DNP_{22}-BSA at 37°C for 20 minutes, majority of A488-IgE clusters appear to be inside the cells, and therefore not labeled by Cy5/anti-Alexa 488. The amount of surface accessible A488-IgE is quantitatively measured on a flow cytometer, where monitoring the far red fluorescence (Figure 2.2B) shows that the amount of surface accessible IgE in cells incubated with DNP_{22}-BSA at 37°C is significantly less (~65%) than samples in which cells are not treated with DNP_{22}-BSA or are treated with DNP_{22}-BSA at 4°C, where, in both cases, internalization is minimalWe also observe that 100 nM bafilomycin pretreatment does not inhibit the loss of surface accessiblity of IgE receptor upon antigen treatment, as measured by flow cytometry. This result verifies the validity of this assay for quantitative assessment of the extent of surface accessibility of IgE in a manner that does not depend on the acidification of IgE containing endosomes.

IgE-FcεRI crosslinked with anti-IgE or DNP_{22}-BSA can be in different states, as depicted in Figure 2.3A. Crosslinked IgE-FcεRI complexes can be on the surface and labeled by the anti-Alexa-488 antibody, and this is detectable by flow cytometry, as illustrated for state I in Figure 2.3A. However, if crosslinked complexes are in membrane invaginations that are not cleaved

Figure 2.1 FITC-IgE acidification assay determines the extent of acidification of IgE containing endosomes: A) RBL-2H3 cells, sensitized with FITC-IgE and suspended at 10^6 cells/mL at 37°C, were treated with 1:200 dilution of rabbit anti-IgE serum or 500 ng/mL DNP_{22}-BSA (antigen). As shown in this representative experiment, FITC fluorescence of the samples was monitored on a fluorimeter for 20 minutes after the addition of anti-IgE serum or antigen. B) The extent of acidification was quantified with Eqn 1 by calculating the percentage of FITC fluorescence quenching in 20 minutes starting from 120 seconds after the addition of anti-IgE or DNP_{22}-BSA. Error bars represent the SEM for 3 individual fluorescence quenching experients.

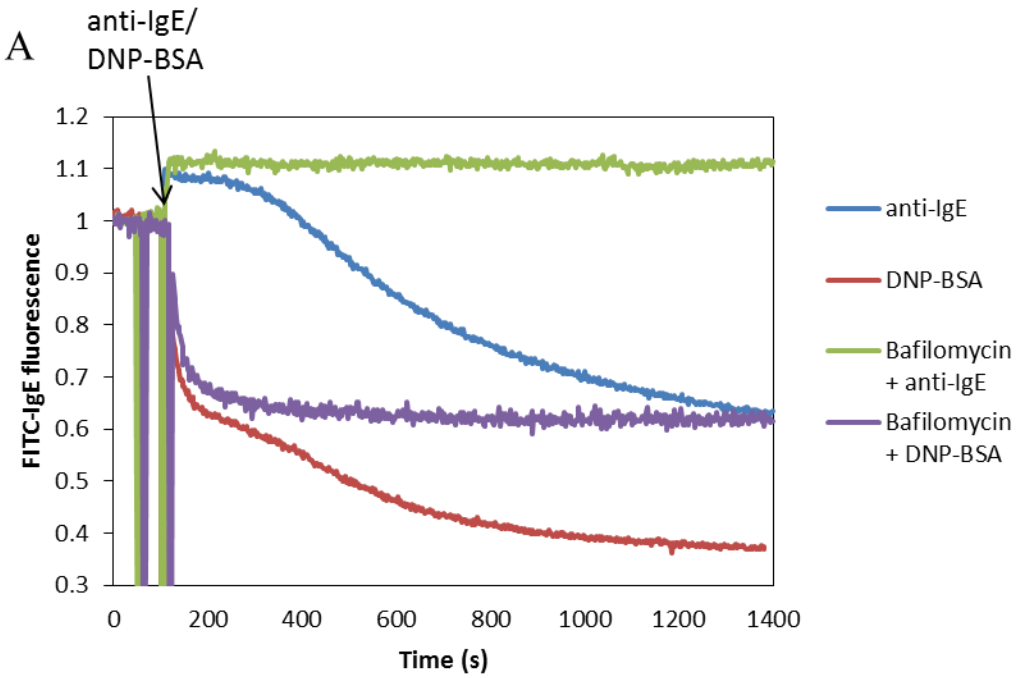
A
anti-IgE/
DNP-BSA
1.2
1.1
1
0.9
0.8
0.7
0.6
0.5
0.4
0.3
FITC-IgE fluorescence
0
200
400
600
800
1000
1200
1400
Time (s)
anti-IgE
DNP-BSA
Bafilomycin
+ anti-IgE
Bafilomycin
+ DNP-BSA

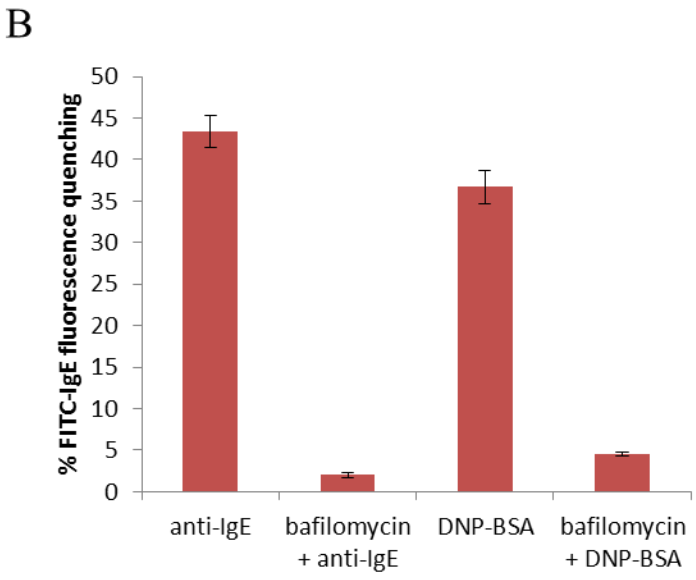
B
% FITC-IgE fluorescence quenching
50
45
40
35
30
25
20
15
10
5
0
anti-IgE
bafilomycin
+ anti-IgE
DNP-BSA
bafilomycin
+ DNP-BSA

Figure 2.2 Confocal imaging and flow cytometry for quantification of surface accessible IgE: A) RBL-2H3 cells, suspended in BSS-BSA at a concentration of 5 x 10^6 cells/mL, were sensitized with A488-IgE then incubated with or without antigen and labeled with anti–Alexa 488 primary antibody followed by washing and labeling with Cy5 labeled secondary antibody at 4°C (as described in Materials and Methods). The cells were then fixed, and two-color fluorescence images of the equatorial slice were taken by a confocal microscope (Scale bar 10μm). B) The amount of surface-accessible of A488-IgE is quantified using flow cytometry by measuring the far red fluorescence corresponding to A647 or Cy5 secondary antibodies bound to anti-Alexa 488 primary antibodies. Values are normalized such that 100% A488-IgE on surface is characterized from the 'no antigen' sample. Error bars represent SEM over 3 different experiments.

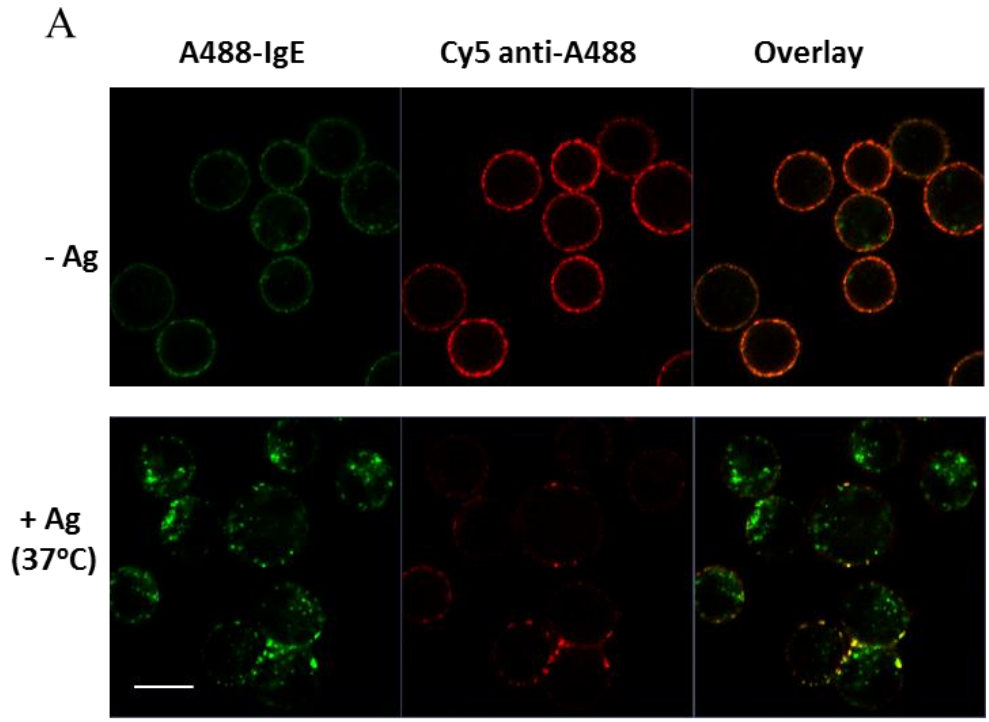
A
A488-IgE
Cy5 anti-A488
Overlay
- Ag
+ Ag
(37°C)

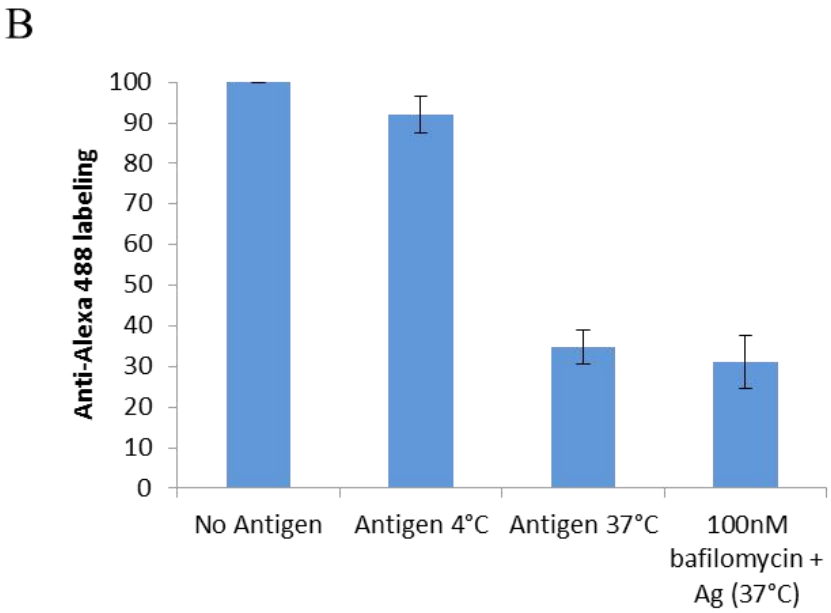
B
Anti-Alexa 488 labeling
100
90
80
70
60
50
40
30
20
10
0
No Antigen
Antigen 4°C
Antigen 37°C
100nM bafilomycin + Ag (37°C)

Figure 2.3: States of IgE bound to FcεRI before and after crosslinking: A) Cartoon represents the possible states of IgE: **(I)** IgE, present on the surface of the plasma membrane, can be labeled by fluorescent primary secondary antibodies without cell permeabilization. **(II)** IgE, present in membrane invaginations that are not cleaved from the surface of the plasma membrane, is not accessible to labeling by fluorescent primary and secondary antibodies. However, IgE in this location continues to experience extracellular pH levels. **(III)** IgE, present in endosomes that are cleaved from the plasma membrane, but not acidified. **(IV)** IgE, present in endosomes that are acidified, which results in quenching of FITC-IgE fluorescence. In these studies, we refer to IgE as being internalized after endosomes pinch off from the plasma membrane (states III or IV). **B)** Likely state(s) of crosslinked IgE under different experimental conditons, as determined from three independent and quantitative internalization assays.

A

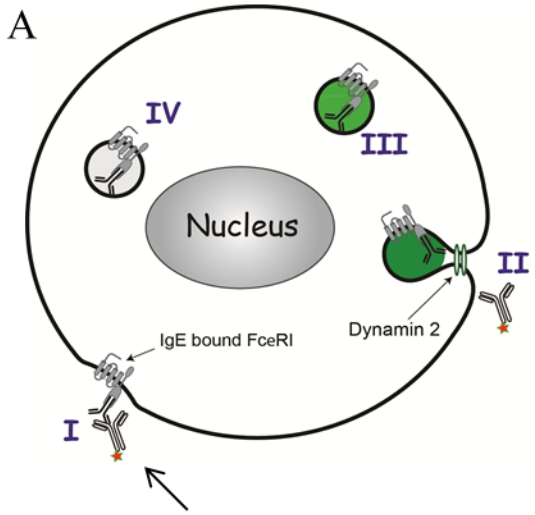

anti-Alexa 488 Ab labeling surface accessible IgE

B

	Flow Cytometry	FITC-IgE acidification	pH sensitivity	Likely State
Unstimulated	I	I,II,III	I,II	I
DNP_{22}-BSA/anti-IgE	II,III,IV	IV	IV	IV
MβCD pretreatment	II,III,IV	I,II,III	I,II	II
Cytochalasin-D	II,III,IV	I,II,III	I,II	II
Syk -/- cells	I	I,II,III	ND	I
PAO/quercetin	II,III,IV	I,II,III	I,II	II
Bafilomycin	II, III, IV	II,III,I	III	III
Dynamin-II KD	ND	I,II,III	ND	I,II,III

from the plasma membrane (State II), they may not be surface labeled by the anti-Alexa 488 antibody yet remain sensitive to the pH of the extracellular medium. Alternatively, internalized IgE may be in endosomes that are cleaved from plasma membrane but not acidified, as is the case with bafilomycin pretreatment (State III), in which case the fluorescence FITC-IgE will not be quenched. The FITC-IgE acidification assay detects internalization only after the IgE containing endosomes are pinched off and acidified (State IV). The possible states of crosslinked IgE receptors are depicted in the Figure 2.3A and summarized in in Figure 2.3B, where the possible conclusions from each individual assay used to assess state of IgE-FcεRI complexes after crosslinking are indicated. Out of the four possible states, the one state that is common in three different assays has been listed as the most probable state of FcεRI post aggregation in those conditions. The result listed under the column pH sensitivity indicates that in those conditions, crosslinked FITC-IgE is sensitive to changes in extracellular pH.

2.3.2 Internalization of crosslinked IgE-FcεRI is sensitive to the size of the clusters and to mild cholesterol reduction

Previously, we developed and characterized structurally rigid Y-shaped DNA ligands that are conjugated with dinitrophenyl (DNP) on each 5' end (Figure 2.4A). We used these ligands to probe the structural requirements of FcεRI signaling, and showed that some of these ligands stimulate robust degranulation responses (5). The level of stimulation varied with the spacing between DNP moieties in the trivalent ligand. In comparison, various studies using bivalent ligands have shown that they stimulate only very limited degranulation responses (28). These studies indicate that IgE-FcεRI signaling is regulated by the geometry, valency, and spacer length of the crosslinking ligands. We performed experiments using these structurally rigid DNP-conjugated Y-DNA ligands to probe the structural constraints of IgE-FcεRI complexes in

the process of IgE-FcεRI internalization. We found that 50 nM Y-16 DNP_3 caused maximal degranulation in presence of 2 μM cytochalasin D (~50%; data not shown), and somewhat weaker responses (~25%) in absence of cytochalasin D, consistent with previous observations (5). Treatment of FITC-IgE sensitized RBL-2H3 cells with 50 nM Y-16 DNP_3 caused minimal quenching of FITC-IgE fluorescence (<5%) subsequent to initial quenching due to binding (Figure 2.4 B,C). 50 nM Y-16 DNP_3 is sufficient to saturate IgE binding sites on the surface of mast cells, as additional Y-16 DNP_3 doesn't cause further quenching of FITC-IgE fluorescence (data not shown). Flow cytometry measurements showed that, in contrast to cells treated with multivalent antigen, 50 nM Y-16 DNP_3 causes only a slight reduction of A488-IgE at the cell surface 20 minutes after incubation with this ligand at 37°C (Figure 2.4D). These results indicate that IgE-FcεRI clusters formed by Y-16 DNP_3 are sufficient to stimulate degranulation but do not lead to internalization of IgE-FcεRI complexes.

Ordered membrane domains enriched in cholesterol and sphingolipids, have been strongly implicated in IgE receptor signaling (44). A previous study reported a decrease in the extent of IgE receptor endocytosis, assessed via flow cytometry, upon cholesterol reduction by 10 mM MβCD pretreatment for 30 min at 37°C (27). We found that, following cholesterol depletion with 4 mM MβCD for 20 min at 37°C, no quenching of FITC-IgE fluorescence due to acidification of the IgE containing endosomes could be detected (Figure 2.5A). In contrast, our flow cytometry data shows reduction in surface accessibility of A488-IgE after antigen treatment both with and without MβCD pretreatment (Figure 2.5D). These results do not distinguish whether, after cholesterol reduction, crosslinked IgE-FcεRI are retained in membrane invaginations that are not cleaved from the plasma membrane (State II, Figure 2.3A), or are in endosomes that are cleaved from plasma membrane but not acidified (State III, Figure 2.3A).

Figure 2.4: The trivalent ligand – Y-16DNP$_3$ does not lead to internalization of FcεRI receptor: A) A schematic of trivalent Y-DNP$_3$ ligands. The chains represent DNA strands where the 5' end of each DNA is conjugated to DNP via a flexible linker (adopted from (5)). B) RBL-2H3 cells sensitized with FITC-IgE are treated with Y-16DNP$_3$ or antigen. FITC fluorescence is measured on a fluorimeter, and the data plotted are from one representative experiment. C) Quantification of FITC-IgE acidification, carried out as described for Figure 2.1. D) The amount of surface-accessible A488-IgE before and after crosslinking with antigen or Y-16DNP$_3$ is analyzed and quantified using flow cytometry as described for Figure 2.2, the error bars for both the assays represent SEM over 3 individual experiments.

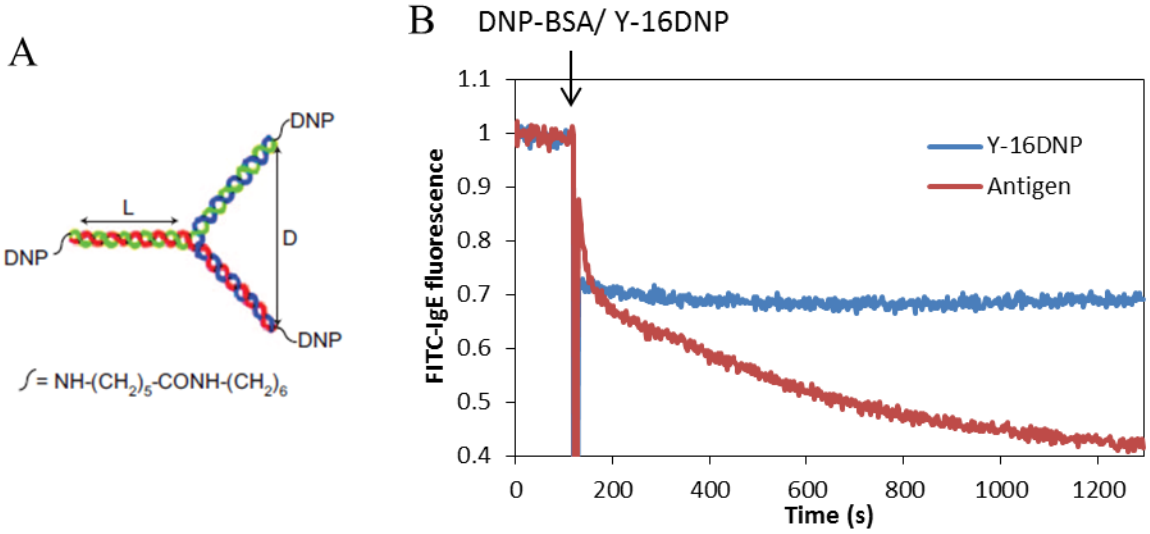
A
DNP
L
D
DNP
DNP
∫ = NH-(CH2)5-CONH-(CH2)6
B
DNP-BSA/ Y-16DNP
FITC-IgE fluorescence
Time (s)
Y-16DNP
Antigen

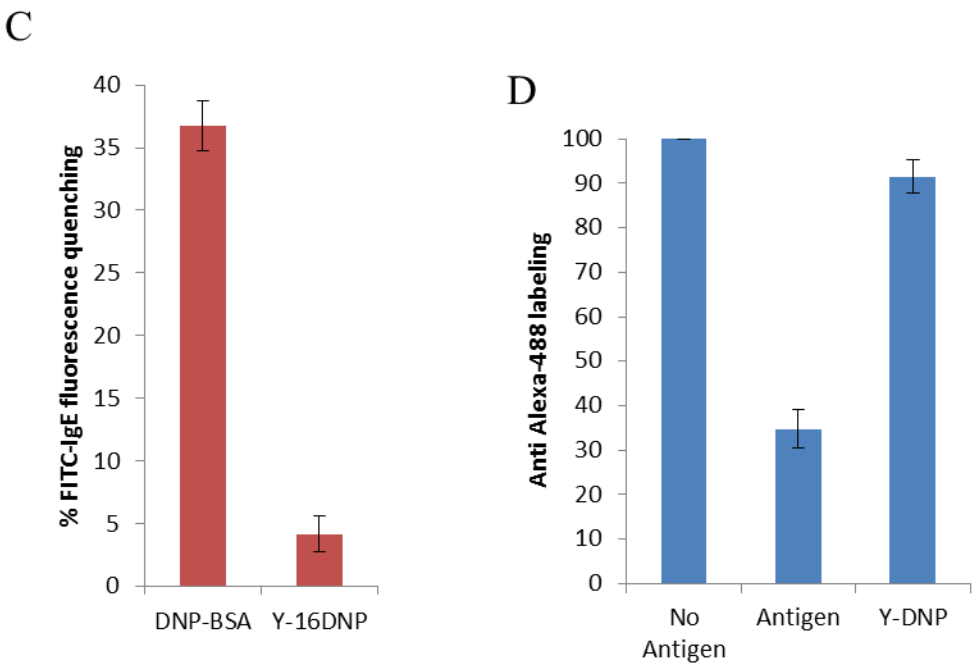
C
% FITC-IgE fluorescence quenching
DNP-BSA
Y-16DNP
D
Anti Alexa-488 labeling
No Antigen
Antigen
Y-DNP

Figure 2.5: Mild cholesterol reduction with MβCD inhibits FITC-IgE quenching, but not surface inaccessibility of IgE: A) RBL-2H3 cells are sensitized with FITC-IgE. Mild cholesterol reduction is performed by pretreatment of RBL-2H3 cells with 4 mM MβCD for 20 minutes at 37°C. Cells are subsequently treated with 1:200 dilution of rabbit anti-IgE serum, and FITC fluorescence is measured on a fluorimeter. The plot shows fluorescence levels from one representative experiment. B) Quantification of FITC-IgE acidification is performed, as described in Figure 2.1. C) The amount of surface-accessible A488-IgE before and after crosslinking with antigen in the presence or absence of MβCD treatment is quantified using flow cytometry as described for Figure 2.2. The error bars in B and C represent SEM over 3 individual experiments.

A

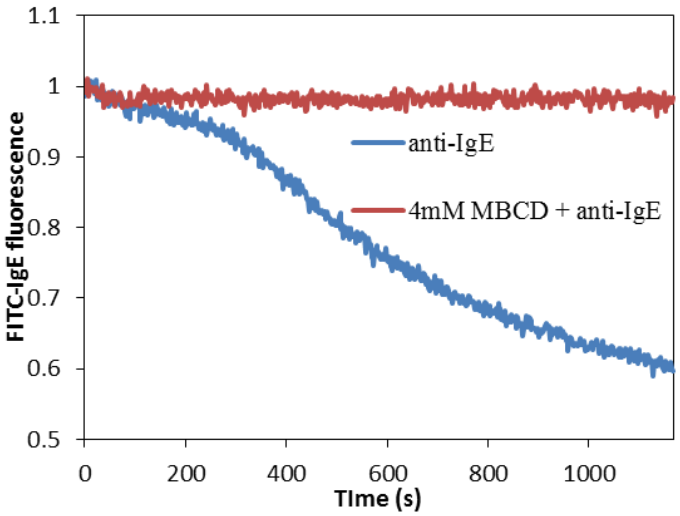
1.1
1
0.9
0.8
0.7
0.6
0.5
FITC-IgE fluorescence
0
200
400
600
800
1000
TIme (s)
anti-IgE
4mM MBCD + anti-IgE

B

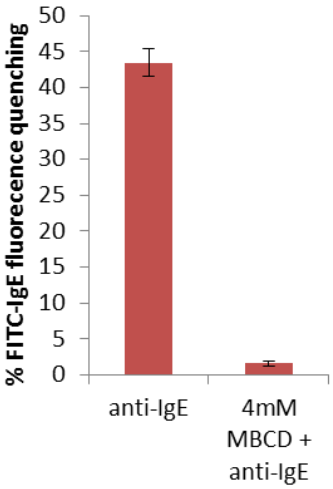
50
45
40
35
30
25
20
15
10
5
0
% FITC-IgE fluorecence quenching
anti-IgE
4mM MBCD + anti-IgE

C

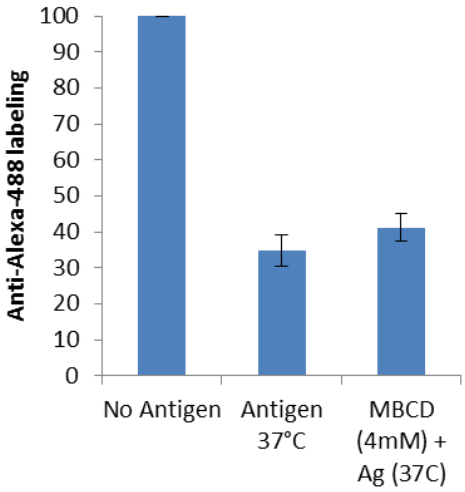
100
90
80
70
60
50
40
30
20
10
0
Anti-Alexa-488 labeling
No Antigen
Antigen 37°C
MBCD (4mM) + Ag (37C)

We designed an experimental scheme to distinguish the above two possibilities. For this purpose, we utilized the dependence of FITC fluorescence on pH to determine whether FITC-IgE retains sensitivity to pH changes in the extracellular environment, which we could vary (45, 46). RBL-2H3 cells sensitized with FITC-IgE were incubated with anti-IgE, with or without MβCD pretreatment, at pH 7.4 for 20 minutes at 37°C. The cells were chilled on ice, washed, and resuspended in MES-buffered BSS- BSA, pH 5.5. Fluorescence of the cells was measured by fluorimetry, before and after the pH was increased to 7.4, via addition of NaOH, followed by addition of 0.1% Triton-X. Raw data, along with the time points of various additions are shown in Figure 2.6A. The average fluorescence readings for multiple experiments, normalized to Triton-X100 values, are plotted in Figure 2.6B. The green bars show the fluorescence values of samples that were maintained at pH 7.4 throughout the experiment, and The lower fluorescence value for samples treated with anti-IgE is due to endosomal acidification, which is inhibited due to MβCD pretreatment. The blue bars represent the FITC fluorescence values at pH 5.5, and the red bars represent the FITC fluorescence values after the pH is increased to 7.4. These results indicate that crosslinked FITC-IgE in samples following mild cholesterol depletion are sensitive to changes in extracellular pH, and thus these IgE-containing endosomes are not cleaved from the plasma membrane. Thus, the results are consistent with the crosslinked IgE concentrating in membrane invaginations that are not pinched off from the plasma membrane following mild cholesterol reduction via MβCD pretreatment.

2.3.3 Syk is necessary for internalization of IgE receptors

Syk is a tyrosine kinase activated early in the signaling cascade of FcεRI following clustering and tyrosine phosphorylation of FcεRI (47). There have been contradicting reports for the role of Syk kinase in internalization of clustered IgE-FcεRI. For example, it was found that this

Figure 2.6 Upon mild cholesterol reduction, the majority of crosslinked IgE is sensitive to changes in extracellular environment: RBL-2H3 cells are sensitized with FITC-IgE and stimulated (or not) with anti-IgE for 20 minutes at 37°C prior to being chilled and resuspended in fresh buffer with indicated pH. Designated samples were treated with 4 mM MβCD for 20 minutes at 37°C prior to antigen addition. A) (left side) FITC fluorescence intensity of cell samples resuspended in BSS, pH 7.4, before and after addition of tritonX-100; (right side), cell samples resuspended in BSS at pH 5.5, which is then adjusted to pH 7.4 by addition of NaOH, before addition of triton-X. All fluorescence values are normalized to the values obtained after triton-X addition. B) Quantification of data for each sample is done by first normalizing all fluorescence values to that obtained after triton-X addition and then plotting the normalized fluorescence values for the samples subjected to different pH conditions, as represented in (A). Error bars represent the SEM over 3 different experiments.

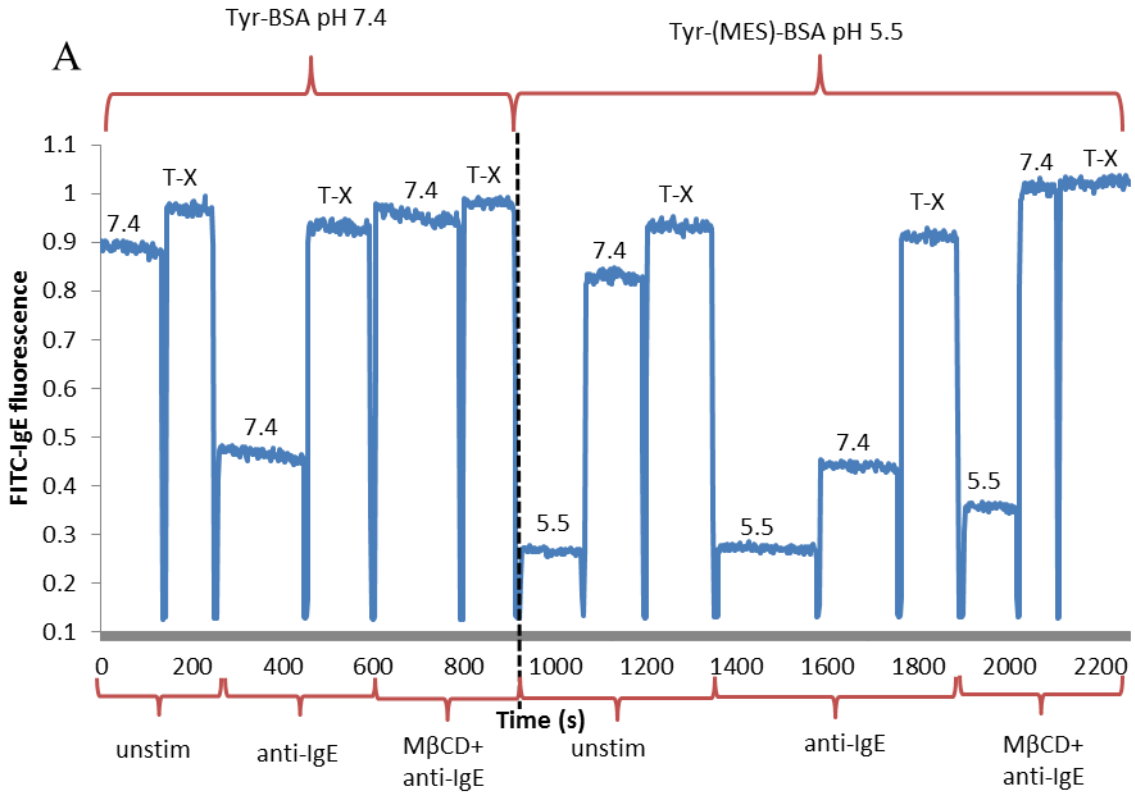
A
Tyr-BSA pH 7.4
Tyr-(MES)-BSA pH 5.5
FITC-IgE fluorescence
1.1
1
0.9
0.8
0.7
0.6
0.5
0.4
0.3
0.2
0.1
7.4
T-X
7.4
T-X
7.4
T-X
5.5
7.4
T-X
5.5
7.4
T-X
5.5
7.4
T-X
0
200
400
600
800
1000
1200
1400
1600
1800
2000
2200
Time (s)
unstim
anti-IgE
MβCD+ anti-IgE
unstim
anti-IgE
MβCD+ anti-IgE

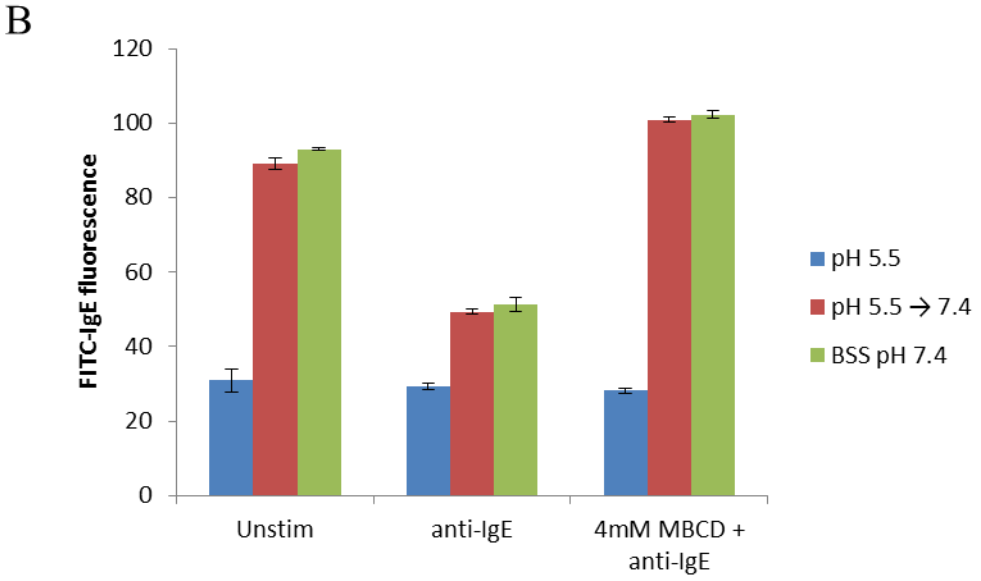
B
FITC-IgE fluorescence
120
100
80
60
40
20
0
Unstim
anti-IgE
4mM MBCD + anti-IgE
pH 5.5
pH 5.5 → 7.4
BSS pH 7.4

Figure 2.7 Syk -/- cells do not show internalization of IgE: A) RBL-2H3 cells or Syk -/- cells are sensitized with FITC-IgE before stimulation with 500 ng/mL antigen. FITC fluorescence is measured on a fluorimeter. Normalized FITC fluorescence is plotted for one representative experiment,120 seconds after the addition of antigen. B) Quantification of FITC-IgE acidification is performed as described in Figure 2.1. C) Flow cytometry analysis for quantification of surface accessible A488-IgE in RBL-2H3 and Syk -/- cells is performed as described in Figure 2.2. The error bars in B and C represent SEM over 3 individual experiments.

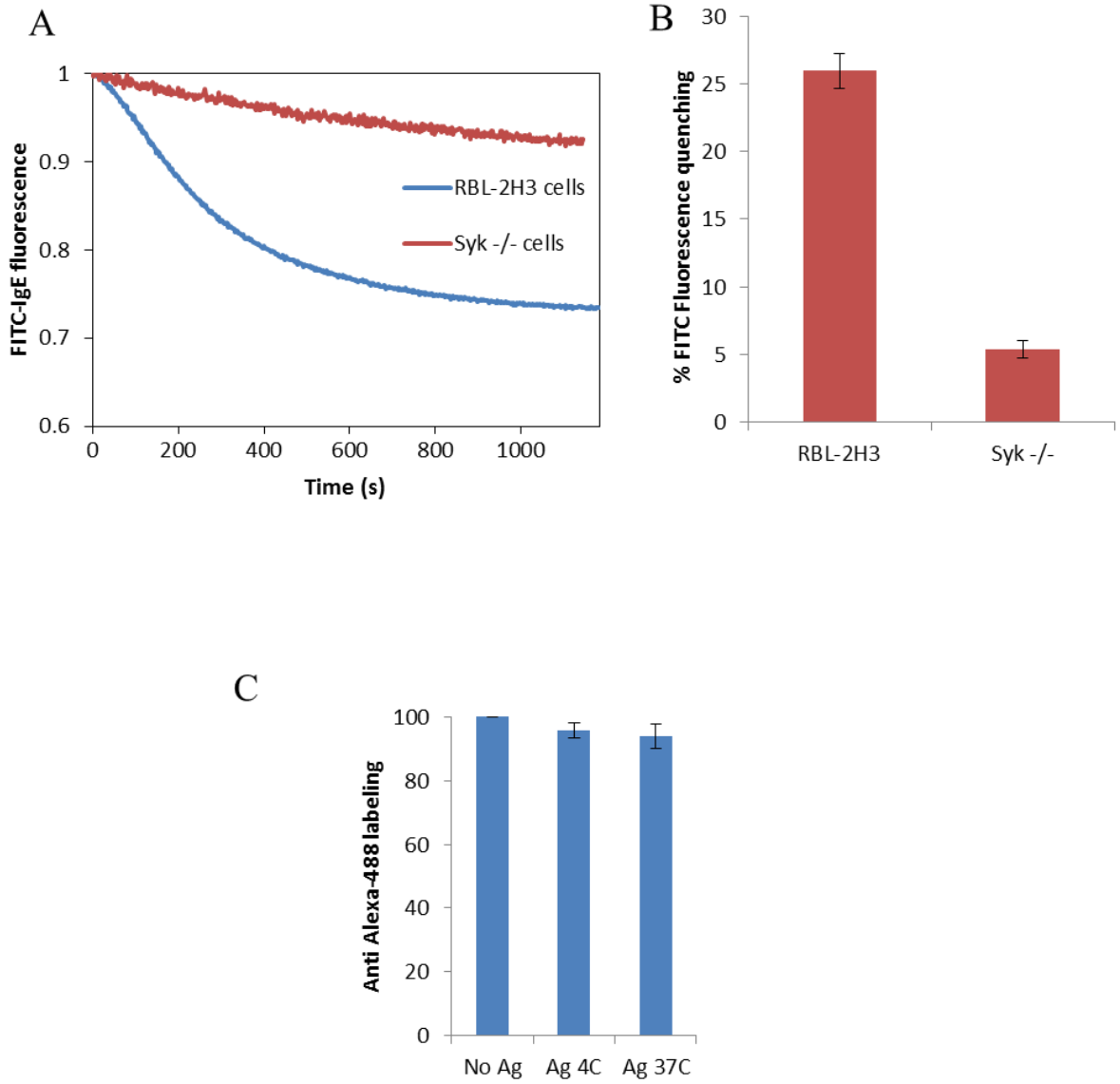
A
1
0.9
0.8
0.7
0.6
FITC-IgE fluorescence
0
200
400
600
800
1000
Time (s)
RBL-2H3 cells
Syk -/- cells
B
30
25
20
15
10
5
0
% FITC Fluorescence quenching
RBL-2H3
Syk -/-
C
100
80
60
40
20
0
Anti Alexa-488 labeling
No Ag
Ag 4C
Ag 37C

endocytosis of crosslinked IgE-FcεRI is reduced in Syk deficient cells as measured by flow cytometry (48), while others using similar cell lines report no effect on extent of IgE-FcεRI internalization and an enhanced rate of internalized receptor transport to lysosomes as measured via flow cytometry and confocal microscopy in fixed cells (13). We find that endocytosis of IgE receptors in Syk-/- cells (TB1A2 cell line, (49)) is substantially inhibited as detected by FITC-IgE acidification assay (Figure 2.7B). Consistent with this, our flow cytometry measurements show that most of the Alexa 488-IgE remains surface accessible upon binding by antigen at 37°C (Figure 2.7C). The presence of Syk appears to be essential for the signaling pathway leading to the internalization of activated FcεRI receptor at the cell surface.

2.3.4 F-actin cycling is important for pinching off of IgE-containing endosomes from the plasma membrane.

Inhibition of crosslink-dependent IgE receptor endocytosis by the inhibitor of actin polymerization, cytochalasin D, was first reported in 1989 (40). Using our acidification assay, we find that 2 μM cytochalasin D prevents crosslink-dependent acidification of IgE receptor complexes, as does another inhibitor of actin polymerization, latrunculin A at 1 μM (Figure 2.8A and B). This inhibition of acidification is dose dependent, such that cells treated with 0.25 μM cytochalasin D exhibited negligible inhibition of FITC-IgE acidification (data not shown).We also observed inhibition of internalization-dependent acidification by jasplakinolide, which stabilizes the actin cytoskeleton. These results indicate that dynamic cycling of F-actin is important for internalization-dependent acidification.

In contrast to effective inhibition of acidification, these agents did not prevent loss of surface accessibility of A488-IgE-FcεRI after crosslinking with antigen (Figure 2.9B). When the

Figure 2.8 Inhibition of F-actin cycling abolishes FITC-IgE quenching upon crosslinking: (A) RBL-2H3 cells sensitized with FITC-IgE and pretreated with 2 μM cytochalasin D or 1 μM latrunculin A for 2 minutes at 37°C, or with 3 μM jasplakinolide for 30 minutes at 37°C, prior to treatment with anti-IgE. FITC fluorescence was measured on a fluorimeter, the plot shows a representative experiment. (B) Quantification of FITC-IgE acidification data is performed as described in Figure 2.1. The error bar represents SEM over 3 individual experiments.

A

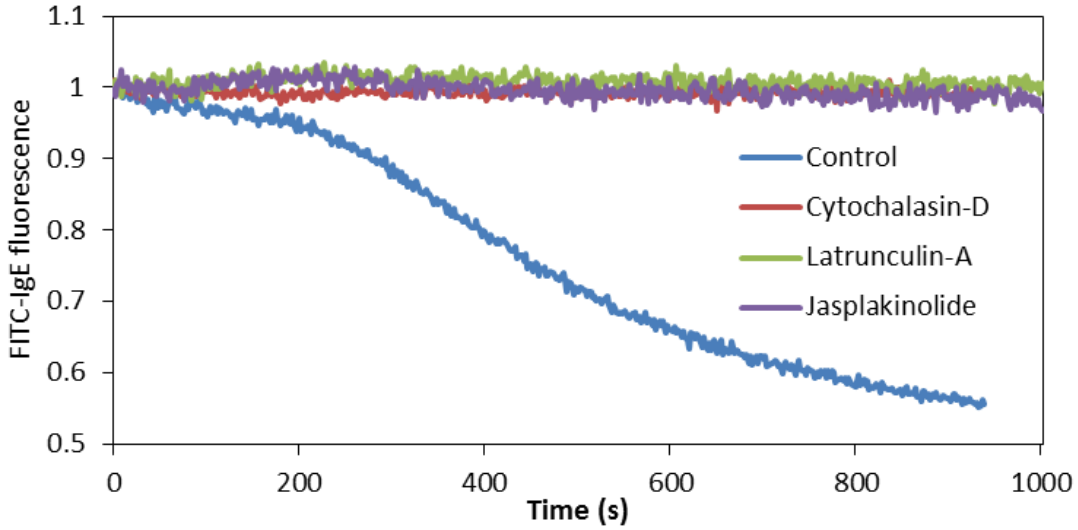
1.1
1
0.9
0.8
0.7
0.6
0.5
FITC-IgE fluorescence
0
200
400
600
800
1000
Time (s)
Control
Cytochalasin-D
Latrunculin-A
Jasplakinolide

B

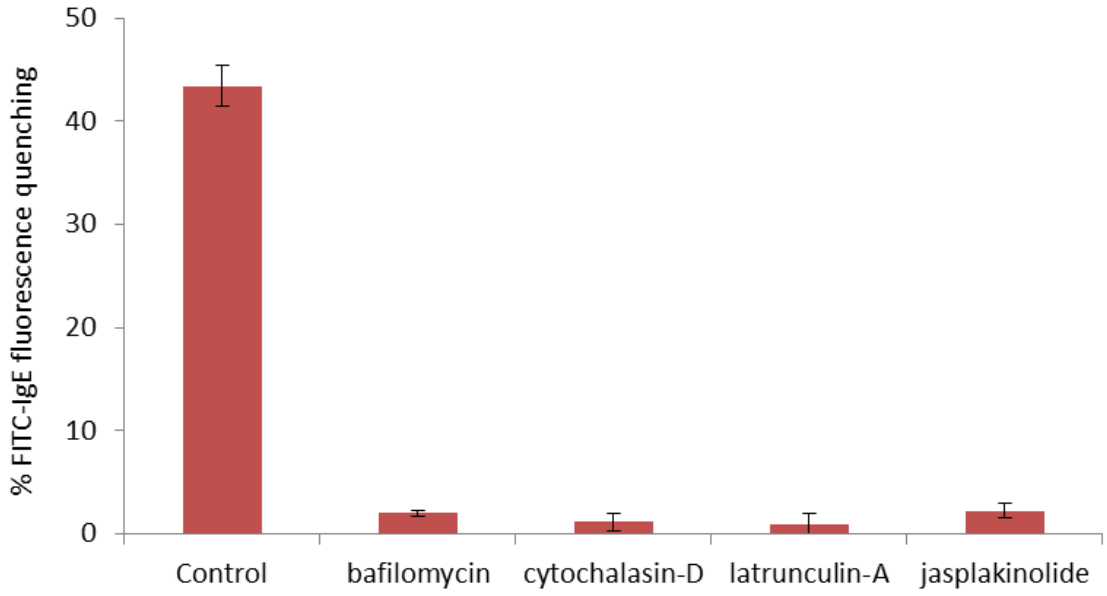
50
40
30
20
10
0
% FITC-IgE fluorescence quenching
Control
bafilomycin
cytochalasin-D
latrunculin-A
jasplakinolide

Figure 2.9 IgE becomes less surface-inaccessible upon treatment with antigen in presence or absence of F-actin cycling inhibitors: A) RBL-2H3, suspended in BSS (5 x 10^6/mL) are sensitized with A488-IgE. They are subsequently treated with 2 μM cytochalasin D (or not), followed by treatment with antigen for 20 minutes at 37°C (or not). The cells are subsequently chilled, labeled with anti-Alexa 488 primary, Cy5 or A647 tagged secondary antibody, and subsequently imaged on a confocal microscope. The top panel shows unstimulated cells, and the bottom panel shows cells treated with cytochalasin D followed by antigen (Scale bar 10μm). B) Quantification of surface accessible A488-IgE is performed as described in Figure 2.2. The error bars represent SEM from 3 individual experiments.

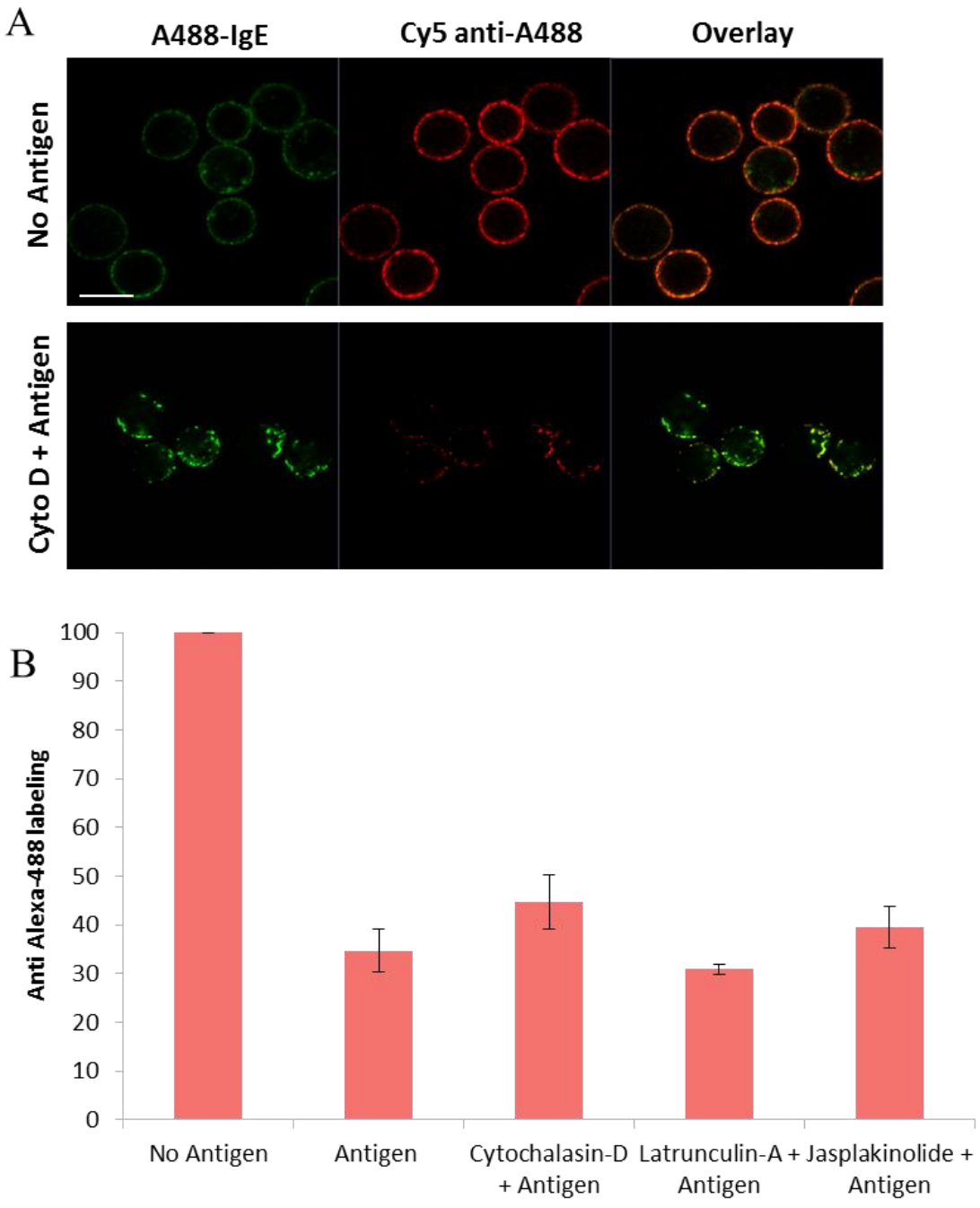
A
A488-IgE
Cy5 anti-A488
Overlay
No Antigen
Cyto D + Antigen
B
Anti Alexa-488 labeling
100
90
80
70
60
50
40
30
20
10
0
No Antigen
Antigen
Cytochalasin-D + Antigen
Latrunculin-A + Antigen
Jasplakinolide + Antigen

cells were visualized via confocal microscopy, we observed formation of IgE-containing endosomes due to antigen crosslinking that were not labeled by the primary (anti-Alexa488) and secondary antibodies (Figure 2.9A). Inhibition of acidification of FITC-IgE after crosslinking in presence of cytochalasin D is reversible.

To further investigate if the endosomes are pinched off from the plasma membrane after antigen treatment in presence of cytochalasin D, we utilized the dependence of fluorescence of crosslinked FITC-IgE on extracellular pH as described in Figure 2.6. Raw data for different samples, along with the time points of additions of reagents are shown in Figure 2.10A. The average fluorescence readings for each sample (normalized to values following 0.1% Triton-X100 treatment) are summarized in Figure 2.10B. These results indicate that crosslinked FITC-IgE in presence of cytochalasin D is sensitive to changes in extracellular pH. These results suggest that crosslinked IgE in the presence of cytochalasin D is not internalized, but becomes inaccessible to the surface labeling anti-Alexa 488 antibodies, as represented by State II in Figure 2.3A. In our experiments, we find that washing out cytochalasin D restores quenching of FITC-IgE fluorescence due to acidification (Figure 2.11A).

When we add 2 μM cytochalasin D to the cells containing acidified FITC-IgE after crosslinking, we find an increase in FITC fluorescence. This increase in FITC-IgE fluorescence may be explained by the increased exocytosis in suspended cells upon addition of inhibitors of F-actin polymerization. Consistent with this explanation, when a similar experiment is performed in absence of extracellular Ca^{2+}, this increase in fluorescence is inhibited. (Figure 2.11B).

Figure 2.10 F-actin inhibition prevents the cleaving of endosomes containing crosslinked IgE from the plasma membrane: Experiment and analysis were performed similarly from Figure 2.6. A) FITC-IgE sensitized RBL-2H3 cells were treated with the 2 μM cytochalasin D or not, prior to stimulation with 1:200 dilultion of rabbit anti-IgE serum. B) The bar graph represents the normalized fluorescence values of FITC-IgE, averaged over there different experiments. Error bar represents SEM over 3 individual experiments.

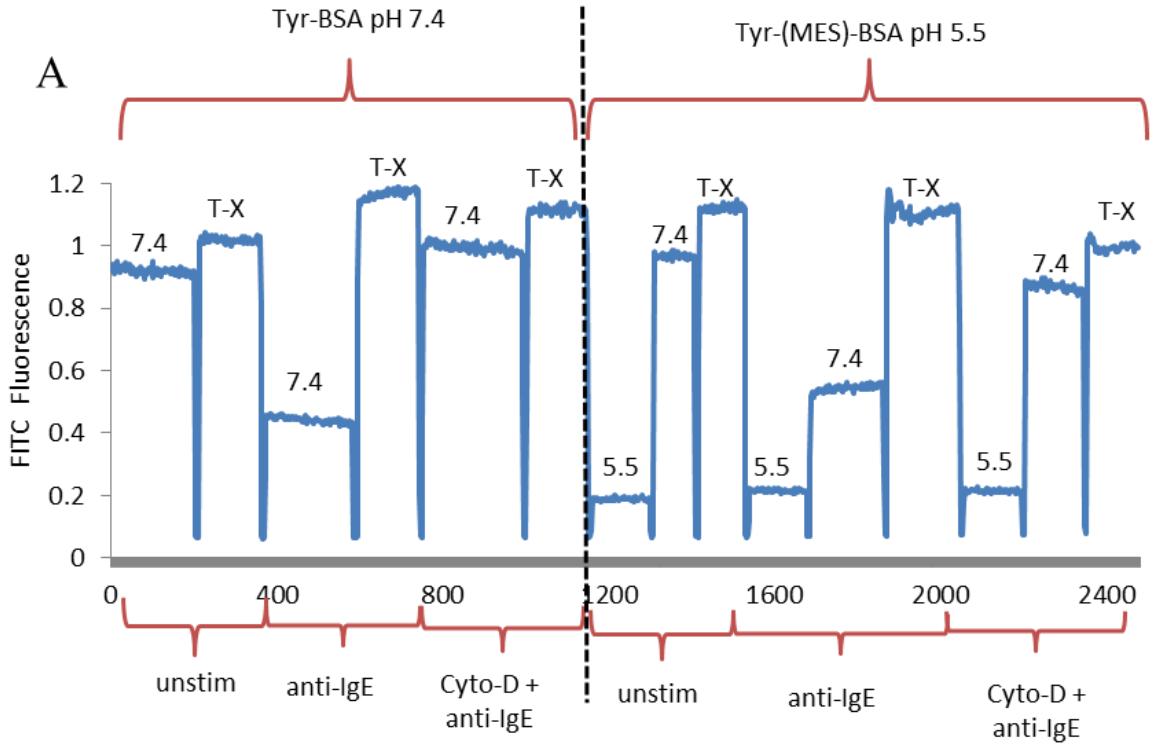
A
Tyr-BSA pH 7.4
Tyr-(MES)-BSA pH 5.5
FITC Fluorescence
1.2
1
0.8
0.6
0.4
0.2
0
7.4
T-X
7.4
T-X
7.4
T-X
5.5
7.4
T-X
5.5
7.4
T-X
5.5
7.4
T-X
0
400
800
1200
1600
2000
2400
unstim
anti-IgE
Cyto-D + anti-IgE
unstim
anti-IgE
Cyto-D + anti-IgE

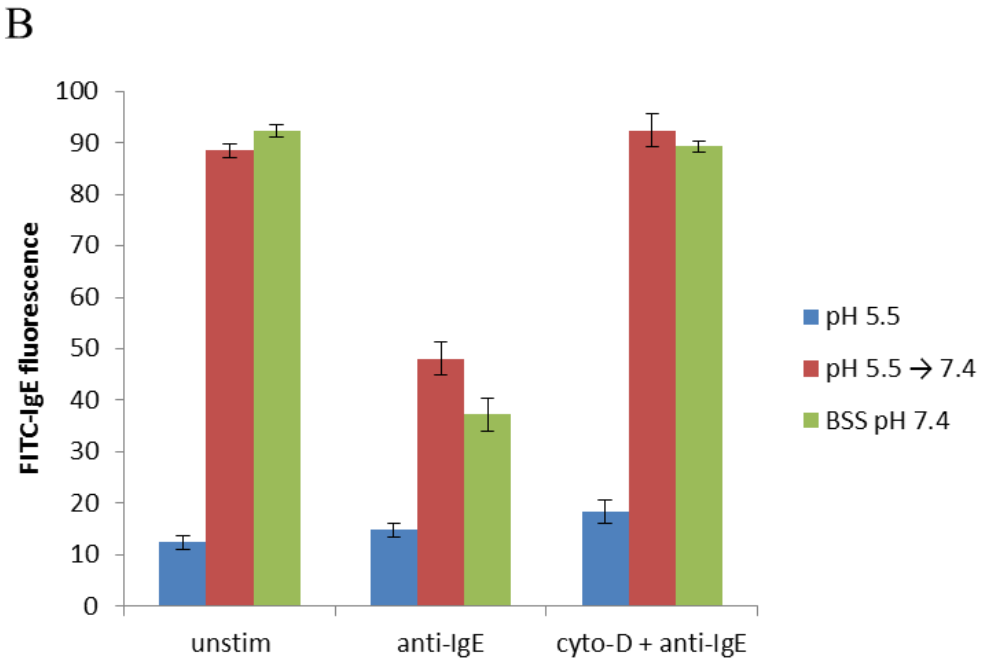
B
FITC-IgE fluorescence
100
90
80
70
60
50
40
30
20
10
0
unstim
anti-IgE
cyto-D + anti-IgE
pH 5.5
pH 5.5 → 7.4
BSS pH 7.4

Figure 2.11 Inhibition of FITC-IgE acidification by inhibition of F-actin cycling is reversible: A) RBL-2H3 cells sensitized with FITC-IgE and treated with 1:200 dilution of rabbit anti-IgE serum (or not) in the presence or absence of 2 μM cytochalasin D at 37°C. The cells are subsequently chilled on ice and centrifuged, and resuspended in BSS-BSA with or without cytochalasin D, and are allowed to incubate for 20 minutes at 37°C. Fluorescence is then measured on a fluorimeter and the values are normalized for each sample, based on the values obtained after adding 0.1% Triton-X. The error bar represents SEM over 3 invididual experiments. B) RBL-2H3 cells, sensitized with FITC-IgE are resuspended in BSS with or without calcium and treated with rabbit anti-IgE serum and fluorescence is measured. 2 μM Cytochalasin D is added to the cells 15 minutes after the addition of anti-IgE. 2 mM Calcium Chlroide was added to the cells suspended in BSS without extracellular calcium, 5 minutes after addition of cytochalasin D. The plot shows values from one representative experiment.

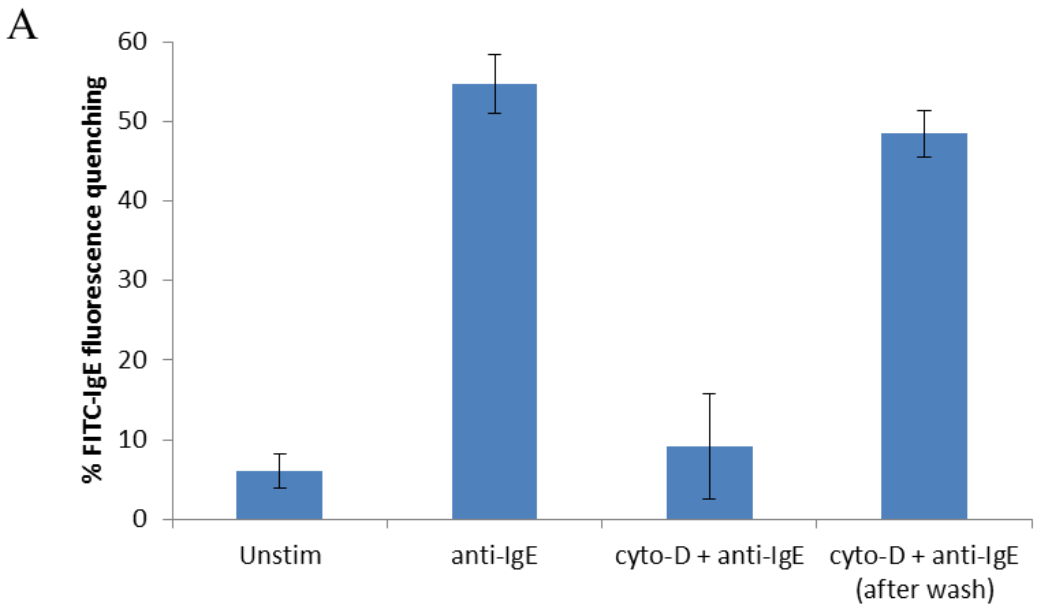
A
% FITC-IgE fluorescence quenching
60
50
40
30
20
10
0
Unstim
anti-IgE
cyto-D + anti-IgE
cyto-D + anti-IgE (after wash)

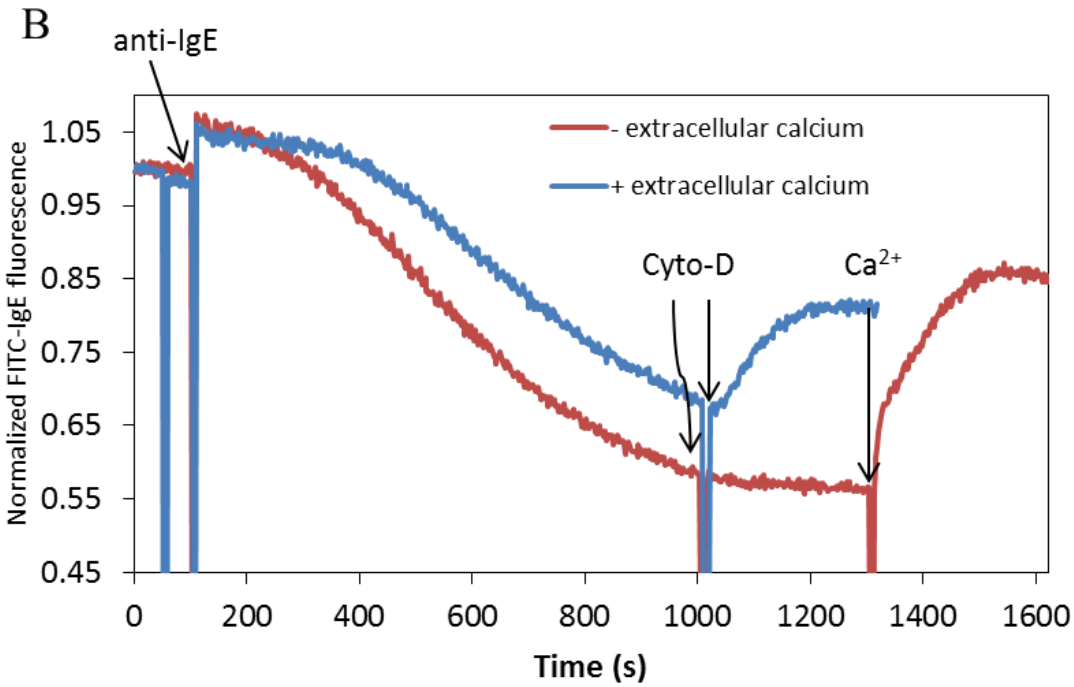
B
anti-IgE
- extracellular calcium
+ extracellular calcium
Cyto-D
Ca2+
Normalized FITC-IgE fluorescence
1.05
0.95
0.85
0.75
0.65
0.55
0.45
0
200
400
600
800
1000
1200
1400
1600
Time (s)

2.3.5 IgE receptor internalization exhibits partial dependence on dynamin 2:

IgE internalization after crosslinking has been found to be clathrin-independent in one study (12), whereas some electron microscopy studies found crosslinked IgE receptor colocalized with clathrin (17, 18). Previous reports in the literature describe the involvement of actin binding proteins, dynamin and cortactin, in clathrin-dependent and clathrin-independent endocytosis (50). To further probe the role of these proteins in the internalization of crosslinked IgE receptors, we employed siRNA to selectively knock down dynamin 2, clathrin heavy chain, cortactin, and the cortactin homolog HS1 (Hematopoietic lineage cell specific protein 1, also known as hematopoietic cell-specific Lyn substrate 1). As shown in Figure 2.12A, we detect >95% knock-down of dynamin 2, clathrin and HS1, and ~75% knock-down of cortactin, as detected by immunoblotting. Cortactin and HS1 were knocked down simultaneously because of the possible functional redundancy between these two closely related homologs (51). Dynamin 2 expression levels were detected by immunoblotting with an anti-dynamin 1 antibody that cross-reacts with dynamin 2. Given that no dynamin is detected under these conditions, it is likely that dynamin 2 is the principal isoform of dynamin expressed in these cells.

Knock-down of cortactin and HS1 or clathrin heavy chain did not cause a significant change in the internalization of antigen-crosslinked IgE receptor, as monitored by FITC-IgE fluorescence quenching due to endosomal acidification (Figure 2.12B). However, knock down of dynamin 2 caused ~ 25% inhibition of FITC-IgE quenching due to endosomal acidification in comparison with cells treated with control siRNA (Figure 2.12B). This result is consistent with a previously detected role of dynamin 2 in the internalization of FcεRI receptor (12). It is notable that > 95% knock down of dynamin 2 led to only a 25% difference in response of IgE internalization. There is a possibility that residual endogenous dynamin 2 after the dynamin 2

siRNA treatment can cause vesicle scission from the plasma membrane. An alternative explanation is that a substantial portion of IgE receptor endocytosis is dynamin 2-independent. Dynamin independent internalization pathways have been reported in literature (reviewed in (15)). As crosslink-dependent IgE receptor endocytosis depends on cholesterol, it is also possible that the mechanism of this process is different from the high membrane curvature required for dynamin-dependent pinching of endocytic vesicles.

2.3.6 Studies with patterned ligand surfaces reveal the role of dynamin in the organization of actin cytoskeleton at sites of IgE receptor clustering.

We previously described the use of micropatterned ligand arrays in combination with fluorescence microscopy to visualize the spatially defined recruitment of signaling components in the IgE receptor signaling cascade (Figure 2.13A) (37, 52). Because IgE-specific ligands are confined to the patterned surface, IgE receptor complexes are not internalized, and accumulation of other components remain stable for relatively long times (> 30 minutes). Utilizing micro-patterned, immobilized DNP-liganded bilayers, and incubating with IgE-sensitized RBL-2H3 cells, we found that dynamin 2 (detected by immunofluorescence) accumulates at the ligand patches (Figure 2.13B). Accumulation of dynamin 2 is maximal by ~30 min after incubation of cells (observed in >70% cells), and remains stable for at least 45 minutes. This time scale is similar to observed accumulation of actin, as we previously reported (53). Dynamin 2-EGFP and the dominant negative mutant Dynamin 2 K44A-EGFP also show recruitment to the clustered receptors (data not shown). Moreover, this selective recruitment of dynamin is not prevented by addition of 2 μM cytochalasin D, and is detected in >65% of imaged cells under these conditions (Figure 2.13B). This indicates that recruitment of dynamin 2 to activated IgE receptors does not depend on actin polymerization. Data adapted from (1).

Figure 2.12 IgE internalization can be independent on clathrin and cortactin, but dependent on Dynamin-2: A) RBL-2H3 cells transfected with control or dynamin 2 or clathrin or cortactin si RNA and western blotting samples were prepared with the appropriate antibodies from the cell lysates. B) Cells transiently transfected with control or dynamin 2, clathrin or cortactin siRNA prior to harvesting and sensitization with FITC-IgE. The cells were then stimulated with antigen, and fluorescence of FITC-IgE was recorded with a fluorimeter. The data plotted in the graphs shows the FITC-IgE fluorescence values 120 sec after the addition of antigen (Figure adopted from PhD Thesis, Alexis Torres). C) Quantification of the quenching of FITC-IgE fluorescence due to acidification was performed as described in Figure 2.1. The error bars represent SEM over 3 individual experiments. * represents $p<0.05$.

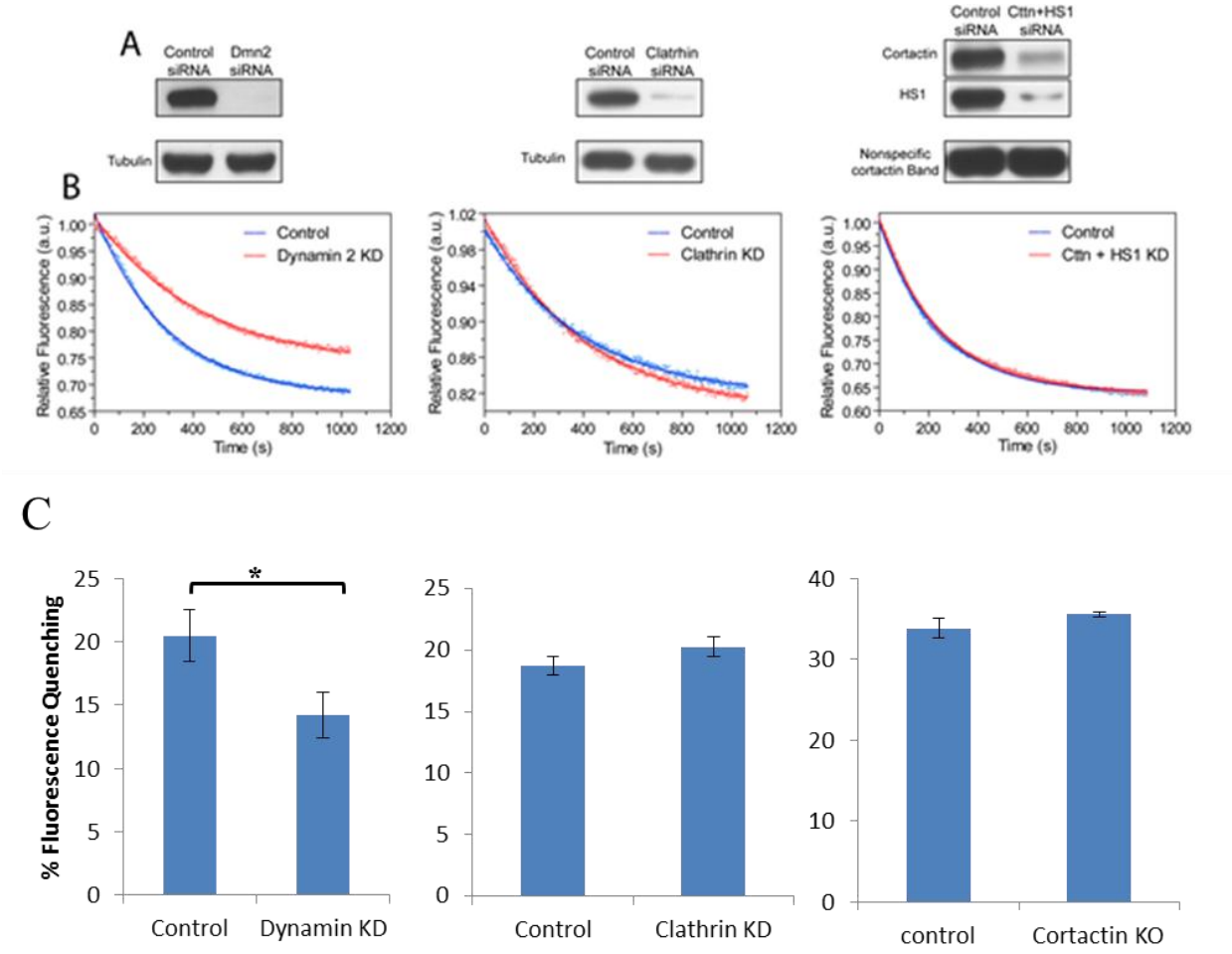
A
Control siRNA
Dmn2 siRNA
Tubulin
Control siRNA
Clatrhin siRNA
Tubulin
Control siRNA
Cttn+HS1 siRNA
Cortactin
HS1
Nonspecific cortactin Band
B
Relative Fluorescence (a.u.)
Time (s)
Control
Dynamin 2 KD
Control
Clathrin KD
Control
Cttn + HS1 KD
C
% Fluorescence Quenching
*
Control
Dynamin KD
Control
Clathrin KD
control
Cortactin KO

Figure 2.13 Dynamin 2 plays a role in recruitment of the actin cytoskeleton to micro-patterned ligand surfaces: A) A schematic showing the use of micro-patterned ligand surfaces to study the spatial recruitment of IgE signaling partners. B) RBL-2H3 cells sensitized with A488-IgE (green channel) are pretreated with 2 μM cytochalasin D or not, and plated onto micropatterned DNP containing lipid bilayers for 40 minutes at 37°C prior to fixation. Cells are subsequently immunolabeled with an anti-dynamin 2 and A568 tagged secondary antibody (red channel). Cells are scored as positive when the fluorescence on top of the antigen clusters is at least 3 times higher than the fluorescence on the cells away from the patterns. More than 70% of the cells were scored positive for the recruitment of dynamin 2 to the activated receptor complex ($n > 90$ cells for each sample). C) RBL-2H3 were transiently transfected with dynamin 2 siRNA or control siRNA, sensitized with A488-IgE, and plated onto micropatterned DNP containing lipid bilayers for 40 minutes at 37°C prior to fixation. Cells are subsequently immunolabeled with A568 phalloidin. D) A bar graph demonstrating that the percentage of cells scored positive for F-actin recruitment to ligand. Cells are scored as positive when the fluorescence on top of the antigen clusters is at least 3 times higher than the fluorescence on the cells away from the patterns. (Modified from PhD thesis - Alexis Torres (1)).

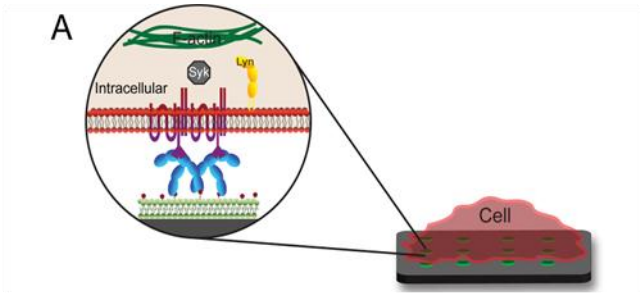
A
Syk
Lyn
Intracellular
Cell

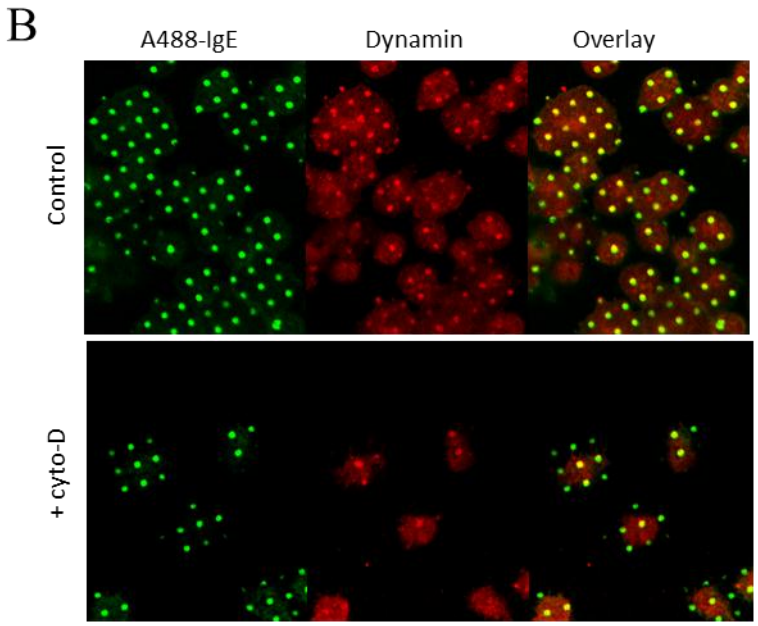
B
A488-IgE
Dynamin
Overlay
Control
+ cyto-D

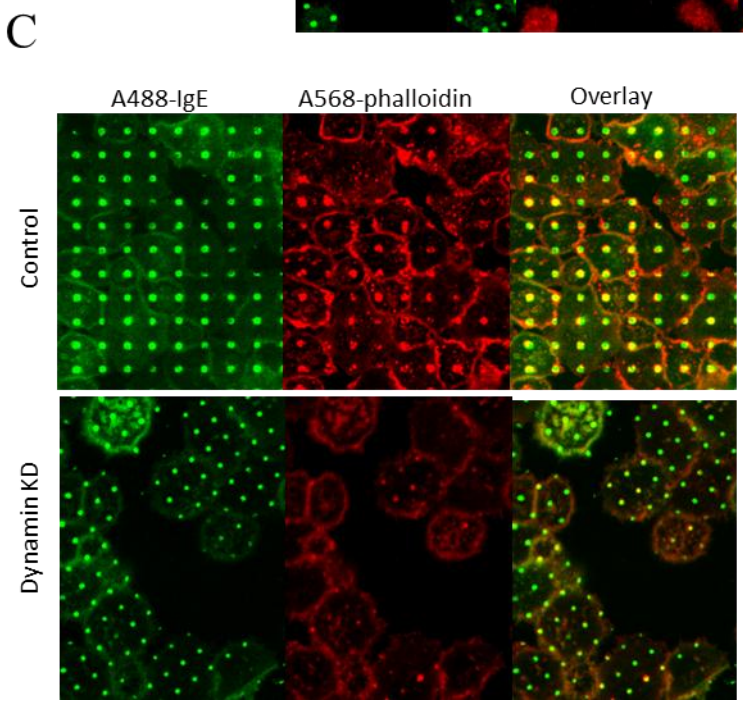
C
A488-IgE
A568-phalloidin
Overlay
Control
Dynamin KD

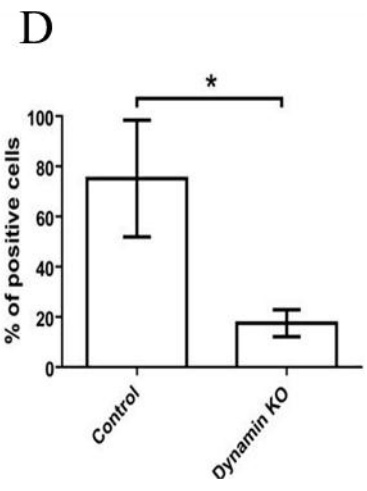
D
*
% of positive cells
100
80
60
40
20
0
Control
Dynamin KO

Dynamin 2 is has been characterized for its role in the later stages of receptor mediated cell signaling, mainly for the scission of endosomal vesicles forming on the plasma membrane of the cells (54, 55). However, our data with micropatterned surfaces suggests that dynamin 2 is recruited to clustered FcεRI receptors, even under conditions where internalization is inhibited. There is evidence for the interactions between dynamin 2 and actin regulating proteins, such as profilin (56) and cortactin (57). To test the involvement of dynamin 2 in the recruitment of actin cytoskeleton to the clustered IgE-FcεRI, we compared F-actin clustering in control and dynamin 2 knock-down (KD) cells. In dynamin 2 KD cells, accumulation of F-actin to aggregated receptors over patterned ligands was highly reduced (Figure 2.13C and D). This dependency of actin cytoskeleton clustering on dynamin 2 might involve direct or indirect interactions of dynamin 2 with actin binding proteins such as Abp1, cortactin, profilin.

To probe the role of actin cytoskeleton in the activity of dynamin 2 with IgE-FcεRI that had been clustered with soluble anti-IgE, we measured colocalization of IgE clusters with dynamin 2-GFP in presence and absence of cytochalasin D. RBL-2H3 cells transiently transfected with dynamin 2-GFP and sensitized with A647-IgE, were treated with anti-IgE for 15 min in presence and absence of cytochalasin D at 37°C. Representative confocal images show increase in colocalization of dynamin2-GFP with crosslinked A647-IgE in the presence of cytochalasin D (Figure 2.14A). This colocalization was quantified by calculating the Pearson's cross correlation coefficient. We find a 2-fold increase in the value of Pearson's coefficient for the cells treated with anti-IgE in presence of cytochalasin-D compared to its absence (Figure 2.14B). These results, taken together provide evidence that dynamin 2 is recruited to clustered IgE-FcεRI complexes independent of its association with F-actin. As shown above, in the absence of actin polymerization, the budding IgE-containing endosomes are not cleaved, and in

the results shown in Figure 2.14, cytochalasin D causes a more stable association of dynamin 2 with clustered IgE-FcεRI at the plasma membrane. In combination, these results indicate that dynamin 2 plays a role in internalization of IgE, either directly, or by regulating the F-actin cytoskeleton.

2.3.7 $PI(4,5)P_2$ is involved in FcεRI internalization:

Previously, we characterized the effects of interfering with $PI(4,5)P_2$ synthesis by treatments with phenylarsine-oxide (PAO), a known inhibitor for PI4K IIIα (58), and quercetin, an inhibitor of PI4K (59) and PI5K, as well as other kinases (2). With these reagents we observed complete inhibition of acidification of FITC-IgE upon treatment with anti-IgE, as well as lack of labeling of surface accessible IgE as labeled by an anti-Alexa 488 antibody (2). Confocal imaging showed that cells treated with antigen in the presence of 20 μM quercetin or 5 μM PAO have crosslinked IgE-containing endosomes, proximal to the plasma membrane but not labeled by a surface labeling antibody (2). These results suggested the formation of crosslinked IgE-containing membrane invaginations that have not been cleaved from plasma membrane.

We used our method to assess the accessibility of crosslinked receptors to the extracellular medium in presence and absence of these PI kinase inhibitors. As shown in Figure 2.15, FITC-IgE on samples treated with anti-IgE in the presence of 20 μM quercetin or 5 μM PAO is sensitive to the changes in extracellular pH, and by this criterion it remains connected to the plasma membrane (state II, Figure 2.3).

2.3.8 Interfering with $PI(4,5)P_2$ synthesis affects recruitment of actin to micropatterned ligand surfaces.

Figure 2.14 Dynamin shows increased colocalization with crosslinked IgE clusters in the presence of cytochalasin-D: A) RBL-2H3, plated on a Mat-tek well are transiently transfected with dynamin 2 GFP. The cells are then sensitized with 2 μg/mL A647-IgE for 1 hour and excess A647-IgE is washed off with BSS-BSA. The cells are then treated with 2 μM cytochalasin D (bottom panel) or not (top panel). They are then stimulated with 1:200 dilution with anti-IgE serum for 15 min at 37°C prior to fixation. The confocal images show dynamin 2-GFP (green channel) and A647-IgE (red channel) and the overlay of cells treated with anti-IgE in absence (top panel) or presence of 2 μM cytochalasin D (bottom panel). B) The data is quantified by calculation of Pearson's coefficients for n > 30 cells for each condition over 2 individual experiments. The error bars represent SEM for all Pearson's coefficient for all the cells analyzed in each condition. Scale Bar: 10μm

A

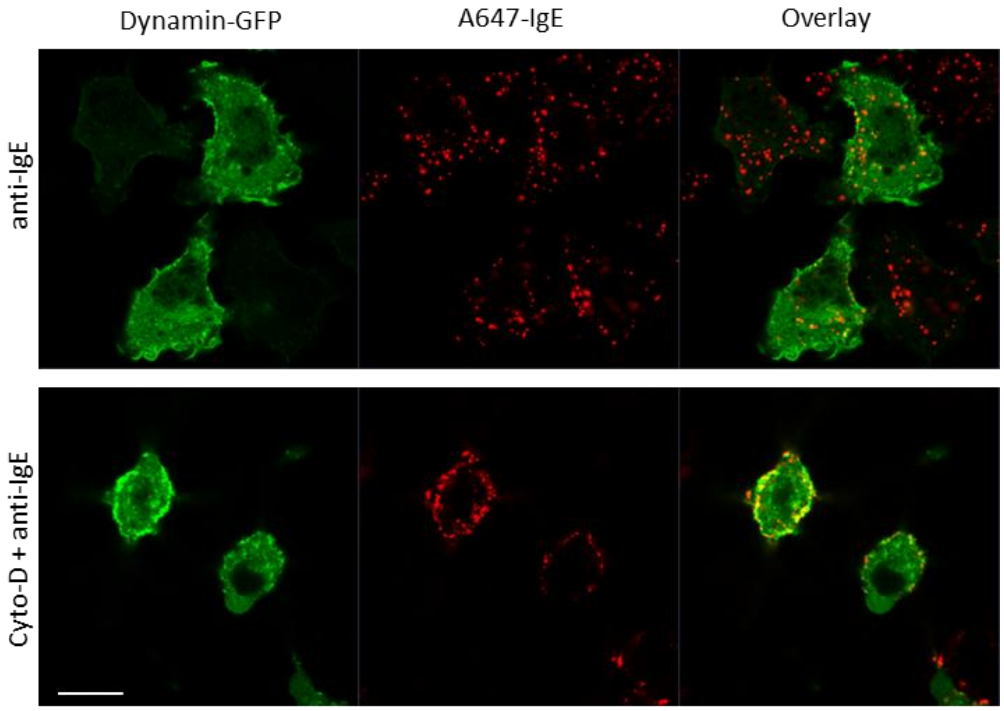
Dynamin-GFP
A647-IgE
Overlay
anti-IgE
Cyto-D + anti-IgE

B

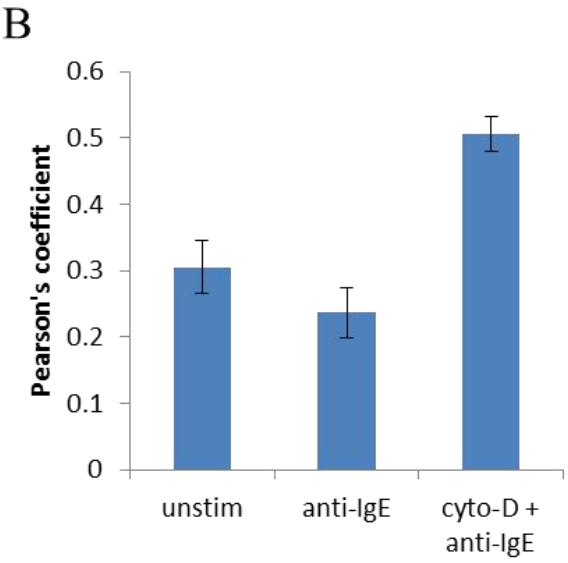
Pearson's coefficient
0.6
0.5
0.4
0.3
0.2
0.1
0
unstim
anti-IgE
cyto-D + anti-IgE

Figure 2.15: Inhibition of PI(4,5)P_2 synthesis prevents the pinching of crosslinked IgE containing endosomes from the plasma membrane. A) RBL-2H3 cells sensitized with FITC-IgE are pretreated with 5 μM PAO or 20 μM quercetin or control and stimulated with 1:200 dilution of anti-IgE serum at 37°C. The fluorescence of FITC-IgE in the samples is measured on a fluorimeter.The plots show data from one representative experiment. B) Flow cytometery samples are prepared and analyzed as described in Figure 2.2. (Data from A and B is adopted (2)) C) Experiments to test the pH sensitivity of crosslinked FITC-IgE were performed as described previously in Figure 2.6. FITC-IgE sensitized RBL-2H3 cells were treated with the 5 μM PAO or 20 μM quercetin prior to stimulation with 1: 200 dilultion of anti-IgE serum. The bar graph represents the normalized fluorescence values of FITC-IgE.. Error bar represents SEM over 3 individual experiments.

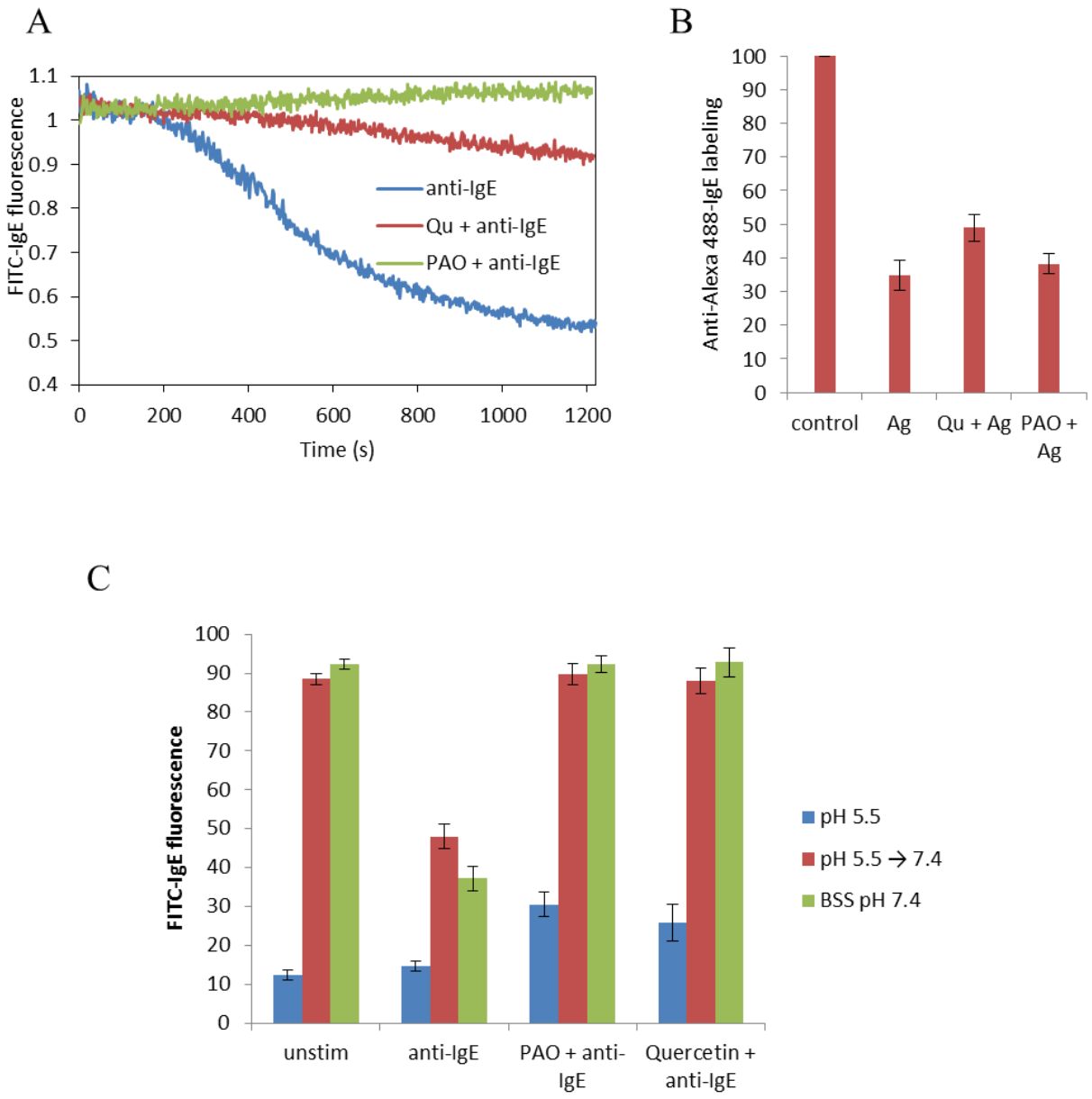
A
FITC-IgE fluorescence
1.1
1
0.9
0.8
0.7
0.6
0.5
0.4
0
200
400
600
800
1000
1200
Time (s)
anti-IgE
Qu + anti-IgE
PAO + anti-IgE
B
Anti-Alexa 488-IgE labeling
100
90
80
70
60
50
40
30
20
10
0
control
Ag
Qu + Ag
PAO + Ag
C
FITC-IgE fluorescence
100
90
80
70
60
50
40
30
20
10
0
unstim
anti-IgE
PAO + anti-IgE
Quercetin + anti-IgE
pH 5.5
pH 5.5 → 7.4
BSS pH 7.4

Figure 2.16: PI(4,5)P_2 synthesis is important for recruitment of F-actin to micro-patterned antigen surfaces: A) RBL-2H3 cells are harvested, sensitized with IgE and resuspended in BSS-BSA (1 mg/mL) at a concentration of 10^6/mL, and treated with 2 µM PAO or 20 µM quercetin or control (no drug added) for 5 minutes. These cells are plated for 40 minutes at 37°C on micro-patterned, covalently attached DNP_{22}-BSA(antigen) conjugated to Cy3 and then fixed. The cells are then stained for F-actin using A488-phalloidin, and are imaged on a confocal microscope. The top panel in the figure shows untreated cells, the middle panel shows the cells treated with 2 µM PAO, and bottom panel shows cells treated with 20 µM quercetin. B) A bar graph demonstrating the percentage of cells scored positive for F-actin recruitment to ligand. Cells are scored as positive when the fluorescence on top of the antigen clusters is at least 3 times higher than the fluorescence on the cells away from the patterns. Data represents an average of >150 cells scored in 3 individual experiments.

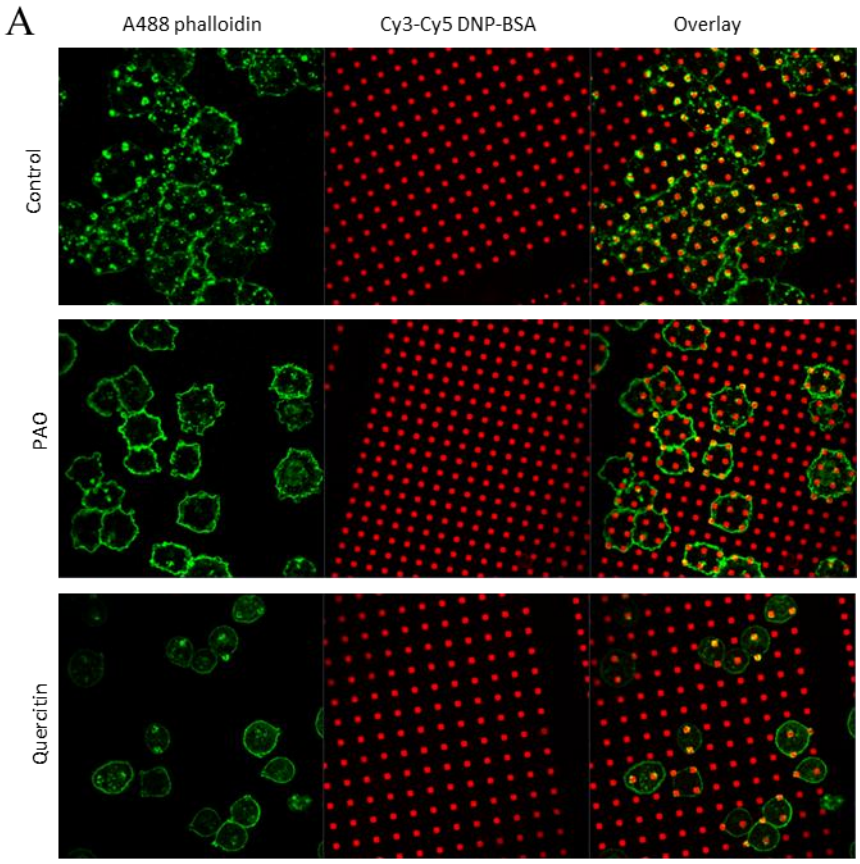
A
A488 phalloidin
Cy3-Cy5 DNP-BSA
Overlay
Control
PAO
Quercitin

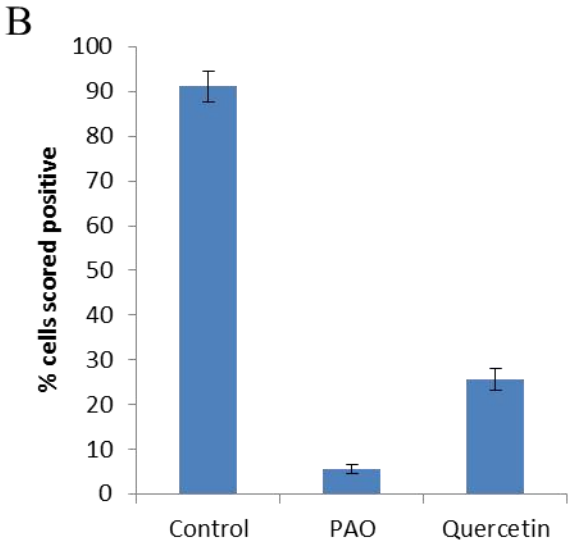
B
% cells scored positive
100
90
80
70
60
50
40
30
20
10
0
Control
PAO
Quercetin

$PI(4,5)P_2$ is known to interact with actin-associated proteins (60), and thus it might participate in the interactions of actin associated-proteins with clustered IgE-FcεRI complexes. Previous studies in our laboratory showed that paxillin, vinculin, and talin are some of the actin-associated proteins that are recruited with IgE receptors to the micro-patterned ligands along with F-actin (36). To investigate the importance of $PI(4,5)P_2$ in mediating these interactions, we plated the RBL cells sensitized with IgE on the micropatterned ligand surfaces. In absence of any pharmacological treatment, we find that >90% cells are positive for recruitment of actin cytoskeleton, as detected by A488-phalloidin. In comparison, we find that incubation with 2 μM PAO or 20 μM quercetin, substantially reduces the number of cells showing F-actin accumulation (Figure 2.16). These results suggest that $PI(4,5)P_2$ participates in interactions of activated IgE receptors with the actin cytoskeleton, either directly or indirectly, probably by recruitment of actin-associated proteins.

2.4 Discussion

When IgE bound to FcεRI receptors on the surface of mast cells is crosslinked with a multivalent antigen, a signaling cascade is initiated leading to release of inflammatory mediators (47). Subsequently, a large fraction of FcεRI/IgE/antigen complexes are internalized in endosomes that mature into lysosomes as the complexes are degraded (13). As described in Figure 2.3A, four states for the crosslinked IgE-FcεRI complexes are possible: 1) Complexes that remain on the surface of the cells and can be labeled by appropriate primary and secondary antibodies without permeabilization (State I, Figure 2.3). 2) Complexes that reside in membrane invaginations but are not pinched from the plasma membrane and are still susceptible to the changes in the extracellular environment (State II, Figure 2.3). 3) Complexes that are in

endosomes, cleaved from plasma membrane, but are not yet acidified (State III, Figure 2.3). 4) Complexes are in acidified endosomes that mature into lysosomes (State IV, Figure 2.3). Commonly, internalization has been studied by radioligand binding and flow cytometry (61). In our experiments with flow cytometry, we label FcεRI/IgE on the surface, but not when the complexes are either in the membrane invaginations or endocytosed. Membrane invaginations that are not cleaved from the plasma membrane have been observed previously via electron microscopy during clathrin mediated endocytosis (62). We also utilize the FITC-IgE acidification assay to assess the extent of internalization of receptor after acidification of IgE-FcεRI containing endosomes. The assay that monitors the effect of decreasing extracellular pH on FITC-IgE fluorescence gives us information about whether crosslinked FITC-IgE is still accessible to the extracellular medium and not internalized. This distinguishes the case when FITC-IgE is in endosomes that have cleaved from plasma membrane but not acidified (such as with bafilomycin treatment) from the case where they are in endosomes that have not been cleaved from plasma membrane. A combination of these methods allows us to specify the state of crosslinked IgE-FcεRI complexes. We refer to IgE as internalized when it is in state III or IV, as depicted in Figure 2.3A.

The signaling cascades leading to degranulation and IgE-FcεRI endocytosis depend on crosslinking of the receptor complexes. Although the initiation of both of these pathways is the same, they diverge after crosslinking, and not much is known about which signaling events are necessary for endocytosis. It is known that IgE receptor endocytosis does not depend on extracellular Ca^{2+} (Figure 2.10B) (63), which is essential for degranulation in RBL-2H3 cells (63). A previous study, in which COS-7 cells were transfected with α,β,γ subunits of FcεRI (64), showed that even reconstituted FcεRI receptors missing the cytoplasmic domain on the α,β,γ

chains and crosslinked by oligomeric IgE can be endocytosed, although at a slower rate in comparison to full length FcεRI receptor in RBL-2H3 (64). This evidence suggests that FcεRI endocytosis differs from signaling requirements for degranulation.

Our laboratory showed previously that FcεRI colocalizes with Lyn kinase, in cholesterol- and sphingolipid-rich ordered membrane domains, (related to "DRMs" or "lipid rafts"), upon activation by aggregation (23, 24). Cholesterol depletion by MβCD pretreatment prevents the localization of aggregated FcεRI into these domains. In addition, it was also demonstrated that cholesterol depletion affects receptor phosphorylation and recruitment of different signaling partners to the ordered membrane domains (24). A previous study using cholesterol depletion by 10mM MβCD for 30 min at 37°C showed increased surface accessibility of crosslinked IgE-FcεRI complexes via flow cytometry (27). Our results with milder cholesterol depletion using 4mM MβCD preatreatment for 20 minutes (Figure 2.5, 2.6), suggest that segregation of IgE-FcεRI in ordered membrane domains is important for the internalization of aggregated IgE receptors. We demonstrate that, under these milder conditions, crosslinked IgE-FcεRI goes in membrane invaginations that are not labeled by anti-Alexa-488 antibody at the cell surface, but they are not cleaved from plasma membrane (Figure 2.6), as depicted in state II, Figure 2.3. These data suggest that translocation of receptor to the ordered membrane domains, which is sensitive to cholesterol depletion, is important for endocytosis of the crosslinked IgE receptor.

We also investigated the dependence of internalization on the length of the rigid ligand spacer in the IgE receptor clusters (28). We previously developed and characterized rigid trivalent DNP-tagged Y-shaped DNA ligands, which stimulated phosphorylation of FcεRI receptor and its signaling partners, including Lyn, Syk, and LAT, together with robust degranulation responses that depended on the distances between DNP moieties in the Y-DNP_3

ligands (5). We also found that treatment with Y-16DNP$_3$ led to aggregation of FcεRI bound to IgE on the surface of mast cells as detected by confocal fluorescent microscopy (data not shown). More recent results quantifying FcεRI receptor aggregation via scanning electron microscopy (SEM) showed that stimulation with Y-16DNP$_3$ causes clustering of IgE/FcεRI that is less extensive that that when the IgE is crosslinked with DNP$_{22}$-BSA (65). We find that although these ligands cause robust degranulation responses in RBL cells in the presence of cytochalasin D, they do not cause any significant internalization of IgE receptor complexes, as detected by FITC-IgE acidification and flow cytometry (Figure 2.4). This is in contrast with studies with the anti-FcεRI antibodies that form receptor dimers and cause significant internalization as seen via FITC-IgE acidification (29). These results, taken together, suggest that the size of aggregated FcεRI clusters is important in initiating the signaling cascade leading to internalization of FcεRI receptor. Although structural constraints and limited crosslinking caused by Y-16DNP$_3$ stimulation is enough to trigger substantial degranulation responses, more robust clustering of IgE-FcεRI complexes appears to be required for internalization of IgE receptor.

Syk, is an early signaling partner coupled to FcεRI activation by crosslinking (47). In our experiments with Syk -/- cells, we find clustering of IgE receptors at optical resolution, but no internalization of the IgE receptor as assessed via FITC-IgE acidification as well as by flow cytometry (Figure 2.7). This argues that Syk is essential in the internalization pathway, and, in absence of Syk, the crosslinked IgE-FcεRI receptor complexes are in state I as depicted in Figure 2.3.

Previous studies in assessing the internalization of transferrin receptors in A431 cells by flow cytometry and Fcγ receptor internalization in RAW 264.7 macrophages by acid stripping found evidence that activation-dependent (Fcγ receptor) and constitutive receptor (transferrin

receptor) endocytosis are insensitive to the disruption of actin cytoskeleton (19, 66). In contrast, there are several examples that the actin cytoskeleton, either directly or via adapter proteins, plays an essential role in endocytosis (67). Previous studies in mast cells, using radiolabeling and acid stripping surface accessible IgE to assess internalization found that IgE in presence of 100 μM cytochalasin B - a drug known to affect formation of microfilaments, doesn't affect IgE internalization after crosslinking with an antigen (63). Other studies using the same method found that IgE internalization is substantially inhibited by 10 μM cytochalasin D (40), supporting dependence on the actin cytoskeleton. We find that in the presence of 1 μM latrunculin A or 2 μM cytochalasin D, which prevent new polymerization of actin, there is no acidification of FITC-IgE upon crosslinking with anti-IgE (Figure 2.7). We see similar results in presence of 3 μM jasplakinolide, which stabilizes the actin cytoskeleton. However, flow cytometry data shows that crosslinked IgE in presence of inhibitors of F-actin polymerization is not labeled with secondary antibodies (Figure 2.8). Upon further investigation, we found that crosslinked IgE under these conditions is located in membrane invaginations that are not cleaved from the plasma membrane (Figure 2.9) (State II, Figure 2.3). Previous studies have shown a role for F-actin in the tubulation (elongation) of membrane invaginations in clathrin dependent endocytosis (68). However, our results show that when F-actin polymerization is inhibited, IgE-FcεRI complexes are trapped in membrane invaginations that are not cleaved from the plasma membrane.

We also find that the inhibition of FITC-IgE acidification by cytochalasin-D is reversible, and, upon removal of the drug, we observe fluorescence quenching of crosslinked FITC-IgE (Figure 2.8A). Once IgE-FcεRI complexes are internalized after crosslinking, IgE-containing endosomes mature into lysosomes and become secretory granules (13). Upon addition of

cytochalasin D or latrunculin A to the IgE in acidified in endosomes, we observe an increase in FITC-IgE fluorescence (Figure 2.10B). It is likely that the increase in FITC-IgE fluorescence upon addition of latrunculin A can be attributed to an increased rate of stimulated exocytosis upon addition of actin cytoskeleton destabilizing agents under these conditions (69). To test this hypothesis, we did the similar experiment in absence of extracellular Ca^{2+}, conditions under which exocytosis does not occur. Consistent with our hypothesis, we do not observe the increase of the FITC-IgE fluorescence upon cytochalasin D or latrunculin A (Figure 2.10B). This indicates that the FITC-IgE fluorescence quenching observed in absence of inhibitors of F-actin polymerization, is a net effect of fluorescence quenching due to the acidification and enhancement when the internalized FITC-IgE, fused with secretory granules are exocytosed.

Various receptor internalization pathways are found to be either clathrin dependent (14), or clathrin independent (15). Previous studies suggested that FcεRI internalization pathway is clathrin mediated, based on colocalization of FcεRI with clathrin coated pits using electron microscopy (17, 18). In contrast with this, more recent studies selectively knocked down clathrin using siRNA, and found that this has no effect on FcεRI internalization via flow cytometry, but it does substantially reduce transferrin internalization (12). Consistent with this, our results using siRNA show that IgE receptor internalization is not affected by clathrin knock-down as measured by FITC-IgE fluorescence quenching (Figure 2.12). Cortactin and its analog, HS1, are also found to be important in both clathrin-mediated (57, 70) and clathrin-independent endocytosis (16). Our results show that selective knock down of cortactin and HS1 does not affect IgE internalization (Figure 2.12).

Dynamin 2 is a GTPase found to be essential for both clathrin-mediated and clathrin-independent endocytosis, primarily for its role in membrane fission to cleave the budding

endosomes from the plasma membrane (71). Previous studies have demonstrated that by over expressing the dominant negative dynamin 2 K44A mutant, there is a significant decrease in FcεRI internalization as measured by flow cytometry (12). We utilize siRNA to selectively knock down >95% dynamin 2 expressed in RBL-2H3 cells, and find only 25% decrease in FcεRI internalization measured by FITC-IgE acidification (Figure 2.12). This result indicates that there is a possibility of some redundancy in the role of dynamin 2 in the FcεRI internalization pathway. Dynamin 2, clathrin and cortactin are all expressed in abundance in RBL-2H3 cells, and upon using siRNA, we achieve > 90% knock down efficiency of all of these proteins. There is a possibility that the residual endogenous proteins after the siRNA treatment are enough to play a role in the internalization of FcεRI. In addition, there might be a different dynamin 2-independent internalization pathways. Therefore, over-expression of dominant negative forms of clathrin and cortactin, may shed light on their effects on FcεRI internalization to provide further insights into the roles of these proteins in IgE receptor internalization. However, there is a possibility that IgE internalization is actin cytoskeleton dependent but dynamin independent pathway.

We previously utilized micropatterned ligand surfaces to study spatially regulated signaling in IgE receptors (53, 72). We demonstrated that several actin binding proteins commonly associated with focal adhesions, including talin, vinculin, and paxillin, are recruited to IgE receptor complexes independently of integrin α-5. We previously hypothesized that these proteins might regulate signaling by playing a role as adaptor proteins in linking the IgE receptor to the actin cytoskeleton (36). However, in light of the role of the actin cytoskeleton in FcεRI internalization, it is possible that recruitment of these actin binding proteins to these micropatterned surfaces is a part of the formation of FcεRI internalization machinery.

We find that dynamin 2 is recruited to the micropatterned surfaces, and this recruitment is independent of actin polymerization (Figure 2.13B). We also find that dynamin 2 knock down inhibits the recruitment of F-actin to the activated FcεRI receptor complexes (Figure 2.13 C). These results suggest that dynamin 2 plays a direct or indirect role via adaptor proteins in the organization of actin cytoskeleton, prior to being involved in vesicle fission, as is commonly perceived role of dynamin in endocytosis. This is consistent with some previous observations which indicate that dynamin 2 is playing a role in the arrangement of actin cytoskeleton (73, 74). The recruitment of dynamin 2 to the receptor clusters might be important for recruitment of other proteins involved in the internalization pathway, including bar domain proteins (75, 76). It should be noted that over-expression of dominant negative dynamin 2 K44A mutant (which is recruited to the activated receptor), did not affect the recruitment of F-actin to micropatterned patches (data not shown) in comparison to control samples, indicating that the role of dynamin 2 in the organization of the actin cytoskeleton is independent of membrane fission activity. However, over expression dynamin 2 K44A mutant reduces crosslinked FcεRI receptor internalization as measured by flow cytometry (12).We also find that when the actin cytoskeleton is disrupted by cytochalasin D pretreatment, dynamin 2 shows increased association with IgE receptor complexes, due to crosslinking by soluble anti-IgE for 15 min at 37°C (Figure 2.14). This suggests that dynamin 2 plays a role in the organization of actin cytoskeleton, and, in turn, the actin cytoskeleton is required for fission of endosomes from the plasma membrane (Figure 2.11). Although our results demonstrate that the actin cytoskeleton is not essential for the formation of FcεRI-containing membrane invaginations in RBL-2H3 cells.

Phosphoinositides mediate a wide variety of signaling processes in cells (22). They are known to play an important role in endocytosis, serving as targeted binding sites for the

recruitment and subsequent regulation of endocytic proteins to the plasma membrane including dynamin (75). $PI(4,5)P_2$ is also known to regulate the actin cytoskeleton at the sites of receptor endocytosis (20). Previous results have shown that clathrin-independent endocytosis is also dependent on Arf 6 (77-79). Given that Arf 6 is known to function in the regulation of the cortical actin cytoskeleton by PIP5K (80), $PI(4,5)P_2$ might be an important regulator in the FcεRI endocytosis, which is known to be clathrin-independent (Figure 2.12) (12). $PI(4,5)P_2$ constitutes ~ 1% of the total lipid content of the plasma membrane, and it needs constant replenishment as it is hydrolyzed by PLCγ, and converted to phosphatitylinositol 3,4,5-triphosphate (PIP_3) by phosphatidylinositol 3- kinases (PI3K). The source of $PI(4,5)P_2$ in cells is by phosphorylation of PI(4)P via PI(4)P-5-Kinase (PI5K) and PI(5)P via PI5P-4-Kinase (PI4K) (22). In mammalian cells, PI4P is a lot more abundant than PI5P. In our experiments, we indirectly reduced the $PI(4,5)P_2$ levels by treatment with PI4K inhibitor PAO and PI5-kinase inhibitor quercetin, whose effects on RBL-2H3 cells are previously characterized (2). We find that the IgE receptors crosslinked in presence of these inhibitors localize in invaginations that are not accessible by surface labeling anti-Alexa 488 antibody, but are not cleaved from the plasma membrane, similar to the response in presence of F-actin polymerization inhibitors (Figure 2.15). Consistent with this, we also observe that pretreatment with PAO or quercetin substantially reduces the recruitment of F-actin to the activated FcεRI receptors complexes formed on the micropatterned ligand surfaces (Figure 2.16). Taken together, these results suggest that $PI(4,5)P_2$ synthesis is important for recruitment of F-actin and other signaling partners that play important roles in fission of IgE containing endosomes from the plasma membrane.

In summary, we have developed assays to probe the different states of IgE-FcεRI complexes during the process of internalization after crosslinking. Using these methods, we

show that FcεRI internalization depends on Syk kinase and F-actin polymerization. We also show that mild depletion of cholesterol prevents crosslinked IgE-FcεRI from pinching off from the plasma membrane. siRNA studies show that IgE internalization does not require clathrin, cortactin or HS1, but it is reduced by dynamin 2 knock down. We utilized micropatterned ligand surfaces to demonstrate the role of dynamin 2 in recruiting actin cytoskeleton to activated IgE receptor complexes. We also provide evidence that synthesis of $PI(4,5)P_2$ is important for internalization of FcεRI.

References:

1. Torres AJ. Investigating cytoskeletal regulation of IgE receptor signaling by micropatterned ligand arrays [PhD thesis]. Ithaca, NY: Cornell University; 2011.
2. Marcela de Souza Santos RMZGN, David Holowka and Barbara Baird. Inhibitors of PI(4,5)P2 Synthesis Reveal Dynamic Regulation of IgE Receptor Signaling by Phosphoinositides in Mast Cells. Journal of cell science.2012;Submitted.
3. Kraft S, Novak N. Fc receptors as determinants of allergic reactions. TRENDS in Immunology.2006;27:88-95.
4. Nimmerjahn F, Ravetch JV. Fc-receptors as regulators of immunity. Advances in immunology.2007;96:179-204.
5. Sil D, Lee JB, Luo D, Holowka D, Baird B. Trivalent ligands with rigid DNA spacers reveal structural requirements for IgE receptor signaling in RBL mast cells. ACS chemical biology.2007;2:674-684.
6. MacGlashan Jr D. IgE receptor and signal transduction in mast cells and basophils. Current opinion in immunology.2008;20:717-723.
7. Kalesnikoff J, Galli SJ. New developments in mast cell biology. Nature immunology.2008;9:1215-1223.
8. Rivera J, Fierro NA, Olivera A, Suzuki R. New Insights on Mast Cell Activation via the High Affinity Receptor for IgE1. Advances in immunology.2008;98:85-120.
9. Liu H, Rhodes M, Wiest DL, Vignali DAA. On the dynamics of TCR: CD3 complex cell surface expression and downmodulation. Immunity.2000;13:665-675.
10. Cheng PC, Steele CR, Gu L, Song W, Pierce SK. MHC class II antigen processing in B cells: accelerated intracellular targeting of antigens. The Journal of Immunology.1999;162:7171.
11. Kitaura J, Xiao W, Maeda-Yamamoto M, Kawakami Y, Lowell CA, Kawakami T. Early divergence of Fc epsilon receptor I signals for receptor up-regulation and internalization from degranulation, cytokine production, and survival. J Immunol.2004;173:4317-4323.
12. Fattakhova G, Masilamani M, Borrego F, Gilfillan AM, Metcalfe DD, Coligan JE. The high-affinity immunoglobulin-E receptor (FcepsilonRI) is endocytosed by an AP-2/clathrin-independent, dynamin-dependent mechanism. Traffic.2006;7:673-685.
13. Fattakhova GnV, et al. Endosomal trafficking of the ligated FceRI receptor. Molecular Immunology.2009;46:793-802.

14. Doherty GJ, McMahon HT. Mechanisms of endocytosis. Annual review of biochemistry.2009;78:857-902.
15. Mayor S, Pagano RE. Pathways of clathrin-independent endocytosis. Nat Rev Mol Cell Biol.2007;8:603-612.
16. Sauvonnet N, Dujeancourt A, Dautry-Varsat A. Cortactin and dynamin are required for the clathrin-independent endocytosis of gammac cytokine receptor. J Cell Biol.2005;168:155-163.
17. Wilson BS, Pfeiffer JR, Oliver JM. Observing FcεRI signaling from the inside of the mast cell membrane. The Journal of cell biology.2000;149:1131-1142.
18. Burns AR, Oliver JM, Pfeiffer JR, Wilson BS. Visualizing Clathrin-Mediated IgE Receptor Internalization by Electron and Atomic Force Microscopy. METHODS IN MOLECULAR BIOLOGY-CLIFTON THEN TOTOWA-.2008;440:235.
19. Fujimoto LM, Roth R, Heuser JE, Schmid SL. Actin assembly plays a variable, but not obligatory role in receptor-mediated endocytosis in mammalian cells. Traffic.2000;1:161-171.
20. Engqvist-Goldstein ÅEY, Drubin DG. Actin assembly and endocytosis: from yeast to mammals. Annual review of cell and developmental biology.2003;19:287-332.
21. Cao H, Chen J, Awoniyi M, Henley JR, McNiven MA. Dynamin 2 mediates fluid-phase micropinocytosis in epithelial cells. Journal of cell science.2007;120:4167-4177.
22. Di Paolo G, De Camilli P. Phosphoinositides in cell regulation and membrane dynamics. Nature.2006;443:651-657.
23. Field KA, Holowka D, Baird B. Fc epsilon RI-mediated recruitment of p53/56lyn to detergent-resistant membrane domains accompanies cellular signaling. Proceedings of the National Academy of Sciences.1995;92:9201.
24. Sheets ED, Holowka D, Baird B. Critical role for cholesterol in Lyn-mediated tyrosine phosphorylation of FcepsilonRI and their association with detergent-resistant membranes. J Cell Biol.1999;145:877-887.
25. Holowka D, et al. Lipid segregation and IgE receptor signaling: a decade of progress. Biochimica et Biophysica Acta (BBA)-Molecular Cell Research.2005;1746:252-259.
26. Parton RG, Richards AA. Lipid rafts and caveolae as portals for endocytosis: new insights and common mechanisms. Traffic.2003;4:724-738.

27. Molfetta R, et al. Lipid raft-dependent FcepsilonRI ubiquitination regulates receptor endocytosis through the action of ubiquitin binding adaptors. PLoS One.2009;4:e5604.
28. Holowka D, Sil D, Torigoe C, Baird B. Insights into immunoglobulin E receptor signaling from structurally defined ligands. Immunological reviews.2007;217:269-279.
29. Robertson DJ. Association of Aggregated Receptors For Immunoglobulin E With The Cytoskeleton of Rat Basophilic Leukimia cells: Detergent insolubility and lateral mobility studies [PhD thesis]; 1990.
30. Pierini L, Holowka D, Baird B. Fc epsilon RI-mediated association of 6-micron beads with RBL-2H3 mast cells results in exclusion of signaling proteins from the forming phagosome and abrogation of normal downstream signaling. J Cell Biol.1996;134:1427-1439.
31. Larson DR, Gosse JA, Holowka DA, Baird BA, Webb WW. Temporally resolved interactions between antigen-stimulated IgE receptors and Lyn kinase on living cells. J Cell Biol.2005;171:527-536.
32. Cao H, Garcia F, McNiven MA. Differential Distribution of Dynamin Isoforms in Mammalian Cells. Mol Biol Cell.1998;9:2595-2609.
33. Ilic B, Craighead HG. Topographical Patterning of Chemically Sensitive Biological Materials Using a Polymer-Based Dry Lift Off. Biomedical Microdevices.2000;2:317-322.
34. Orth RN, Wu M, Holowka DA, Craighead HG, Baird BA. Mast Cell Activation on Patterned Lipid Bilayers of Subcellular Dimensions. Langmuir.2003;19:1599-1605.
35. Torres AJ, Holowka D, Baird BA. Micropatterned Ligand Arrays to Study Spatial Regulation in Fc Receptor Signaling. Methods in molecular biology (Clifton, NJ).2011;748:195.
36. Torres AJ, Vasudevan L, Holowka D, Baird BA. Focal adhesion proteins connect IgE receptors to the cytoskeleton as revealed by micropatterned ligand arrays. Proc Natl Acad Sci U S A.2008;105:17238-17244.
37. Torres AJ, Vasudevan L, Holowka D, Baird BA. Focal adhesion proteins connect IgE receptors to the cytoskeleton as revealed by micropatterned ligand arrays. Proceedings of the National Academy of Sciences.2008;105:17238-17244.
38. Erickson J, Kane P, Goldstein B, Holowka D, Baird B. Cross-linking of IgE-receptor complexes at the cell surface: a fluorescence method for studying the binding of monovalent and bivalent haptens to IgE. Molecular immunology.1986;23:769-781.

39. Xu K, Williams RM, Holowka D, Baird B. Stimulated release of fluorescently labeled IgE fragments that efficiently accumulate in secretory granules after endocytosis in RBL-2H3 mast cells. J Cell Sci.1998;111 (Pt 16):2385-2396.
40. Ra C, Furuichi K, Rivera J, Mullins JM, Isersky C, White KN. Internalization of IgE receptors on rat basophilic leukemic cells by phorbol ester. Comparison with endocytosis induced by receptor aggregation. Eur J Immunol.1989;19:1771-1777.
41. Menon AK, Holowka D, Webb WW, Baird B. Clustering, mobility, and triggering activity of small oligomers of immunoglobulin E on rat basophilic leukemia cells. J Cell Biol.1986;102:534-540.
42. Fattakhova GV, et al. Endosomal trafficking of the ligated FcvarepsilonRI receptor. Mol Immunol.2009;46:793-802.
43. Menon AK, Holowka D, Webb WW, Baird B. Cross-linking of receptor-bound IgE to aggregates larger than dimers leads to rapid immobilization. The Journal of cell biology.1986;102:541-550.
44. Sheets ED, Holowka D, Baird B. Membrane organization in immunoglobulin E receptor signaling. Curr Opin Chem Biol.1999;3:95-99.
45. Yamashiro DJ, Maxfield FR. Kinetics of endosome acidification in mutant and wild-type Chinese hamster ovary cells. J Cell Biol.1987;105:2713-2721.
46. Mamdouh Z, Chen X, Pierini LM, Maxfield FR, Muller WA. Targeted recycling of PECAM from endothelial surface-connected compartments during diapedesis. Nature.2003;421:748-753.
47. Kinet JP. The high-affinity IgE receptor (FcεRI): from physiology to pathology. Annual review of immunology.1999;17:931-972.
48. Molfetta R, et al. Lipid Raft-Dependent FceRI Ubiquitination Regulates Receptor Endocytosis through the Action of Ubiquitin Binding Adaptors. PLoS ONE.2009;4:e5604.
49. Zhang J, Berenstein EH, Evans RL, Siraganian RP. Transfection of Syk protein tyrosine kinase reconstitutes high affinity IgE receptor-mediated degranulation in a Syk-negative variant of rat basophilic leukemia RBL-2H3 cells. J Exp Med.1996;184:71-79.
50. Sauvonnet N, Dujeancourt A, Dautry-Varsat A. Cortactin and dynamin are required for the clathrin-independent endocytosis of {gamma}c cytokine receptor. J Cell Biol.2005;168:155-163.

51. Uruno T, Zhang P, Liu J, Hao J-J, Zhan X. Haematopoietic lineage cell-specific protein 1 (HS1) promotes actin-related protein (Arp) 2/3 complex-mediated actin polymerization. Biochem J.2003;371:485-493.
52. Wu M, Holowka D, Craighead HG, Baird B. Visualization of plasma membrane compartmentalization with patterned lipid bilayers. PNAS.2004;101:13798-13803.
53. Wu M, Holowka D, Craighead HG, Baird B. Visualization of plasma membrane compartmentalization with patterned lipid bilayers. Proc Natl Acad Sci U S A.2004;101:13798-13803.
54. Damke H, Binns DD, Ueda H, Schmid SL, Baba T. Dynamin GTPase Domain Mutants Block Endocytic Vesicle Formation at Morphologically Distinct Stages. Mol Biol Cell.2001;12:2578-2589.
55. Roux Al, Uyhazi K, Frost A, De Camilli P. GTP-dependent twisting of dynamin implicates constriction and tension in membrane fission. Nature.2006;441:528-531.
56. Witke W, et al. In mouse brain profilin I and profilin II associate with regulators of the endocytic pathway and actin assembly. EMBO J.1998;17:967-976.
57. Zhu J, Zhou K, Hao J-J, Liu J, Smith N, Zhan X. Regulation of cortactin/dynamin interaction by actin polymerization during the fission of clathrin-coated pits. J Cell Sci.2005;118:807-817.
58. Balla A, Tuymetova G, Barshishat M, Geiszt M, Balla T. Characterization of type II phosphatidylinositol 4-kinase isoforms reveals association of the enzymes with endosomal vesicular compartments. Journal of Biological Chemistry.2002;277:20041-20050.
59. Middleton Jr E, Kandaswami C, Theoharides TC. The effects of plant flavonoids on mammalian cells: implications for inflammation, heart disease, and cancer. Pharmacological reviews.2000;52:673-751.
60. Johnson CM, Chichili GR, Rodgers W. Compartmentalization of phosphatidylinositol 4, 5-bisphosphate signaling evidenced using targeted phosphatases. Journal of Biological Chemistry.2008;283:29920-29928.
61. Koenig JA. Assessment of receptor internalization and recycling. METHODS IN MOLECULAR BIOLOGY-CLIFTON THEN TOTOWA-.2004;259:249-274.
62. Takei K, McPherson PS, Schmid S, De Camilli P. Tubular membrane invaginations coated by dynamin rings are induced by GTP-7S in nerve terminals. Nature374.1995:186-190.

63. Furuichi K, Ra C, Isersky C, Rivera J. Comparative evaluation of the effect of pharmacological agents on endocytosis and coendocytosis of IgE by rat basophilic leukaemia cells. Immunology.1986;58:105-110.
64. Mao S, Varin-Blank N, Edidin M, Metzger H. Immobilization and internalization of mutated IgE receptors in transfected cells. The Journal of Immunology.1991;146:958.
65. Veatch SL, Machta BB, Shelby SA, Chiang EN, Holowka DA, Baird BA. Correlation functions quantify super-resolution images and estimate apparent clustering due to over-counting. PloS one.2012;7:e31457.
66. Tse SM, et al. Differential role of actin, clathrin, and dynamin in Fc gamma receptor-mediated endocytosis and phagocytosis. J Biol Chem.2003;278:3331-3338.
67. Qualmann B, Mellor H. Regulation of endocytic traffic by Rho GTPases. Biochemical Journal.2003;371:233.
68. Wu M, et al. Coupling between clathrin-dependent endocytic budding and F-BAR-dependent tubulation in a cell-free system. Nature cell biology.2010;12:902-908.
69. Pierini L, Harris NT, Holowka D, Baird B. Evidence supporting a role for microfilaments in regulating the coupling between poorly dissociable IgE-FcεRI aggregates and downstream signaling pathways. Biochemistry.1997;36:7447-7456.
70. Cao H, Orth JD, Chen J, Weller SG, Heuser JE, McNiven MA. Cortactin is a component of clathrin-coated pits and participates in receptor-mediated endocytosis. Mol Cell Biol.2003;23:2162-2170.
71. Damke H, Binns DD, Ueda H, Schmid SL, Baba T. Dynamin GTPase domain mutants block endocytic vesicle formation at morphologically distinct stages. Mol Biol Cell.2001;12:2578-2589.
72. Torres AJ, Wu M, Holowka D, Baird B. Nanobiotechnology and cell biology: micro- and nanofabricated surfaces to investigate receptor-mediated signaling. Annu Rev Biophys.2008;37:265-288.
73. Chua J, Rikhy R, Lippincott-Schwartz J. Dynamin 2 orchestrates the global actomyosin cytoskeleton for epithelial maintenance and apical constriction. Proceedings of the National Academy of Sciences.2009;106:20770-20775.
74. Mooren OL, Kotova TI, Moore AJ, Schafer DA. Dynamin2 GTPase and cortactin remodel actin filaments. Journal of Biological Chemistry.2009;284:23995-24005.

75. Itoh T, Erdmann KS, Roux A, Habermann B, Werner H, De Camilli P. Dynamin and the actin cytoskeleton cooperatively regulate plasma membrane invagination by BAR and F-BAR proteins. Developmental cell.2005;9:791-804.
76. McPherson VA, et al. Contributions of F-BAR and SH2 Domains of Fes Protein Tyrosine Kinase for Coupling to the FcεRI Pathway in Mast Cells. Molecular and cellular biology.2009;29:389-401.
77. Brown FD, Rozelle AL, Yin HL, Balla T, Donaldson JG. Phosphatidylinositol 4, 5-bisphosphate and Arf6-regulated membrane traffic. The Journal of cell biology.2001;154:1007-1018.
78. Naslavsky N, Weigert R, Donaldson JG. Characterization of a nonclathrin endocytic pathway: membrane cargo and lipid requirements. Molecular biology of the cell.2004;15:3542-3552.
79. Aikawa Y, Martin TFJ. ADP-Ribosylation Factor 6 Regulation of Phosphatidylinositol-4, 5-Bisphosphate Synthesis, Endocytosis, and Exocytosis. Methods in enzymology.2005;404:422-431.
80. Honda A, et al. Phosphatidylinositol 4-phosphate 5-kinase [alpha] is a downstream effector of the small G protein ARF6 in membrane ruffle formation. Cell.1999;99:521-532.

Chapter 3[3]

Spatially defined EGF receptor signaling using micro-patterned EGF arrays

3.1 Introduction

Epidermal growth factor receptor (EGFR) belongs to the tyrosine kinase family of receptors and is expressed at the plasma membrane of many cell types. EGFR signaling is known to be an important regulator of cellular responses, including proliferation, migration and apoptosis (1-4). EGFR signaling pathways are highly regulated and they have been a focus of many investigations. Numerous studies have shown that mutations in EGFRs can make them potent oncoproteins (4). Binding of EGF induces dimerization of EGFR that activates the kinase domains in the cytoplasmic segments with consequent transphosphorylation of tyrosine residues in this region of EGFR (1). These phosphorylated tyrosine residues act as docking sites for signaling adaptors, including Grb2, SHC and enzymes such as phospholipase Cγ (PLCγ), thus linking EGFR to their downstream signaling partners. EGFR activation induces initiation of several signaling cascades, including those activating extracellular signal-regulating kinases (Erk) via H-Ras and Akt signaling through phosphatidylinositol 3-kinase (PI3K) activation. EGFR is also known to undergo internalization after stimulation with EGF (5).

Although the series of signaling sequelae is well established, little is known about spatial aspects of signaling partner interactions with activated EGFR. Previous results with beads conjugated with EGF have shown that localized stimulation of EGFR leads to lateral propagation of EGFR activation at the plasma membrane (6), which means that EGFR is phosphorylated even a few micrometers away from the site of stimulation via these beads. The possibility that localization of receptor tyrosine kinases (RTKs) influences signaling consequences has been a

[3] Kirsten Bryant performed the western blotting experiments and paxillin knock down experiments, and she supplied the NIH-3T3 cells stably overexpressing EGFR.

focus of recent studies. There is evidence that EGFRs can continue signaling even from endosomes, and clathrin-mediated endocytosis of EGFR may play a role in the activation of Erk (7, 8). In contrast, another investigation revealed that reduction of endocytosis of EGFR following stimulation with EGF leads to more sustained activation of Akt and suggested that EGFR signaling occurs primarily at the plasma membrane (9). Recent evidence suggests that paxillin, an adaptor protein, participates in Erk activation and its subsequent nuclear translocation downstream of EGFR signaling (10), however, spatial aspects of the interaction of paxillin and other signaling partners like MEK and Erk with activated EGFR have not been elucidated. In addition, the role of F-actin in the recruitment of these signaling partners to activated EGFR on the plasma membrane remains unclear.

We previously demonstrated that micropatterned ligand surfaces are useful tools to study the spatiotemporal aspects of FcεRI signaling (11, 12). We showed that FcεRI bound to anti-DNP-IgE on the surface of mast cells is activated by DNP-liganded lipid bilayers, leading to recruitment of Lyn, a Src family kinase that initiates phosphorylation of FcεRI. In addition, we found that micron-scale recruitment of Lyn to FcεRI complexes involves the actin cytoskeleton, although tyrosine kinase activity associated with catalytic amounts of Lyn does not (11, 12). Previous studies with covalently attached EGF have shown that this configuration can stimulate EGFR, as detected by tyrosine phosphorylation of EGFR (13, 14). In addition, when EGF is covalently attached to a substrate, endocytosis of EGFR cannot occur, resulting in the formation of more stable EGFR signaling complexes at the plasma membrane. These results (13, 14) indicate that micron-scale patches of covalently attached EGF stimulate EGFR.

Here, we utilize NIH-3T3 cells with stably expressed EGFR and micron-sized patches of surface-attached EGF to locally activate EGFR in well-defined geometrical patterns. Under these

conditions, we find that Ras, MAP kinase proteins, MEK and threonine-phosphorylated Erk (pErk) are recruited to the patterned EGFR signaling complexes at the plasma membrane in an actin cytoskeleton-dependent manner. We find that paxillin is recruited to these activated EGFR signaling complexes on the plasma membrane as tyrosine and serine phosphorylated species. We also observe colocalization of F-actin with these EGFR signaling clusters, but GFP-tagged integrin α5 is excluded. Our results provide strong evidence that an extended EGFR signaling complex is established by surface-attached EGF, and its stability depends on coupling to the actin cytoskeleton.

3.2 Materials and Methods:

3.2.1 Materials:

All cell culture reagents, EGF, Lipofectamine 2000, and precast gels for blotting were from Invitrogen. FuGene HD was from Roche Applied Sciences. Alexa488-labeled goat anti-mouse IgG_1, Alexa 488-labeled goat anti-rabbit (H+L), Alexa488-phalloidin, Alexa647-labeled goat anti-mouse IgG (H+L), Alexa568-labeled streptavidin and N-terminal-labeled EGF-biotin were purchased from Invitrogen. Quercetin and phenylarsine oxide (PAO) were purchased from Sigma Aldrich. PP2 was purchased from Enzo LifeSciences. Cytochalasin D and Iressa were purchased from Calbiochem (EMD Chemicals). Rabbit anti-phospho-Erk, rabbit anti-phospho-MEK, rabbit anti-C-terminal EGFR, and anti-phospho-Y1068-EGFR antibodies were purchased from Cell Signaling Corp. Rabbit anti-MEK antibody and FAK-HA cDNA construct were gifts from Dr. R.A. Cerione. Monoclonal anti-phosphotyrosine clone 4G10 was obtained from Upstate Cell Signaling Solutions (Millipore Co.). Anti-phospho-tyrosine paxillin was purchased from Santa Cruz Biotechnology. Dynamin 2-EGFP (15) cDNA was obtained from Dr. Mark McNiven

(Mayo Clinic). Rabbit anti-ezrin and anti-moesin antibodies were gifts from Dr. A. Bretscher (Cornell University). Integrin α5-EGFP and avian paxillin-EGFP cDNA constructs were gifts from Dr. A. Horwitz (University of Virginia). The EGFR-GFP construct from Dr. J. Koland has been described previously (16). Preparation of Lyn-mRFP was described previously (17). The cDNA construct of PLCγ1-EGFP (18) was a gift from Dr. Graham Carpenter, Vanderbilt University. GFP-H-Ras was a gift from Dr. Anne Kenworthy, Vanderbilt University.

3.2.2 Cell Culture and Transfection

RBL-2H3 cells were maintained in monolayer cultures and harvested with trypsin-EDTA (Invitrogen) 3–5 days after passage, as described previously (19). Chemical transfection of RBL-2H3 cells was carried out using a complex of 2 μg cDNA with 8 μL Fugene-HD (Promega) in 100 μL Opti-MEM (Life Technologies) that was added to plated cells in 1mL Opti-MEM per Mat-Tek well, followed by addition of phorbol dibutyrate (0.1μg/mL) as previously described (20).

NIH-3T3 cells stably over-expressing wild type (wt)-EGFR, hereafter referred to as NIH-3T3 (EGFR) cells, were cultured as monolayers in DMEM containing 10% (v/v) calf serum (CS) as described elsewhere (21). Briefly described, NIH3T3 cells were transfected with the wt-EGFR-pkH3 vector, using FuGene HD (Roche). The transfection complex for NIH-3T3 cells was prepared similarly as for RBL-2H3 cells: plating the complex with the cells in DMEM (GIBCO) for 2 hours at 37°C, before washing away the complex and incubating with NIH-3T3 media. Transfected cells were maintained in DMEM supplemented with 10% CS and 2μg/ml puromycin (Invitrogen). After 10–14 days, puromycin-resistant colonies were selected and subcultured in DMEM supplemented with 10% CS and 0.5 μg/ml puromycin. The clones were

then assessed for expression of EGFR. For use in experiments, NIH-3T3 (EGFR) (clone A13) cells were serum starved for 12-14 hours prior to harvesting.

3.2.3 Microfabrication of patterned EGF surfaces.

Surfaces with 1.5 to 4 μm features were patterned with a parylene layer as described previously (22, 23). An 8 x 8 mm parylene-patterned silicon substrate was prepared for functionalization by plasma cleaning for 5 minutes at room temperature under vacuum in a glass dish. The surface was rinsed with acetone and dried under nitrogen, followed by treatment with 3-mercaptopropyltrimethyoxy silane (MPTS) for 30 minute at room temperature. The substrate was then washed with absolute ethanol (3x) and was incubated in 2 mM N-(γ-maleimidobutyryloxy) succinimide (GMBS) in absolute ethanol for 1 hour at room temperature (24). The samples were rinsed with phosphate buffered saline (PBS, pH 7.4) and placed on parafilm, followed by incubation with 50 μg/mL Alexa568-streptavidin for 1 hour at room temperature. The substrates were thoroughly rinsed with PBS at room temperature, followed by incubation with 500 ng/mL EGF-biotin for 30 minutes at room temperature. The samples were rinsed thoroughly once more with PBS, and parylene was mechanically peeled away to yield patterned EGF on the substrate. For negative controls, incubation with EGF-biotin was omitted. Non-specific binding to the micro-patterned substrate is minimized by incubation with 1 mg/mL BSA for 5 minutes before plating the cells for experiments.

3.2.4 Fluorescence Microscopy

For experiments involving patterned EGF surfaces, ~100 μl of cells suspended at a concentration of 0.5 x 10^6 cells per mL in buffered salt solution (BSS:135 mM NaCl, 5.0 mM

KCl, 1.8 mM $CaCl_2$, 1.0 mM $MgCl_2$, 5.6 mM glucose and 20 mM Hepes pH 7.4) with 1 mg/ml BSA were added to a patterned substrate (8 × 8 mm) in the center of a 35-mm Petri dish with coverglass bottom (0.16–0.19 mm; MatTek Corp.) to minimize the volume of cell suspension utilized for each experiment. After 40 minutes of incubation at 37°C, cells were fixed with 4% paraformaldehyde in PBS for 20 minutes at room temperature followed by quenching with 10 mg/ml BSA in PBS with 0.01% NaN_3 (PBS/BSA). For immunofluorescence after fixation, cells were labeled with a primary antibody at room temperature for 1 hour in presence of 0.1% Triton-X in PBS/BSA. After washing with PBS/BSA, a fluorophore-labeled secondary antibody was incubated with samples at room temperature for 1 hour in presence of 0.1% Triton-X in PBS/BSA. For labeling of F-actin, cells were incubated with 5 μg/mL Alexa 488-phalloidin in PBS-BSA with 0.1% Triton-X for 30 minutes at room temperature prior to rinsing with PBS before inverting the chip for imaging using a Zeiss LSM 710 inverted microscope and a 63x Oil Plan-Apochromat lens. A DF 488/561/647 filter set was used to perform sequential 1/2/3 color imaging of the samples. The width of the focal plane was adjusted for optimal image quality. Quantification of colocalization was carried out by calculating Pearson's cross-correlation coefficients for each cell using a Matlab code as described elsewhere (12). The equation used to calculate Pearson's cross-correlation coefficient is:

$$\rho = \frac{\sum(x_i - x)(y_i - y)}{\sqrt{\sum(x_i - x)^2 \sum(y_i - y)^2}}$$

Where, x_i and y_i are the pixel intensity values for green and red channel, respectively, and x, y are the average values of x_i and y_i in the image. A mask is drawn around the cell of interest using a Matlab script, and ρ values are calculated for each individual cell. Statistical analyses were carried out by calculating the p values using Student's t-test, and a value of $p \leq 0.05$ was considered to be statistically significant.

3.2.5 Knockdown Experiments

Small interfering RNA (siRNA) knockdown experiments were performed using siGENOME SMARTpool siRNA (Dharmacon) to knockdown mouse paxillin using a specific RNA sequence. A siRNA (ON-TARGETplus siCONTROL, Dharmacon) with the sequence UGGUUUACAUGUCGACUAA was used as the nonspecific (sham knock-down) control (12). The RNA interference oligonucleotides were transiently transfected in NIH-3T3 (EGFR) cells using Lipofectamine 2000, and the relative knockdown efficiency was determined using anti-mouse paxillin antibody against paxillin by western blotting (BD Biosciences).

3.2.6 Immunoblot Analysis

Cells were lysed in 25mM Tris, 100mM NaCl, 1mM EDTA, 1% (v/v) Triton X-100, 1 mM DTT, 1 mM sodium orthovanadate, 1 mM β-glycerol phosphate and 1μg/mL of leupeptin and aprotinin (lysis buffer), and whole-cell lysates (WCL) were recovered in the supernatant following microfuge centrifugation. Protein concentrations of the WCL were determined using the Bio-Rad DC protein assay. WCL (40μg) were resolved by SDS/PAGE, and proteins were transferred to PVDF membranes. Membranes were blocked by 10% (w/v) BSA diluted in 20 mM Tris, 135 mM NaCl, and 0.02% Tween 20 and incubated with the indicated primary antibodies diluted in the same buffer. The primary antibodies were detected with HRP-conjugated anti-mouse IgG (GE Healthcare) followed by exposure to ECL reagent (Invitrogen).

3.3 Results

3.3.1 Cellular EGFR is activated on micropatterned EGF surfaces

Micropatterned surfaces, with A568-streptavidin covalently attached to silicon substrates, were prepared as described in Materials and Methods. Figure 3.1A schematically depicts the preparation of micropatterned surfaces via the parylene lift-off method, and cell association with these. In initial experiments, RBL-2H3 cells transiently transfected with GFP-tagged EGFR were incubated with silicon substrates containing micro-patterned, covalently attached A568-streptavidin saturated with EGF-biotin. After 40 minutes at 37°C, we observed concentration of EGFR-GFP co-localized with the micron-sized EGF patches on the substrate, as detected via confocal fluorescence microscopy (Figure 3.1B). This clustering was not observed when the EGF-biotin was not attached to the micropatterned surfaces (data not shown).

NIH-3T3 cells endogenously express a small amount of EGFR that is hard to detect at micro-patterned, immobilized EGF on silicon substrates (data not shown). To visualize EGFR more clearly, we used NIH-3T3 cells stably over-expressing EGFR, which is localized primarily at the plasma membrane in these cells (21). All further experiments were done using these cloned NIH-3T3 (EGFR) cells, so that transfection efficiency of EGFR is not a variable in our experiments. As shown in Figures 3.1B and 3.2A, we find that EGFR, labeled with an anti-EGFR in these cells, is recruited to the EGF patches. Under these conditions, we detect robust tyrosine phosphorylation, colocalized with the clustered EGFR, most likely due to the EGFR kinase activity (Figure 3.2A – blue channel). The clustering of EGFR and enhanced tyrosine phosphorylation depends on the presence of EGF in the patterns (Figure 3.2A). This tyrosine phosphorylation can be detected as early as 10 minutes after plating in >90% of the imaged cells, and it increases in intensity with times up to 40 minutes after plating at 37^{o}C (data not shown).

Recruitment of signaling partners to micron-sized patches can be quantified by calculation of Pearson's cross-correlation coefficient, which evaluates the spatial coincidence of

two distinct labels. Consistent with our qualitative observations in confocal images, we find that the Pearson's cross-correlation coefficient is ~0.7 for EGFR localized to EGF patterns, and ~ 0.05 in absence of EGF-biotin at these patterns (Figure 3.2C). Similarly, the Pearson's coefficient for tyrosine phosphorylation at the patterns is ~0.8 in presence of EGF and ~ 0.06 in its absence.

We also detect tyrosine phosphorylation of EGFR specifically at tyrosine 1068 by labeling with an anti-phospho-tyrosine 1068 EGFR antibody (Figure 3.3A). Iressa is a potent inhibitor of the tyrosine kinase activity of EGFR (25), and when NIH-3T3 (EGFR) cells are serum starved overnight and plated in the presence of 10 μM Iressa for 40 minutes at 37°C on patterned EGF substrates, there is no detectable phosphorylation of EGF receptors at Tyr-1068 in EGF patterns (Figure 3.3A). None-the-less, in presence of Iressa, EGFR is recruited to the EGF patterns, even though there is no enhancement or concentration of tyrosine phosphorylation as detected by a more general anti-phospho-tyrosine antibody (Figure 3.3B). These results show that micro-patterned, immobilized EGF binds to and clusters EGFRs on the surface of the cells, but receptor activation and its consequent tyrosine phosphorylation depend on the EGFR kinase activity.

3.3.2 Paxillin is recruited and phosphorylated within activated EGFR clusters at the plasma membrane:

Paxillin, a multi-domain adaptor protein, is known to participate in integrin mediated signaling as a part of focal adhesions (26). In this role, it interacts with several actin cytoskeleton regulating proteins, including vinculin and talin (26, 27). We previously found that paxillin is recruited to clustered IgE receptor complexes, and it contributes to the regulation of IgE receptor signaling (12). Prior studies have shown that paxillin plays an important role in the activation of

Figure 3.1: EGFR binds to patterned EGF: A) A schematic showing fabrication of EGF patterned surfaces and subsequent incubation of cells on the patterned substrate. B) RBL-2H3 cells transiently transfected with EGFR-GFP (top panel), incubated on covalently immobilized EGF patterns for 40 minutes at 37°C, prior to fixation by 4% paraformaldehyde for 20 minutes at room temperature. The bottom panel shows NIH-3T3 cells stably over expressing wt-EGFR, plated on micro-patterned EGF surfaces for 40 min at 37°C. EGFR is labeled with an anti-EGFR primary, and an A488 tagged secondary antibody. (Scale bar: 20 μm)

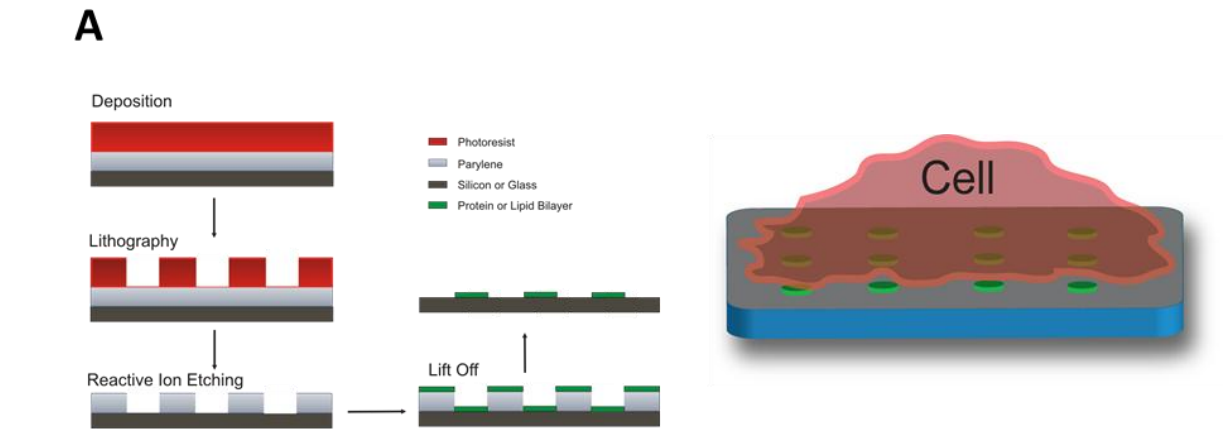
A
Deposition
Lithography
Reactive Ion Etching
Lift Off
Photoresist
Parylene
Silicon or Glass
Protein or Lipid Bilayer
Cell

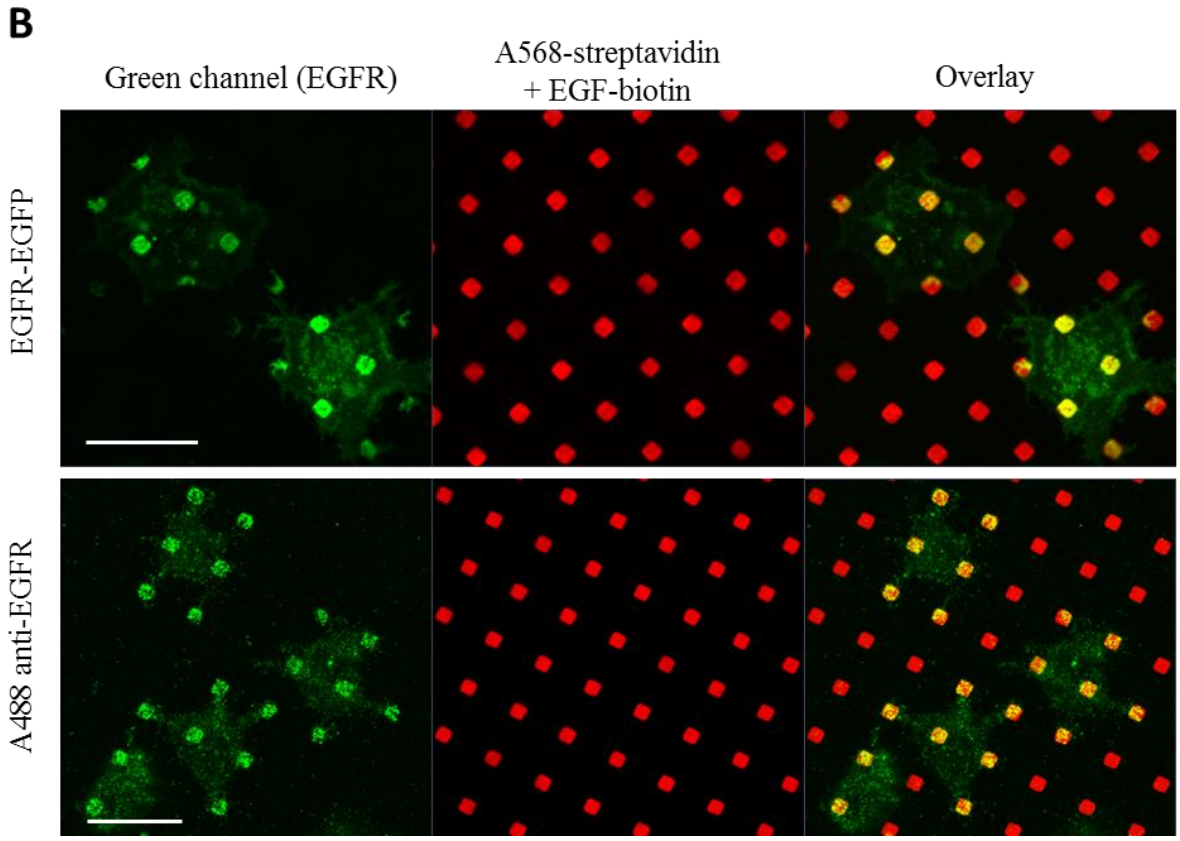
B
Green channel (EGFR)
A568-streptavidin
+ EGF-biotin
Overlay
EGFR-EGFP
A488 anti-EGFR

Figure 3.2 EGFR is activated in a ligand dependent manner on patterns: A) NIH-3T3 cells stably over-expressing EGFR were plated onto micro-patterned, covalently immobilized EGF (labeled by A568-streptavidin – red channel), for 40 minutes at 37°C prior to fixation with paraformaldehyde. The same conditions were used for incubating the cells in all the subsequent experiments, unless specified otherwise. The cells were subsequently immunolabeled with anti-EGFR primary antibody and A488 tagged secondary antibody (green channel). These cells were also immunolabeled with an anti-phospho-tyrosine primary antibody and A647 tagged secondary antibody (blue channel). The bottom panel shows the NIH-3T3 (EGFR) cells plated on micro-patterned surfaces without EGF-biotin bound to the covalently immobilized A568-streptavidin. B) Quantification of colocalization by calculating Pearson's correlation coefficients for green channel with red channel, and blue channel with red channel, as described in Materials and Methods. Error bars represent SEM; **** indicates $p \leq 0.0001$, $n > 40$ cells over 3 independent experiments. Scale bar: 20 μm

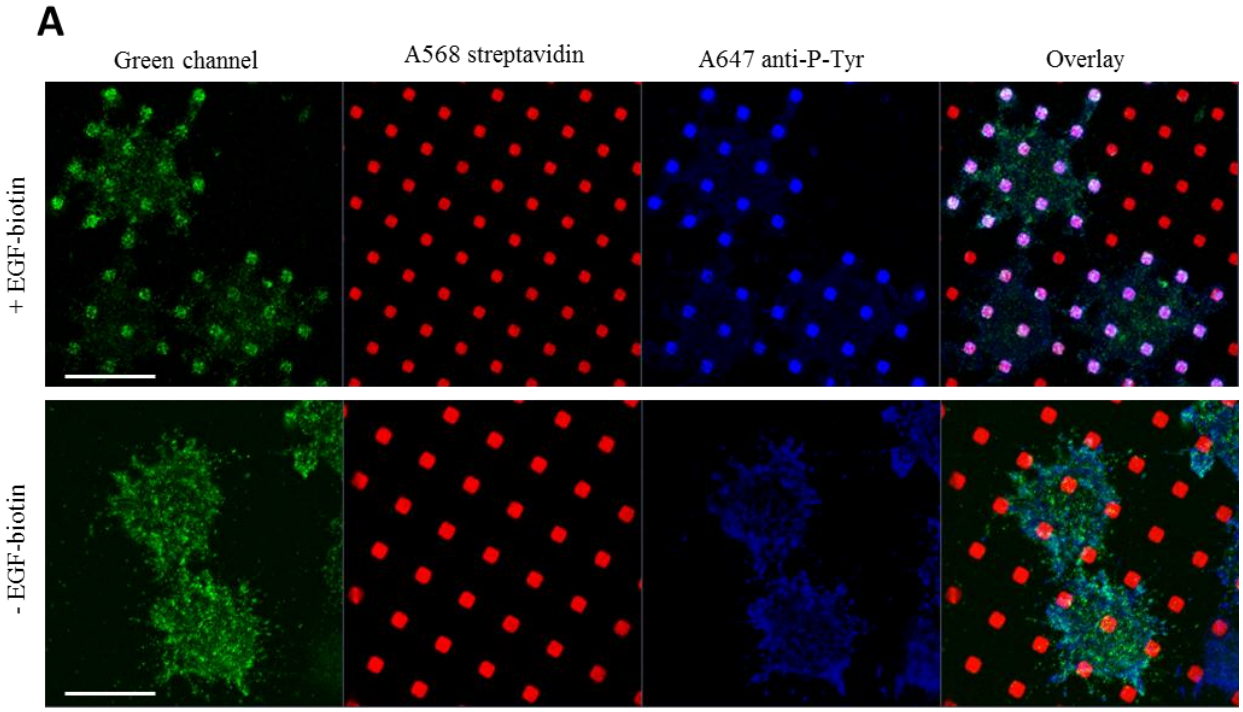
A
Green channel
A568 streptavidin
A647 anti-P-Tyr
Overlay
+ EGF-biotin
- EGF-biotin

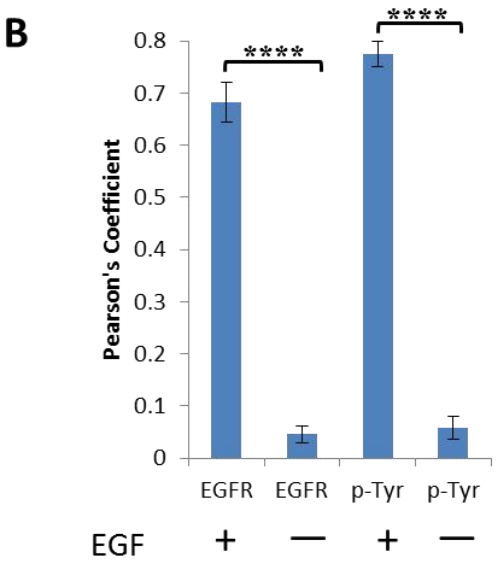
B
****
****
Pearson's Coefficient
0.8
0.7
0.6
0.5
0.4
0.3
0.2
0.1
0
EGFR
EGFR
p-Tyr
p-Tyr
EGF
+
—
+
—

Erk after EGFR stimulation (10). We examined the distribution of paxillin-GFP in NIH-3T3 (EGFR) cells under conditions of EGFR clustering at the patterns, and we observed that paxillin-GFP is visibly concentrated at these patterned features (Figure 3.4A, top panel). This concentration at patterned surfaces is not observed in the absence of EGF-biotin (Figure 3.4A, middle panel). Quantification of this co-localization using Pearson's cross-correlation coefficient gives a value of ~0.25 for paxillin-GFP colocalization with A568-streptavidin patches when EGF is present on the surface, substantially higher than the value when EGF-biotin is absent from the surface (~0.05, Figure 3.4B). In addition, this recruitment of paxillin-GFP is also inhibited by treatment of cells with EGFR kinase inhibitor Iressa, demonstrating its dependence on tyrosine kinase activation (Figure 3.4A, bottom panel, and Figure 3.4B).

Paxillin has several sites of phosphorylation that mediate its binding to several different proteins (28). Paxillin is phosphorylated at Tyr 31 and Tyr118 by Src kinase (29), and at Ser 83 (30) and Ser 126 (31) by Erk kinase. We find that paxillin recruited to clustered EGFR is phosphorylated at Tyr 31 and/or 118 residues, identified by labeling with anti-paxillin Tyr 118 antibody (Figure 3.5). Paxillin recruited to clustered EGFR is also phosphorylated at Ser 126 as detected by labeling with anti-paxillin phospho-Ser126 antibody (Figure 3.5A). Quantification of these results using Pearson's analysis shows that there is significant association of tyrosine phosphorylated paxillin (~0.41) and serine phosphorylated paxillin (~0.28) on EGF patterns (Figure 3.5B).

To examine the dependence of paxillin recruitment and phosphorylation on Src kinase activity, we tested the effect of PP2, a well-known Src kinase inhibitor. As expected, tyrosine phosphorylation of recruited paxillin is inhibited by pretreatment with 20 μM PP2. However,

Figure 3.3: Activation, but not recruitment of EGFR to EGF patches, depends on EGFR kinase activity: A) NIH-3T3 (EGFR) cells were plated onto micro-patterned EGF surfaces (red channel) for 40 minutes at 37°C prior to fixation. These cells were then immunolabeled with anti-phospho-Tyr-1068 EGFR primary antibody and A488 tagged secondary antibody (green channel). Bottom panel: NIH-3T3 (EGFR) cells pretreated with 10 μM Iressa overnight and plated in presence of 10 μM Iressa on micro-patterned EGF surfaces. B) NIH-3T3 (EGFR) cells plated on micro-patterned EGF surfaces without (top panel) and with (bottom panel) Iressa pretreatment. Cells were then immunolabeled with anti EGFR antibody (A488 – green channel) and 4G-10 anti-phospho-Tyr antibody (A647 secondary – blue channel). Scale bar: 20 μm

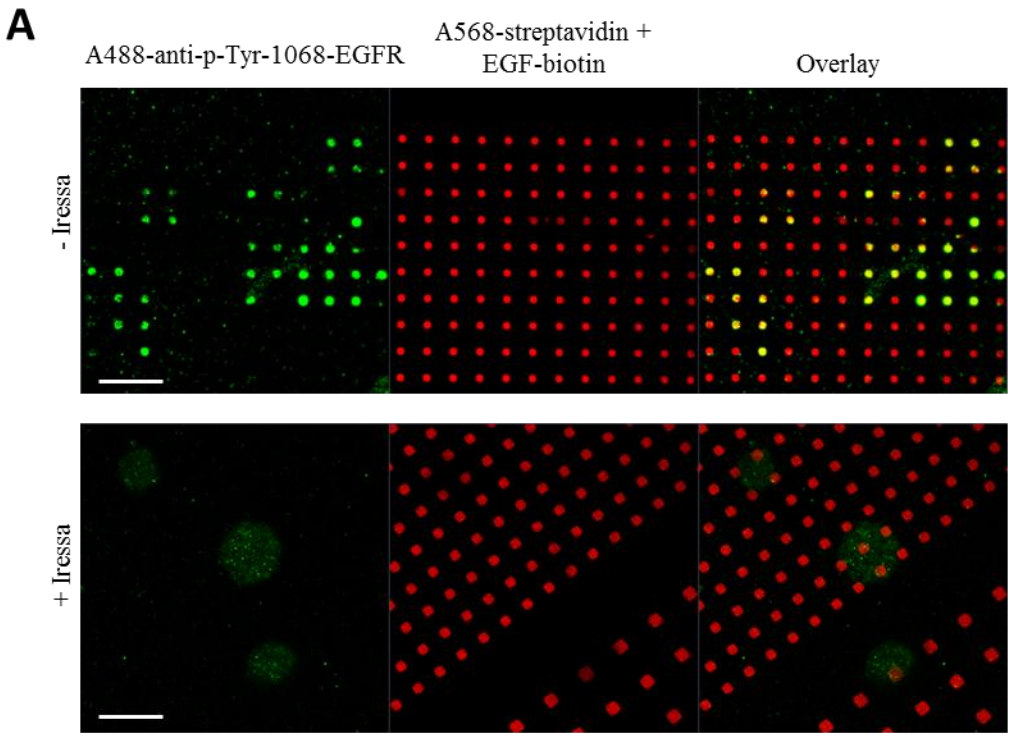
A
A488-anti-p-Tyr-1068-EGFR
A568-streptavidin +
EGF-biotin
Overlay
- Iressa
+ Iressa

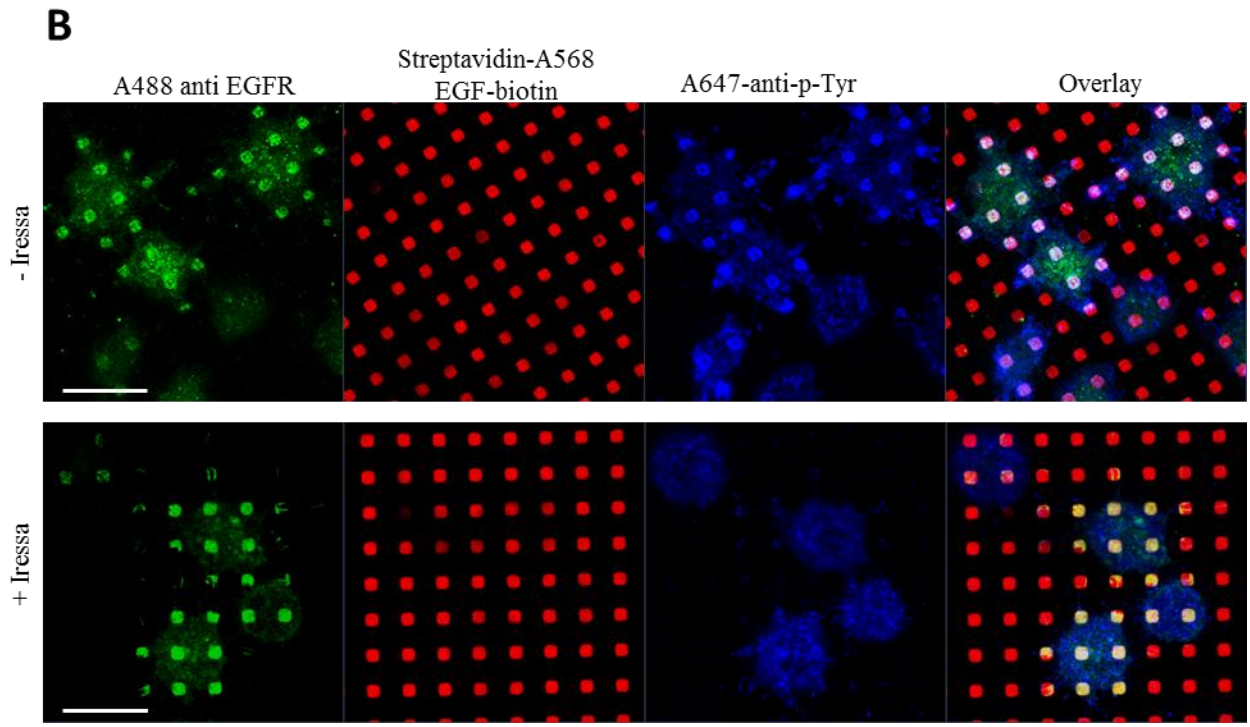
B
A488 anti EGFR
Streptavidin-A568
EGF-biotin
A647-anti-p-Tyr
Overlay
- Iressa
+ Iressa

Figure 3.4: Paxillin is recruited to the EGF patterns in a ligand dependent manner: A) NIH-3T3 (EGFR) cells transiently transfected with paxillin-GFP (green channel), were plated on micro-patterned, covalently attached A568-streptavidin (red channel) surfaces with EGF-biotin (top panel), or without EGF-biotin (middle panel). The bottom panel shows the NIH-3T3 (EGFR) cells transiently transfected with paxillin-GFP and pretreated with 10 μM Iressa overnight, prior to incubation on micropatterned EGF surfaces. B) Quantification with Pearson's cross correlation coefficients to compare red and green channels; N > 20 cells for each sample at least 2 independent experiments. Error bars represent SEM; **** indicates $p \leq 0.0001$, *** indicates $p \leq 0.001$. Scale bar: 20 μm.

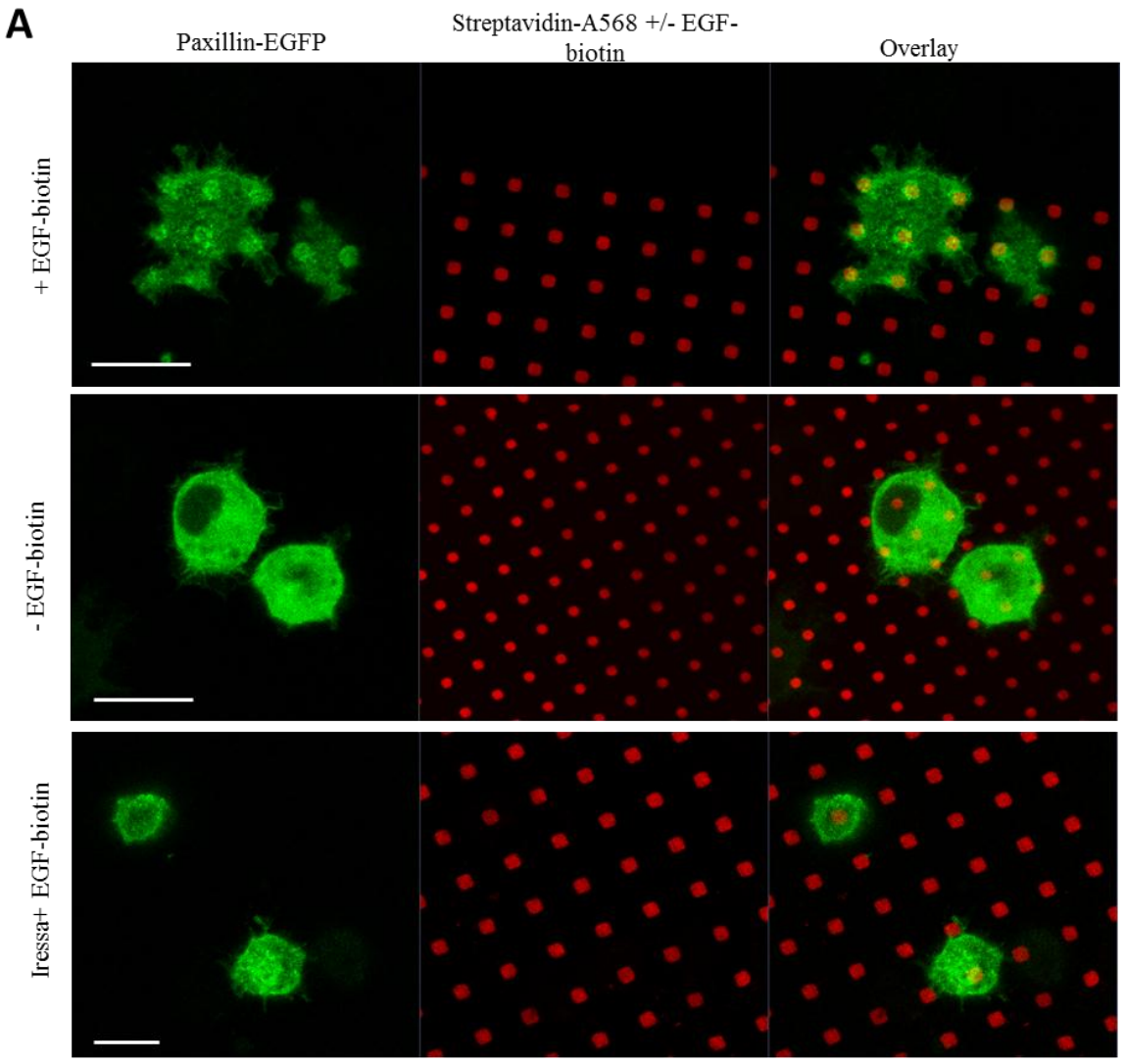
A
Paxillin-EGFP
Streptavidin-A568 +/- EGF-biotin
Overlay
+ EGF-biotin
- EGF-biotin
Iressa+ EGF-biotin

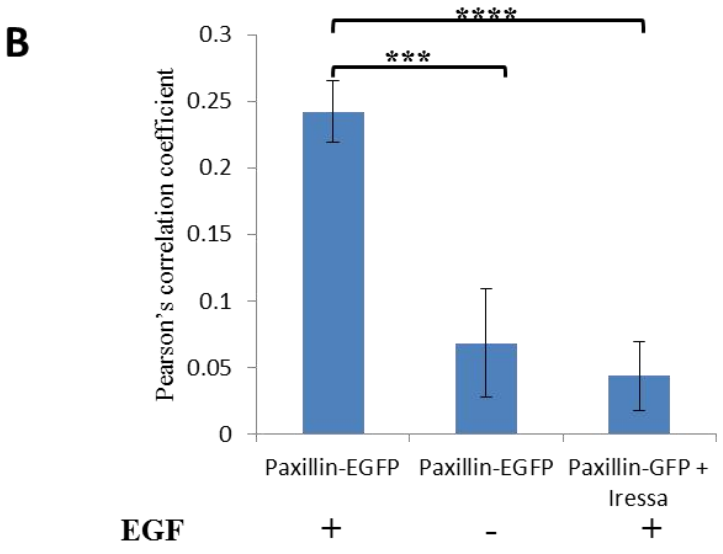
B
****
***
Pearson's correlation coefficient
0.3
0.25
0.2
0.15
0.1
0.05
0
Paxillin-EGFP
Paxillin-EGFP
Paxillin-GFP + Iressa
EGF
+
-
+

Figure 3.5 Paxillin is phosphorylated in EGFR signaling complexes at the plasma membrane: A) NIH-3T3 (EGFR) cells transiently transfected with paxillin-EGFP (top panel, green channel) were incubated with micro-patterned EGF surfaces (red channel). NIH-3T3 (EGFR) cells, incubated with micropatterned EGF surfaces prior to fixation, were immunolabled with anti-phospho-Tyr 118 anti-paxillin antibody (green channel, middle panel) or anti-phospho-Ser paxillin antibody (green channel, bottom panel). B) Co-localization of paxillin with micro-patterned EGF is quantified by Pearson's cross correlation coefficients between green and red channels; N > 30 cells per sample, from at least 2 independent experiments. Error bars represent SEM. Scale bar: 20μm

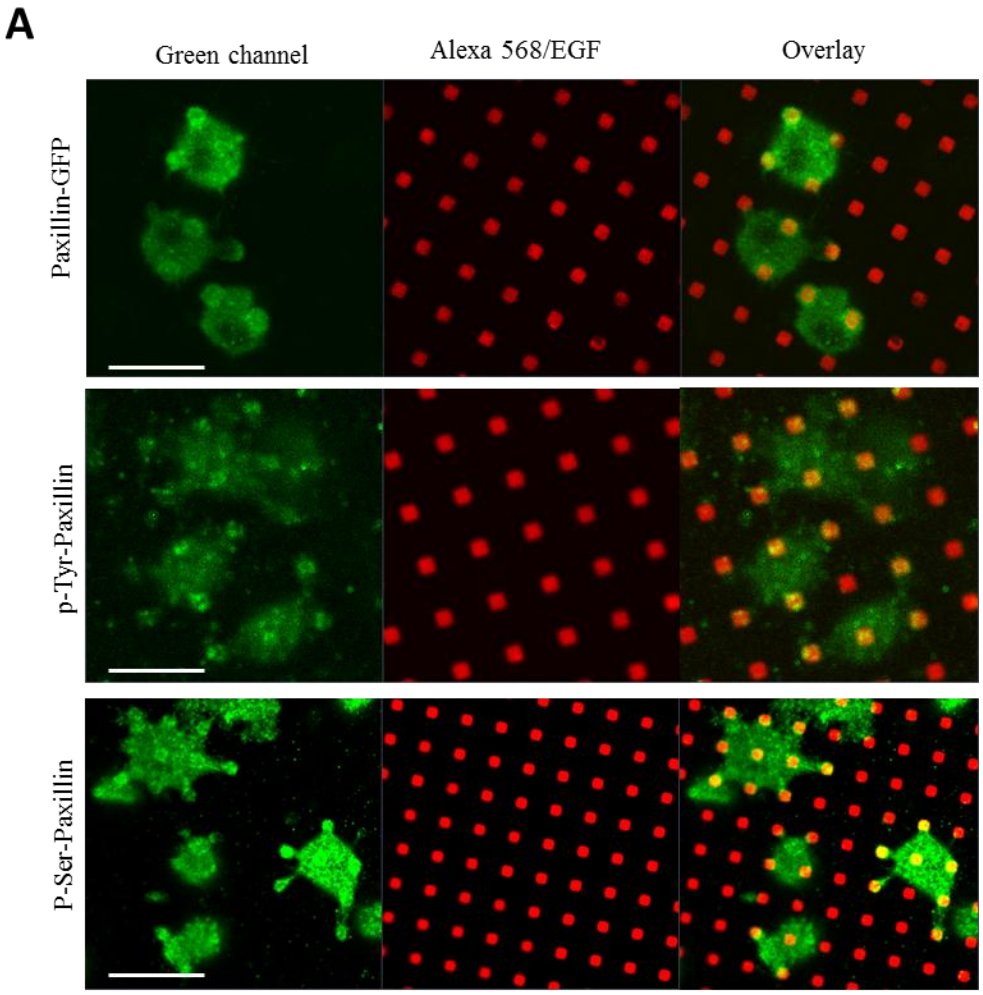
A
Green channel
Alexa 568/EGF
Overlay
Paxillin-GFP
p-Tyr-Paxillin
P-Ser-Paxillin

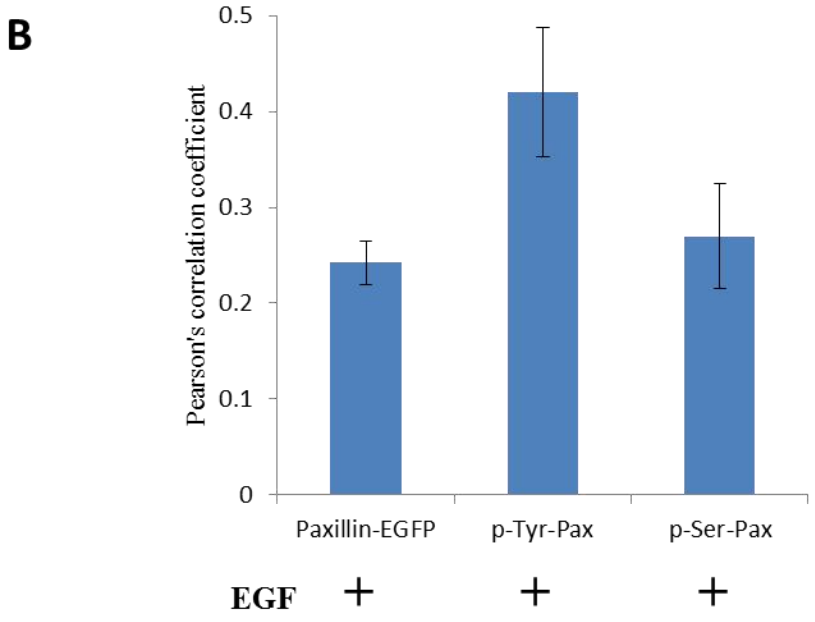
B
Pearson's correlation coefficient
0.5
0.4
0.3
0.2
0.1
0
Paxillin-EGFP
p-Tyr-Pax
p-Ser-Pax
EGF
+
+
+

PP2 does not inhibit recruitment of paxillin-GFP or paxillin phosphorylation at serine residues (Figure 3.6A, B). Quantification of cross-correlation between these labels and Alexa568-streptavidin shows very low Pearson's correlation coefficient values for tyrosine phosphorylated paxillin and EGF patterns in presence of PP2. In contrast, a slight enhancement in colocalization of paxillin-GFP and serine phosphorylated paxillin is detected with EGF patterns under these conditions (Figure 3.6C). Together, these results indicate that paxillin is recruited to clustered EGFR at the plasma membrane in a ligand-dependent and EGFR kinase activity-dependent manner. Furthermore, recruited paxillin is phosphorylated on tyrosine residues by Src, and paxillin recruitment and serine phosphorylation do not depend on Src activity.

3.3.3 F-actin is recruited to the activated EGFR complexes, whereas α5 integrin is excluded.

A previous study showed that F-actin co-localizes with IgE receptors clustered in micron-scale patterns (11). Similarly, we found that F-actin labeled with Alexa488-phalloidin in NIH-3T3(EGFR) cells concentrates at with the patterned EGF(Figure 3.7A). This clustering of F-actin can be observed as soon as 10 minutes after plating the cells and is maximal after 30 minutes of plating. Inhibition of actin polymerization by 2 μM cytochalasin D during cell attachment substantially reduces this local accumulation. Quantification by Pearson's analysis shows substantial co-localization of F-actin with patterned EGF in the absence of cytochalasin D (Figure 3.7B). We evaluated whether ezrin or moesin, which connect the actin cytoskeleton to the plasma membrane under some conditions (32), become concentrated in the location of clustered EGFR. We detected no such concentration of these labeled proteins in three separate experiments (Figure 3.7A and B).

Because paxillin and F-actin are often concentrated in focal adhesions as modulated by integrins (33), we examined whether integrins are also localized to the EGFR signaling complexes. Integrin α5 is the most abundant integrin alpha subunit in NIH-3T3 cells (34), and we expressed a GFP-tagged form of this protein. As shown in Figure 3.8, we find that this protein is excluded from EGFR clusters on the patterned surfaces. In > 80% cells, we find that integrin α5-GFP is depleted from the regions of patterned EGF. This contrasts with F-actin and paxillin, which are concentrated in these regions. This exclusion of integrin α5-GFP is observed even in the presence of cytochalasin D, suggesting that it is independent of focal adhesion complexes (data not shown).

3.3.4 The Erk signaling pathway is recruited to patterned EGF.

EGFR activated by EGF initiates a signaling cascade leading to activation of Ras (Figure 1.5), MEK, and Erk (35, 36). EGFR phosphotyrosine residues are the docking sites for binding of Grb2, which in turn activates son of sevenless (SOS), a guanine nucleotide exchange factor (GEF) that activates Ras (37). To investigate whether proteins in the Erk signaling pathway co-localize with clustered, activated EGFR, GFP-H-Ras was transiently expressed in NIH 3T3 (EGFR) cells, and these cells were plated on EGF-patterned surfaces for 40 minutes at 37°C. Confocal imaging shows concentration of GFP-H-Ras fluorescence with patterned EGF in >95% of imaged cells (Figure 3.9A). We see similar recruitment of transiently transfected GFP-N-Ras to these patterned EGF (data not shown). This recruitment of GFP-H-Ras to the patterned EGF is not reduced by 20 μM PP2, indicating no dependence on Src kinase activity (data not shown).

Figure 3.6: Tyrosine phosphorylation, but not recruitment of paxillin, depends on Src kinase: A) NIH-3T3 (EGFR) cells, transiently transfected with paxillin-GFP (green channel) and pretreated with 20 μM PP2, a Src kinase inhibitor, were incubated with micropatterned EGF surfaces (red channel). B) NIH-3T3 (EGFR) cells, pretreated with 20 μM PP2 and incubated with micropatterned EGF surfaces and subsequently immunolabeled with anti-phospho-Tyr 118 anti-paxillin antibody (green channel, top panel) or anti-phospho-Ser paxillin antibody (green channel, bottom panel). C) Quantification of colocalization by calculation of Pearson's cross correlation coefficients for green channel with red channel, N > 20 cells, from at least 2 independent experiments. Error bars represent SEM; *** indicates $p \leq 0.001$. Scale bar: 20 μm.

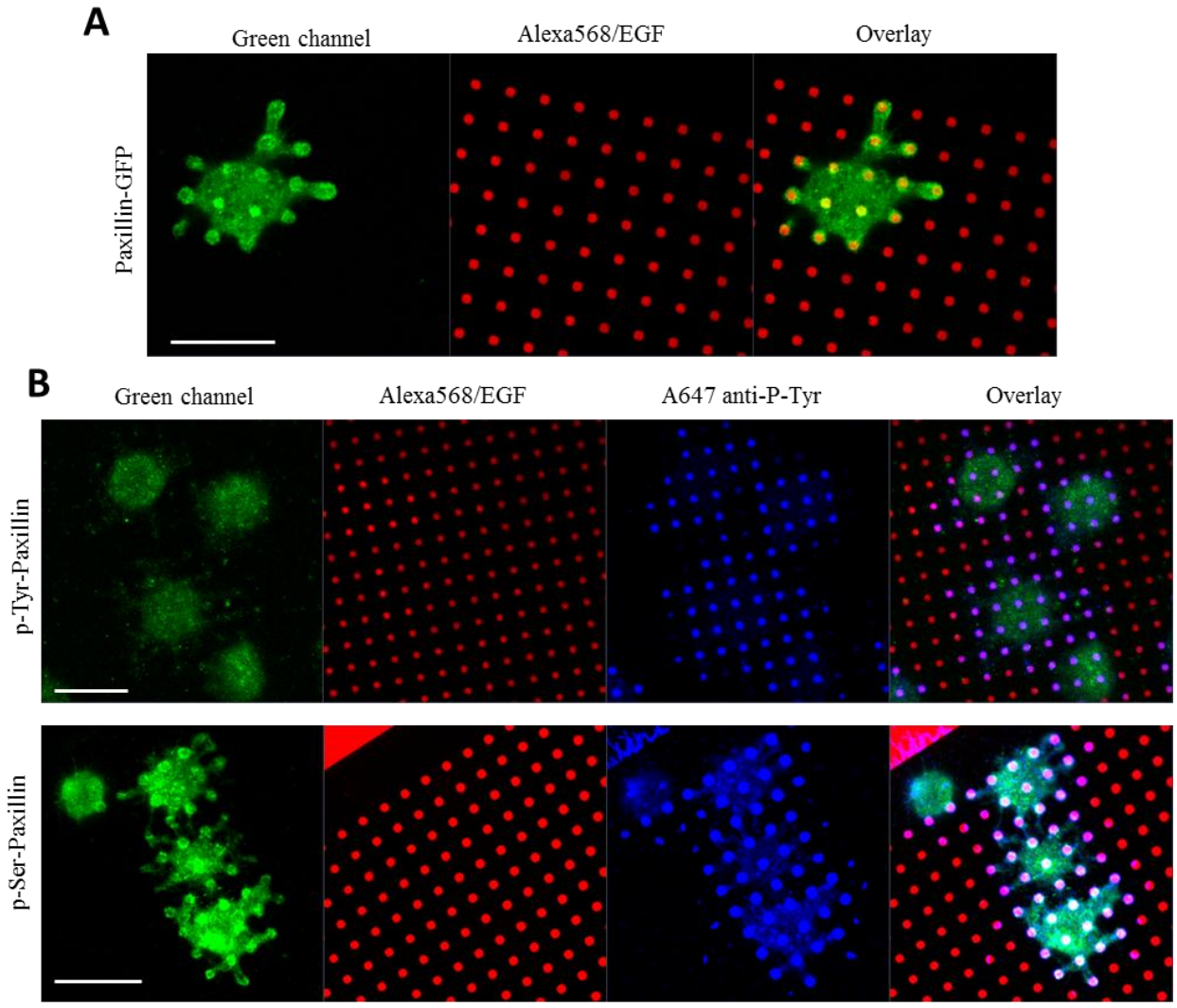
A
Green channel
Alexa568/EGF
Overlay
Paxillin-GFP
B
Green channel
Alexa568/EGF
A647 anti-P-Tyr
Overlay
p-Tyr-Paxillin
p-Ser-Paxillin

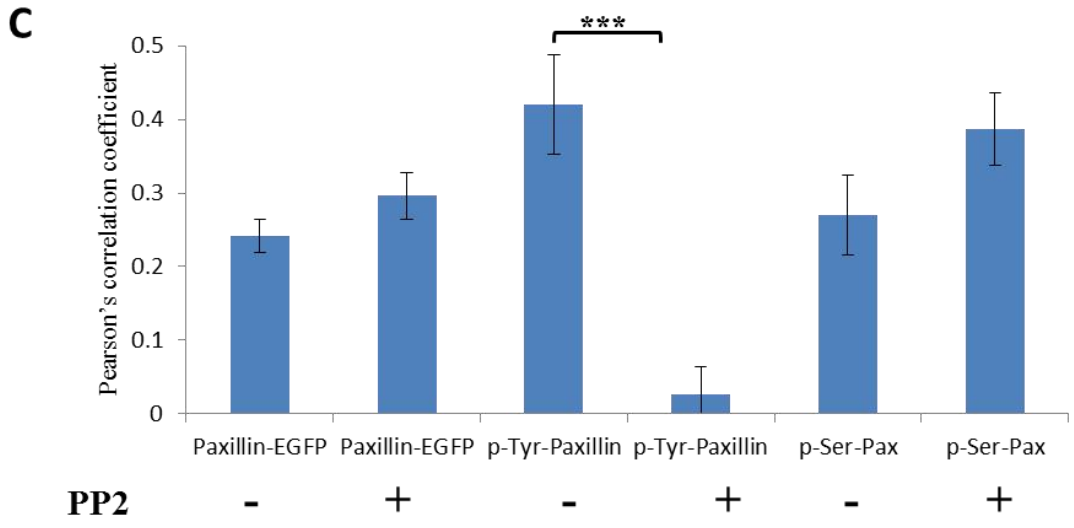
C
***
Pearson's correlation coefficient
0.5
0.4
0.3
0.2
0.1
0
Paxillin-EGFP
Paxillin-EGFP
p-Tyr-Paxillin
p-Tyr-Paxillin
p-Ser-Pax
p-Ser-Pax
PP2
-
+
-
+
-
+

Figure 3.7: F-actin co-redistributes with EGFR complexes on the plasma membrane: A) NIH-3T3 (EGFR) cells were plated onto micropatterned EGF surfaces (red channel) and immunolabeled with A488-phalloidin (green channel, top panel), anti-moesin (middle panel), or anti-ezrin (bottom panel). B) Quantification of colocalization by calculation of Pearson's cross-correlation coefficients for green channel with red channel, N > 20 cells per sample, from 2 independent experiments. Error bars represent SEM; **** indicates $p \leq 0.0001$, *** indicates $p \leq 0.001$. Scale bar: 20 μm.

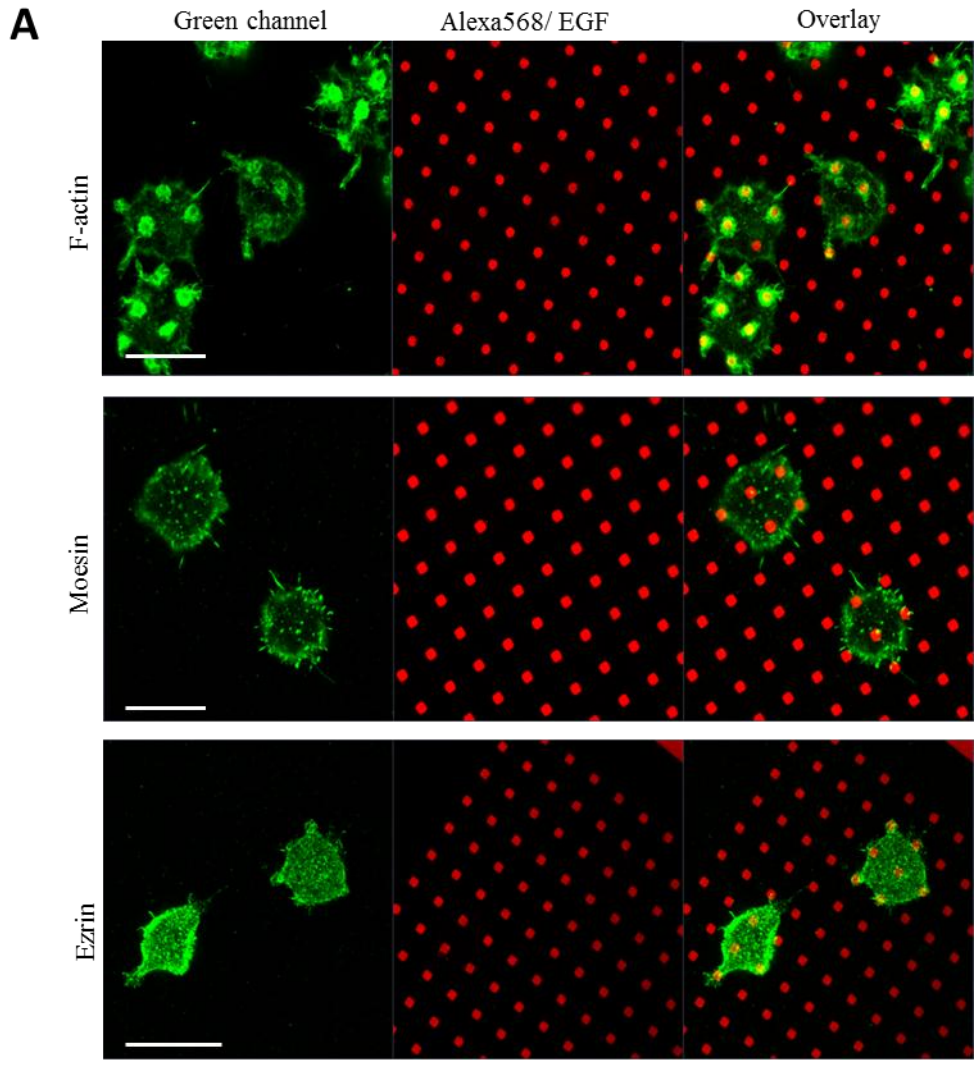
A
Green channel
Alexa568/ EGF
Overlay
F-actin
Moesin
Ezrin
B
Pearson's correlation coefficeint
0.5
0.45
0.4
0.35
0.3
0.25
0.2
0.15
0.1
0.05
0
***
F-actin
F-actin
Moesin
Ezrin
Cyto D
-
+
-
-

Figure 3.8: Integrin α-5 is excluded from EGF-bound EGFR signaling complexes: A) NIH-3T3 (EGFR) cells transiently transfected with integrin α5-EGFP (green channel) were plated on micro-patterned A568-streptavidin (red channel) with EGF-biotin (top panel) or without EGF-biotin (bottom panel). B) Quantification by calculation of Pearson's cross-correlation coefficients for green channel with red channel. N > 20 cells, in 2 independent experiments. Error bars represent SEM; *** indicates $p \leq 0.001$, ** indicates $p \leq 0.01$. Scale bar: 20 μm.

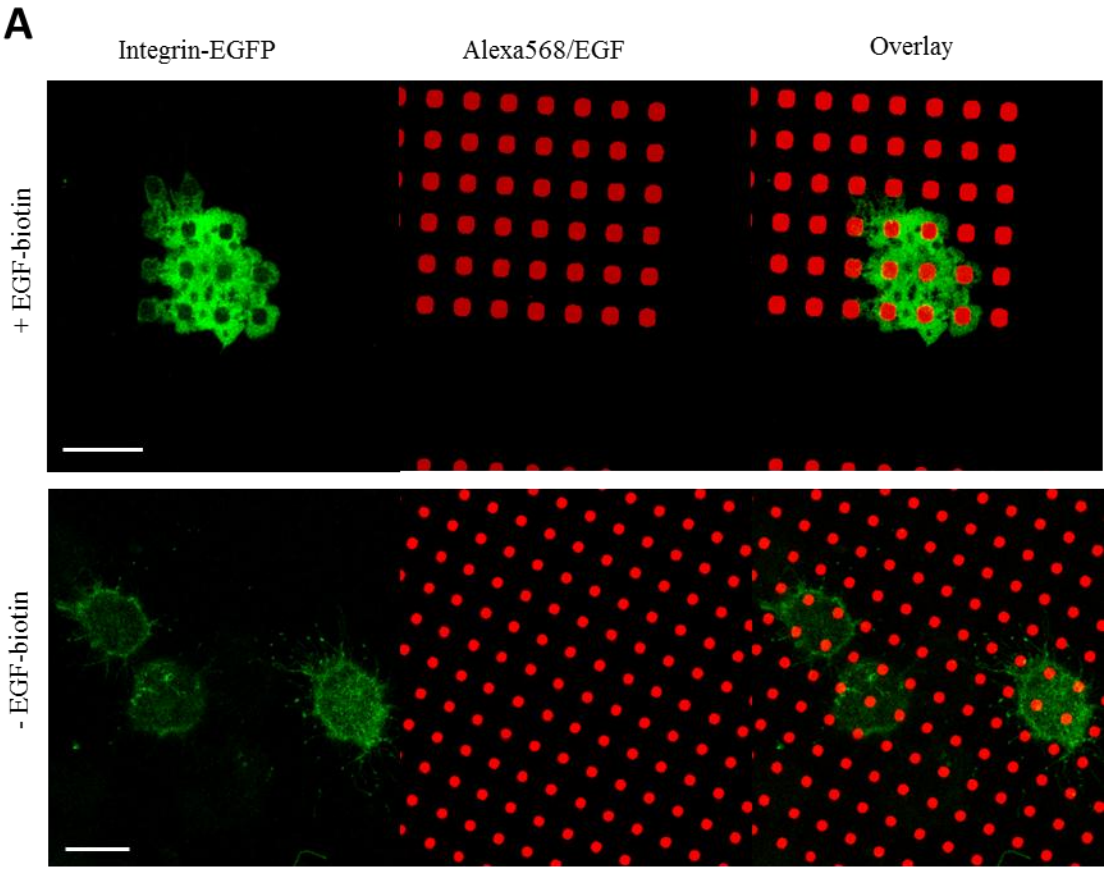
A
Integrin-EGFP
Alexa568/EGF
Overlay
+ EGF-biotin
- EGF-biotin

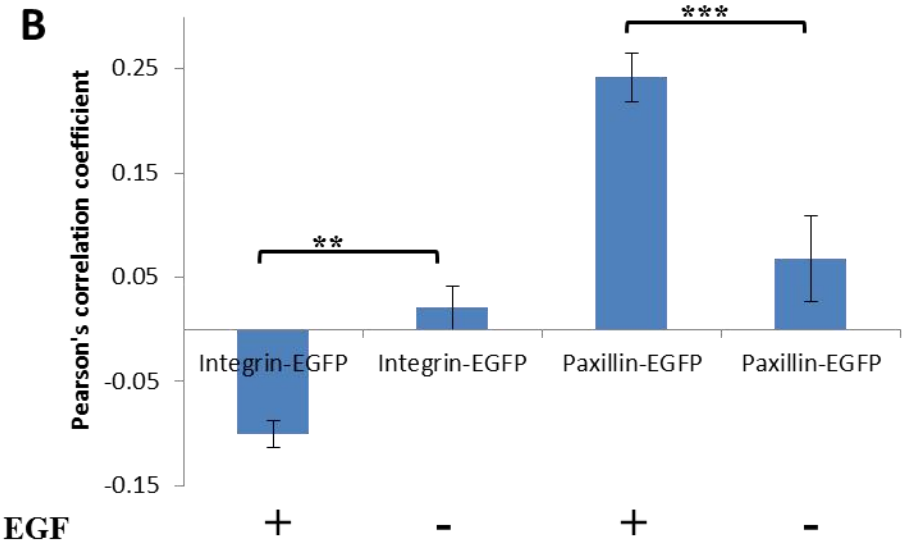
B
Pearson's correlation coefficient
0.25
0.15
0.05
-0.05
-0.15
**
***
Integrin-EGFP
Integrin-EGFP
Paxillin-EGFP
Paxillin-EGFP
EGF
+
-
+
-

Figure 3.9: Proteins involved in the Erk signaling cascade -- Ras, MEK and Erk -- co-redistribute with EGFR signaling complexes on plasma membrane: A) NIH-3T3 (EGFR) cells transiently transfected with GFP-H-Ras (green channel, top panel), were plated on micro-patterned EGF surfaces. NIH-3T3 (EGFR) cells were plated on micro-patterned EGF surfaces, and after fixation they were immunolabeled with anti-MEK (green channel, middle panel) or anti-phospho-Erk (green channel, bottom panel) antibodies, followed by A488 labeled secondary antibodies. B) Quantification by calculation of Pearson's cross-correlation coefficients of green channel with red channel; $N > 30$ cells from 3 independent experiments. Error bars represent SEM; *** indicates $p \leq 0.001$, ** indicates $p \leq 0.01$. Scale bar: 20 μm.

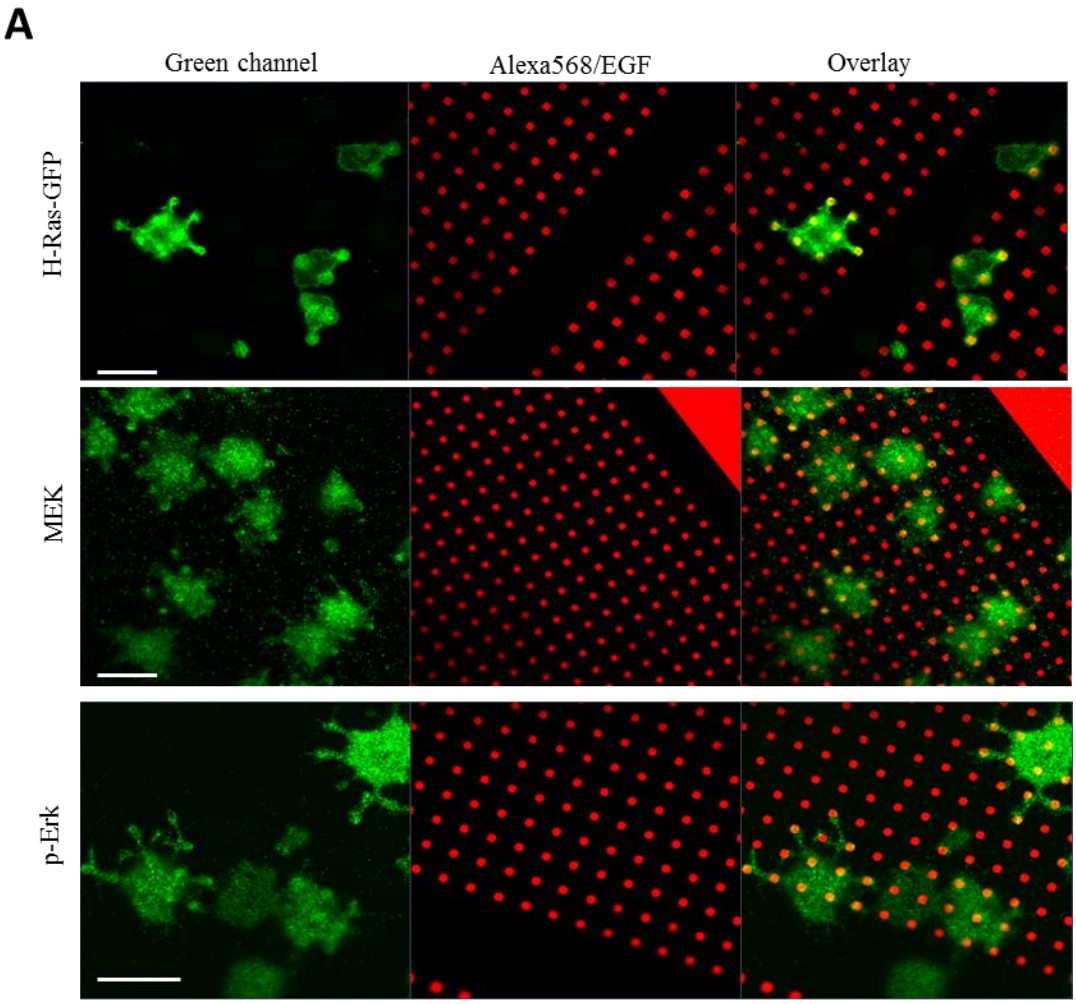
A
Green channel
Alexa568/EGF
Overlay
H-Ras-GFP
MEK
p-Erk

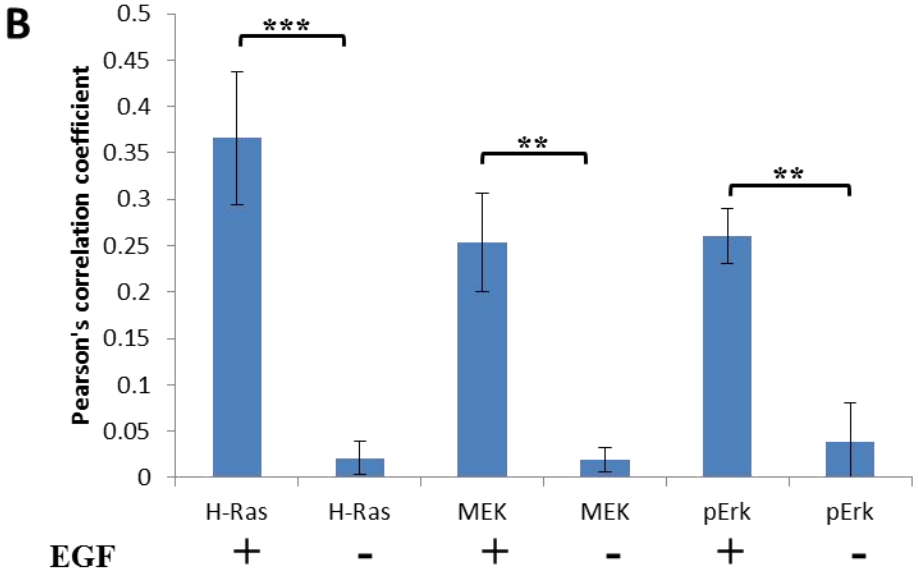
B
Pearson's correlation coefficient
0.5
0.45
0.4
0.35
0.3
0.25
0.2
0.15
0.1
0.05
0
***
**
**
H-Ras
H-Ras
MEK
MEK
pErk
pErk
EGF
+
-
+
-
+
-

Similar to results with GFP-H-Ras, we also observed colocalization of MEK and pErk with the patterned EGF using specific antibodies post fixation (Figure 3.9A). Quantitative analysis of co-localization by cross-correlation analysis shows limited but statistically significant recruitment of these more downstream partners in the Erk activation pathway in a ligand-dependent manner (Figure 3.9B). In addition to their recruitment to clustered EGFR, a noticeable fraction of the fluorescent label for MEK and pErk becomes localized in the nucleus under these conditions of cell activation (observed with z-sectioning; data not shown). These results provide evidence for the formation of a macromolecular signaling complex colocalized with clustered EGFR on the patterned surface that includes all of the principal proteins in the Erk signaling cascade.

3.3.5 Recruitment of EGFR signaling partners to patterned EGF depends on the actin cytoskeleton.

Our laboratory previously reported actin cytoskeleton-dependent recruitment of Lyn to clustered IgE on patterned ligands, even though catalytic amounts of Lyn required for phosphorylation of FcεRI is not inhibited by cytochalasin D (11). In the present experiments, we observe that recruitment of paxillin and p-Erk to patterned EGF is inhibited by cytochalasin D (Figure 3.10A), even though cytochalasin D does not inhibit the recruitment or activation of the EGFR to EGF on patterns, as observed by localized, concentrated labeling of EGFR and phosphotyrosine detected by 4G10 mAb (Figure 3.10A – blue channel). We further found that treatment with cytochalasin D does not inhibit phosphorylation of recruited EGFR at tyrosine 1068, consistent with a lack of cytoskeletal dependence of these early events under these conditions (data not shown). We did not detect recruitment of H-Ras and MEK to patterned EGF in presence of cytochalasin D (data not shown).

Quantification by Pearson's correlation coefficient shows that there is a significant decrease in the colocalization of p-Erk and paxillin with patterned EGF in presence of cytochalasin D (Figure 3.10B). In a previous study, cytochalasin D did not inhibit activation of Erk in Rat 1a fibroblasts by soluble EGF (38). In our experiments with cytochalasin D, we observe that stimulation of surface-attached NIH-3T3 (EGFR) cells by soluble EGF (50 ng/mL) caused a partial decrease in the activation of Erk, as compared to cells stimulated in absence of cytochalasin D, as detected by western blotting (Figure 3.10C). Quantification of this Erk phosphorylation stimulated by soluble EGF indicates ~50% inhibition due to cytochalasin D (Figure 3.10D). This suggests that the actin cytoskeleton stabilizes the EGFR signaling complexes formed by either soluble or immobilized EGF and thereby participates in Erk activation due to stimulation of EGFR.

3.3.6: Dynamin 2, PLCγ-1, and Lyn are recruited to patterned EGF:

Dynamin 2 is a GTPase that is commonly implicated in internalization of receptors on cell surfaces by facilitating fission of the forming endosomes from the plasma membrane (39). In Chapter 2, we showed that dynamin 2 plays a role in the organization of actin cytoskeleton at the sites of IgE receptor endocytosis. Here, we find that dynamin 2-GFP expressed in NIH-3T3 (EGFR) cells is recruited to patterned EGF in >90% of the dynamin 2-GFP expressing cells (Figure 3.11A). This recruitment is not inhibited by cytochalasin D (data not shown), similar to previous observations with IgE receptors concentrated in micron-scale patterns (Chapter 2, Figure 2.13)

Phospholipase Cγ1 (PLCγ1) is an enzyme that mediates hydrolysis of $PI(4,5)P_2$ to inositol 1,4,5 triphosphate (IP_3) and diacylglycerol (DAG), and it was previously shown to bind directly to activated EGFR via its tandem SH2 domains (40). NIH-3T3 (EGFR) cells transiently

Figure 3.10: Recruitment of pErk and paxillin depend on F-actin polymerization: A) NIH-3T3 (EGFR) cells transiently transfected with paxillin-EGFP (top panel, green channel) were pretreated with 2 μM cytochalasin D prior to incubation on the micro-patterned EGF surfaces. NIH-3T3 (EGFR) cells incubated with micro-patterned EGF surfaces in presence of 2 μM cytochalasin D and immunolabeled with anti-phospho-Erk primary and an A488 tagged secondary antibody (green channel, bottom panel). B) Pearson's cross-correlation coefficient of green channel with red channel. N > 30 cells over 2 independent experiments. C) Surface adhered NIH-3T3 (EGFR) cells, treated with or without cytochalasin D, EGF are solubilized and prepared for western blotting. Proteins separated on SDS gels were labeled with anti-EGFR, anti-phospho-Tyr-1068, and anti-phospho-Erk antibodies. D) Calculated intensities of phospho-Erk bands from the western blots over 3 independent experiments. The intensities were normalized for each individual experiment (where pErk band intensity of sample stimulated with EGF in absence of cytochalasin D was normalized to 1, and the remaining intensities were normalized accordingly), where band intensity obtained for EGF treatment in absence of cytochalasin D was normalized to 1. Error bars represent SEM; *** indicates $p \leq 0.001$, * indicates $p \leq 0.05$. Scale bar: 20 μm.

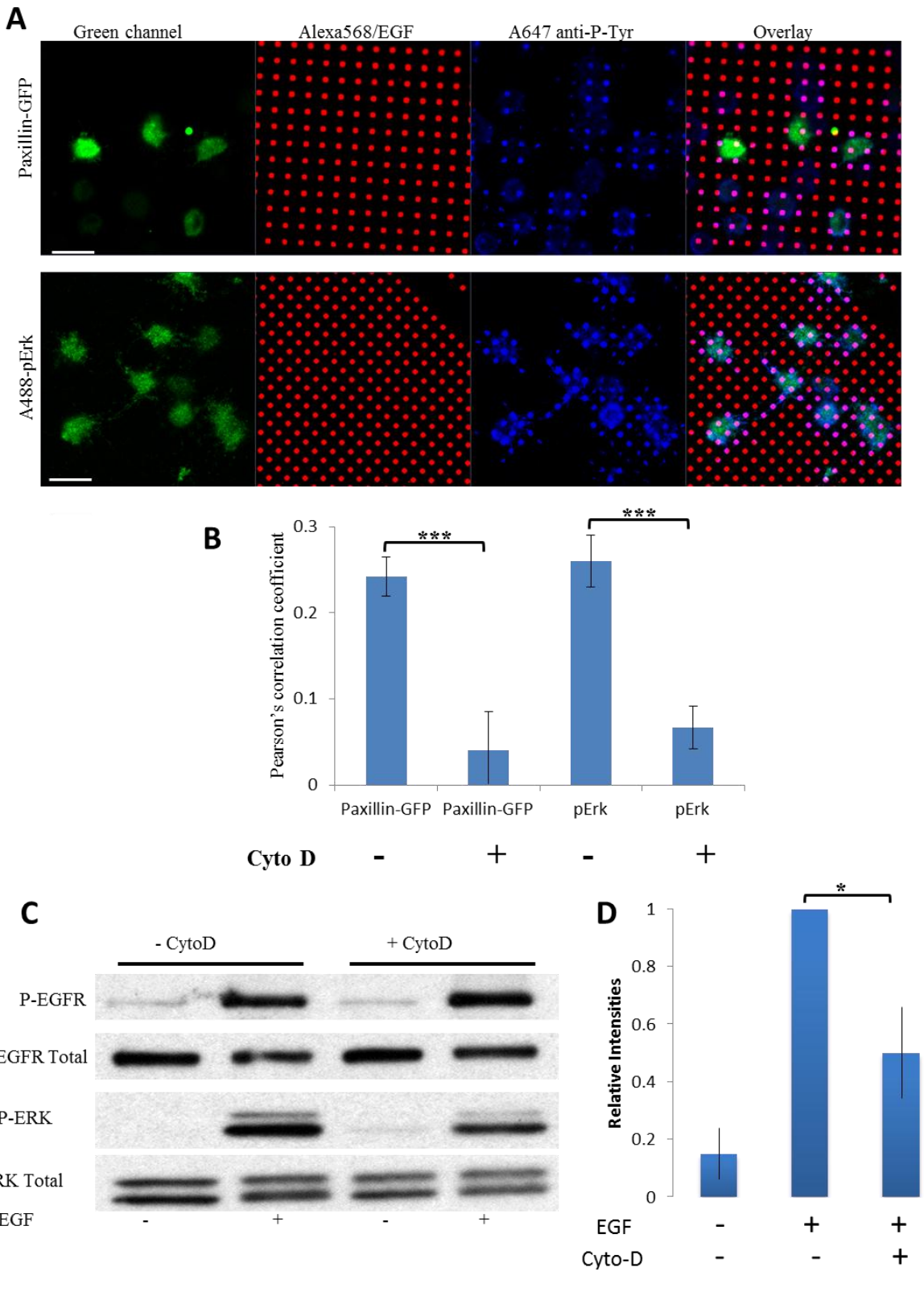
A
Green channel
Alexa568/EGF
A647 anti-P-Tyr
Overlay
Paxillin-GFP
A488-pErk
B
Pearson's correlation ceofficient
0.3
0.2
0.1
0
***
***
Paxillin-GFP
Paxillin-GFP
pErk
pErk
Cyto D
-
+
-
+
C
- CytoD
+ CytoD
P-EGFR
EGFR Total
P-ERK
ERK Total
EGF
-
+
-
+
D
*
Relative Intensities
1
0.8
0.6
0.4
0.2
0
EGF
-
+
+
Cyto-D
-
-
+

Figure 3.11: PLCγ-1, Dynamin2, and Lyn are recruited to patterned EGF: NIH-3T3 (EGFR) cells were transiently transfected with dynamin 2-GFP (top panel) or PLCγ-GFP (middle panel) and plated on micro-patterned EGF surfaces (red channel) prior to fixation. NIH-3T3 (EGFR) cells transiently transfected with Lyn-mRFP (bottom panel, red channel) were incubated on EGF-biotin bound micro-patterned FITC-streptavidin (bottom panel, green channel) prior to fixation. Scale bar: 20 μm.

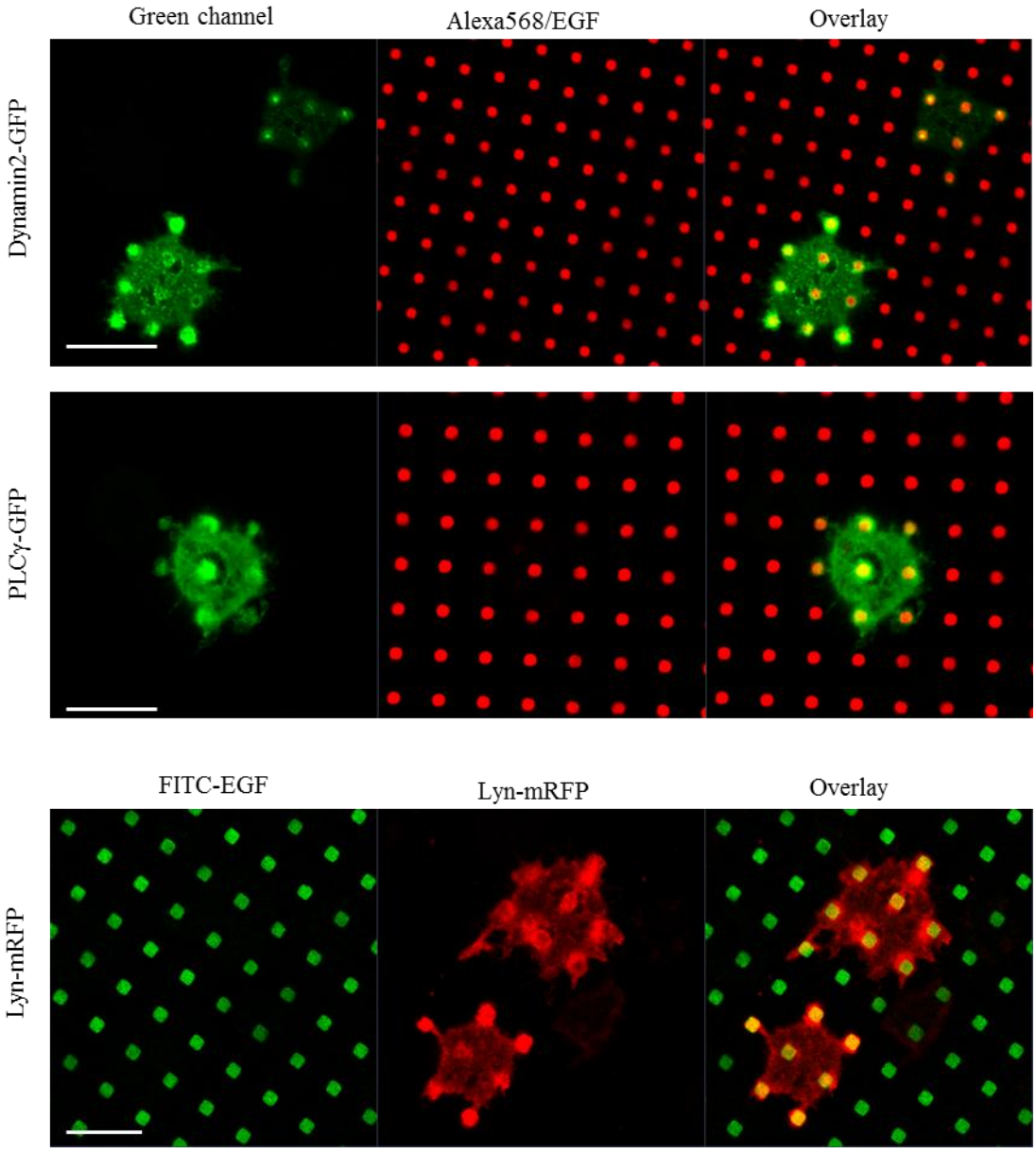
Green channel
Alexa568/EGF
Overlay
Dynamin2-GFP
PLCγ-GFP
FITC-EGF
Lyn-mRFP
Overlay
Lyn-mRFP

transfected with a GFP-tagged construct of PLCγ-1 show recruitment of this enzyme to patterned EGF (Figure 3.11A) in a ligand-dependent manner (data not shown).

Sen et al. (2010) previously showed that Src kinase phosphorylates paxillin at Tyr118 as a consequence of EGFR activation in prostate cancer cells (10). To investigate the association of a Src family kinase with EGF patterns, we transiently transfected NIH-3T3(EGFR) cells with Lyn-mRFP and examined its localization using EGF-biotin bound to FITC-streptavidin. As shown in Figure 3.11, panel 3, we observe concentration of Lyn-mRFP with the patterns in ~60% of the positively transfected cells. This suggests that Src family kinases can be recruited to activated EGFR complexes, providing a mechanism by which they can mediate phosphorylation of Tyr 118 in paxillin, also associated with the activated EGFR signaling complexes.

3.3.7 Inhibitors of PI(4,5)P_2 synthesis interfere with recruitment of F-actin, Erk, and dynamin 2 to pattern-localized EGFR complexes:

It is now well-established that PI(4,5)P_2 plays multiple roles in regulating cell signaling (41). We recently showed that two inhibitors of phosphoinositide synthesis, PAO and quercetin, effectively inhibit multiple consequences of IgE receptor signaling in mast cells, including stimulated Ca^{2+} mobilization, cell morphological changes, and endocytosis of FcεRI (42). We also found that these compounds inhibit recruitment of F-actin to IgE receptor complexes localized to micro-patterned antigen (Chapter 2). In NIH-3T3 (EGFR) cells, we find that pretreatment of cells with 2 μM PAO or 20 μM quercetin leads to substantial reduction in F-actin recruitment to EGF patterns, as detected by A488-phalloidin labeling (Figure 3.12A and B). In addition, treatment with PAO or quercetin reduces the recruitment of p-Erk at EGFR signaling complexes on patterned EGF surfaces (Figure 3.13A and B).

We previously provided evidence for a role for dynamin 2 in the organization of the actin cytoskeleton at the sites of micro-patterned FcεRI receptor complexes (Chapter 2). Dynamin 2 is known to have a PI(4,5)P_2-binding pleckstrin homology (PH) domain (43), and this could be relevant for this role. To investigate this issue with regard to the pattern-localized EGFR signaling complexes, NIH-3T3 (EGFR) cells were transiently transfected with dynamin2-GFP, then briefly pretreated with 2 μM PAO or 20μM quercetin prior to plating on EGF patterned surfaces. As shown in Figure 3.14, these compounds prevent the concentration of dynamin 2 at EGF patterns. (observed for > 95% of the imaged cells). These results suggest that phosphoinositides play a role in the co-localization of dynamin 2 with the clustered EGFR bound to patterned EGF.

3.3.8 Paxillin is required for recruitment of p-Erk to the EGF patterns, but not its activation by soluble EGF.

A previous study showed that paxillin plays a role in the phosphorylation of Erk after activation of EGFR as well as androgen receptors (AR) in prostate cancer cells (10). Paxillin has been previously shown to participate in integrin-mediated activation of Erk by stabilizing the signaling complex (44). We utilized siRNA knock down of paxillin in NIH 3T3 (EGFR) cells to assess its role in Erk activation by patterned EGF. Under our conditions, >95% knock down is achieved 48 hrs after transfection (Figure 3.15A,B). Knock down of paxillin does not inhibit enhanced tyrosine phosphorylation stimulated by patterned EGF or recruitment of F-actin to these clusters, early events in this response (Figure 3.15C). By comparison, this knock down reduces co-localization of p-Erk with the patterned EGF (Figure 3.16A,B), a later response in the signaling sequelae. Knock down of paxillin does not inhibit Erk activation in NIH-3T3(EGFR)

cells by soluble EGF, as detected by western blotting (Figure 3.16C). These results indicate some differences in the signaling requirements for paxillin in these cells depending on the physical presentation of the stimulus. Surprisingly, paxillin knock down does not inhibit recruitment of GFP-H-Ras to patterned EGF (Figure 3.17), despite its inhibiting p-Erk recruitment occurring more down-stream in this MAP kinase cascade. These results suggest that paxillin plays a nuanced role in regulating the activation of this cascade by surface-associated EGF.

3.4 Discussion:

Receptor tyrosine kinases are key regulators of cellular processes such as proliferation, migration, and differentiation (1). Upon binding its ligand EGF at its extracellular domain, EGFR dimerizes, leading to transphosphorylation of the tyrosine residues in the cytoplasmic region of the receptor. Signal transduction propagates through the recruitment via phosphotyrosine binding to adaptor proteins such as Grb2 and enzymes such as PLCγ-1. These recruited adaptor proteins activate downstream signaling cascade involving Ras, MEK, Erk and PI3-kinase-dependent activation of Akt (Figure 3.18). The signaling pathways leading to activation of these proteins are well-established (37, 45), but less is known about the spatial redistribution of these proteins with activated EGFR at the plasma membrane. Micro-patterned ligand arrays have been a valuable tool to study the interactions of cytoplasmic and membrane bound proteins with ligand-activated plasma membrane receptors. We previously utilized these surfaces to probe the recruitment of signaling partners of activated FcεRI receptor (11, 12). In that situation, the size of the ligand – dinitrophenyl (DNP) (~ 266 Da) was substantially smaller than EGF (~6500 Da) in the present case (2).

There has been prior evidence that covalently immobilized EGF stimulates tyrosine phosphorylation of proteins in chinese hamster overy (CHO) cells over-expressing EGFR

Figure 3.12 PI(4,5)P_2 synthesis is involved recruitment of F-actin to EGFR signaling complexes: A) NIH-3T3 (EGFR) cells were pretreated with 2 μM PAO (middle panel) or 20 μM quercetin (bottom panel) or not treated (control; top panel) prior to plating on micro-patterned EGF surfaces. The cells were labeled with A488-phalloidin after fixation. B) Pearson's cross-correlation coefficient of green channel with red channel; N > 30 cells, for at least 2 independent experiments. Error bars represent SEM; **** indicates $p \leq 0.0001$, *** indicates $p \leq 0.001$. Scale bar: 20 μm.

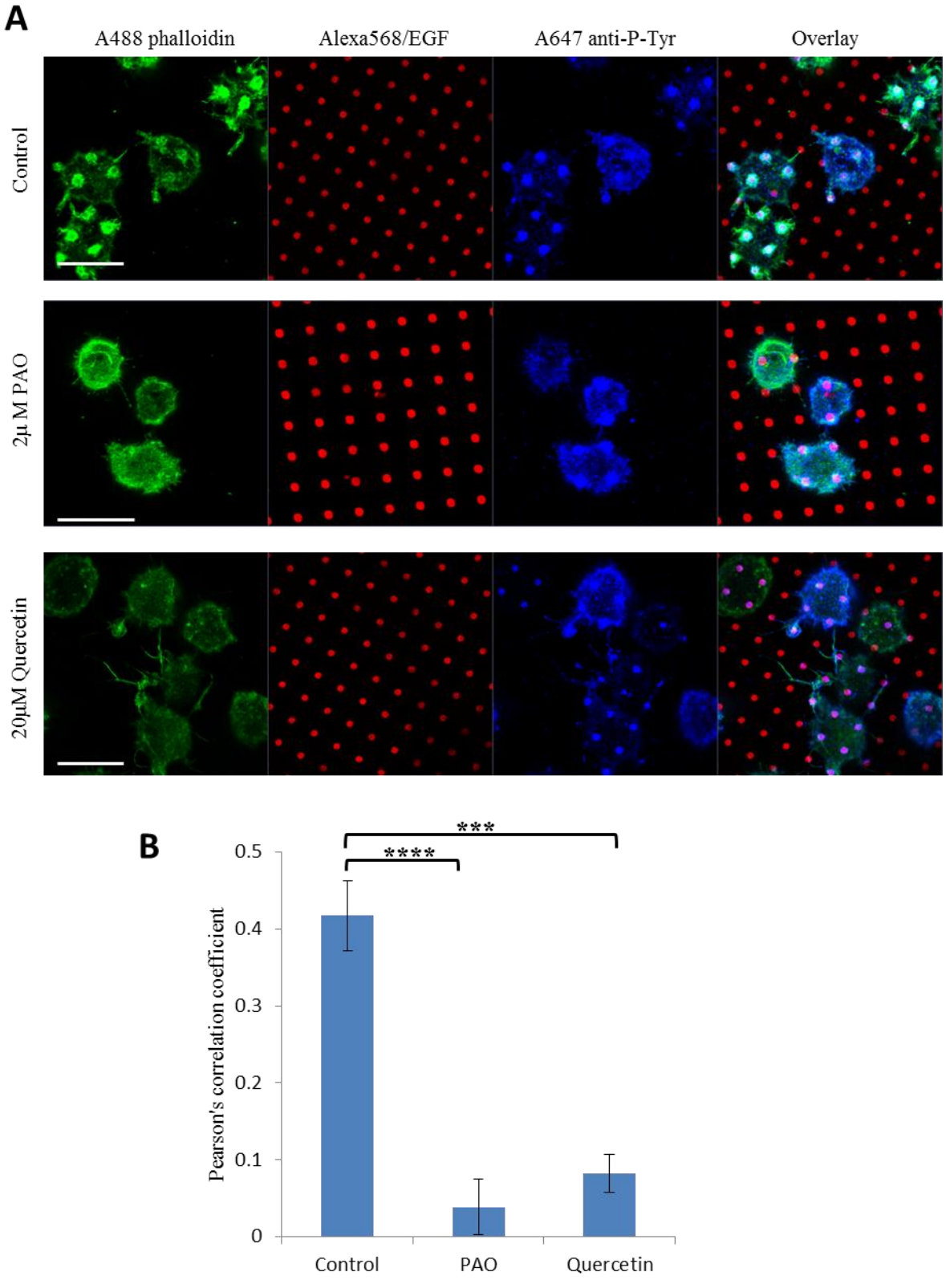
A
A488 phalloidin
Alexa568/EGF
A647 anti-P-Tyr
Overlay
Control
2µ M PAO
20µM Quercetin
B
***
****
0.5
0.4
0.3
0.2
0.1
0
Pearson's correlation coefficient
Control
PAO
Quercetin

Figure 3.13: PI(4,5)P_2 synthesis is involved in recruitment of pErk to EGFR signaling complexes A) NIH-3T3 (EGFR) cells were pretreated with 2 μM PAO (middle panel) or 20 μM quercetin (bottom panel) or not treated (control; top panel) prior to plating on micro-patterned EGF surfaces. The cells were immunolabeled with phospho-Erk primary and A488 tagged secondary antibody after fixation. B) Pearson's cross-correlation coefficients of green channel with red channel; N > 30 cells from 2 independent experiments. Error bars represent SEM, **** indicates $p \leq 0.0001$, *** indicates $p \leq 0.001$. Scale bar: 20 μm.

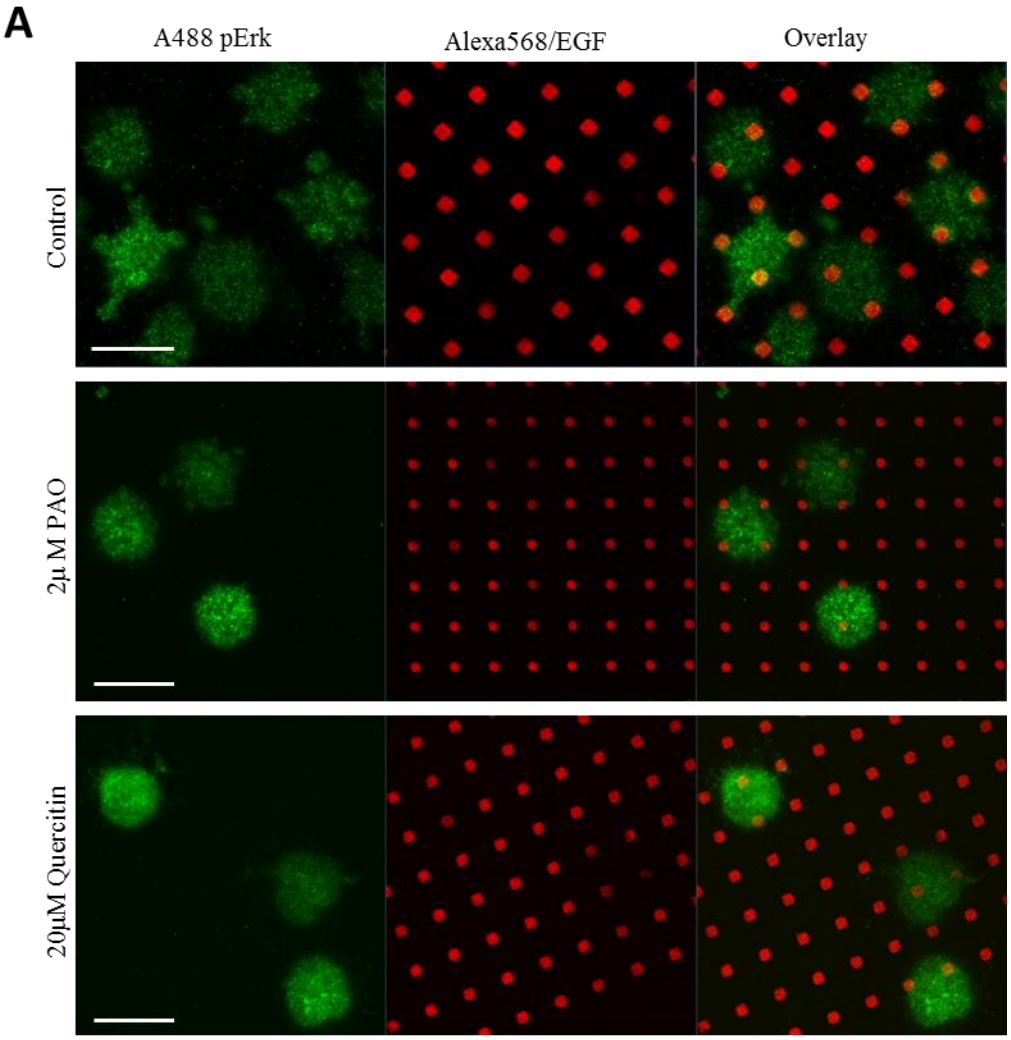
A
A488 pErk
Alexa568/EGF
Overlay
Control
2µ M PAO
20µM Quercitin

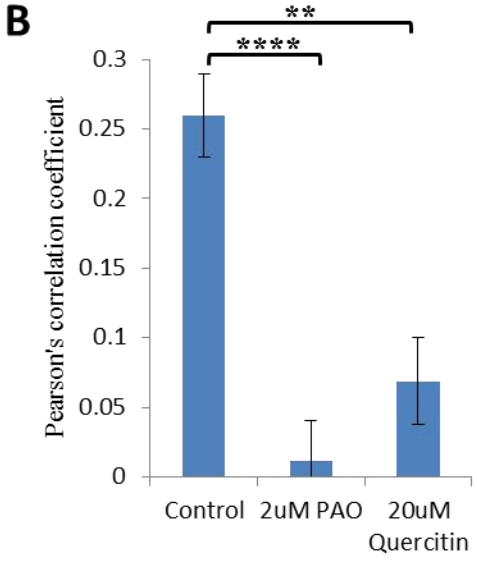
B
**
****
Pearson's correlation coefficient
0.3
0.25
0.2
0.15
0.1
0.05
0
Control
2uM PAO
20uM Quercitin

Figure 3.14: PI(4,5)P_2 synthesis is involved in the recruitment of dynamin 2 to patterned EGF: NIH-3T3 (EGFR) were cells transiently transfected with dynamin 2-GFP, pretreated with 2 μM PAO (middle panel) or 20 μM quercetin (bottom panel) or control (untransfected, top panel) prior to plating on micro-patterned EGF surfaces. Scale bar: 20 μm.

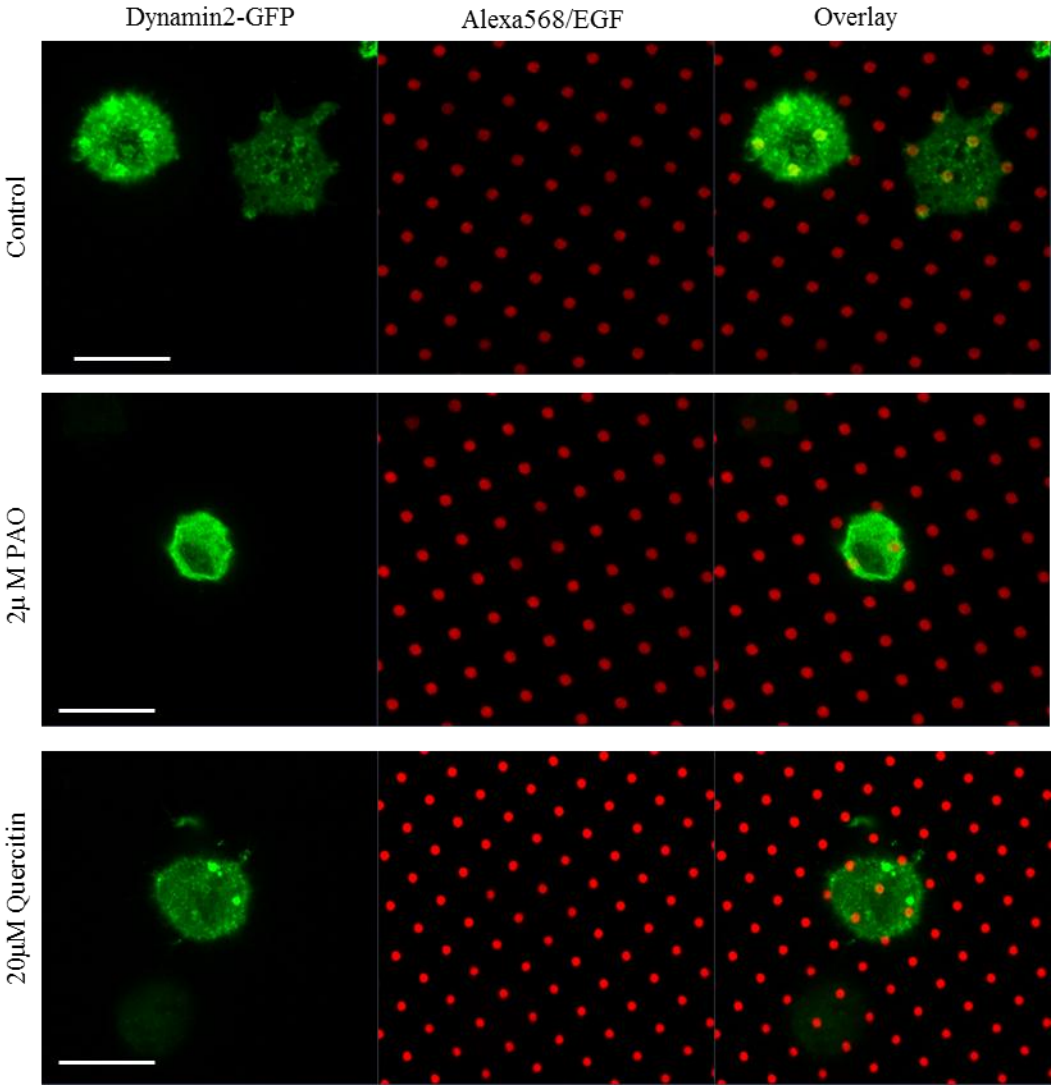
Dynamin2-GFP
Alexa568/EGF
Overlay
Control
2μ M PAO
20μM Quercitin

Figure 3.15: Paxillin knockdown does not inhibit recruitment of F-actin or enhance tyrosine phosphorylation at patterned EGF: A) Plated NIH-3T3 (EGFR) cells were transfected with 80 pmol paxillin siRNA and lysed after 24, 48, 72, 96 hours to prepare samples for western blotting. Bands were labeled with anti-paxillin antibody. B) Plated NIH-3T3 (EGFR) cells were transfected with 80 pmol control siRNA or 80 pmol paxillin siRNA, treated with 100 ng/mL soluble EGF for 30 minutes 48 hours after the siRNA treatment. The cells are subsequently lysed and samples were prepared for western blotting. C) NIH-3T3 (EGFR) cells were treated with paxillin siRNA or control siRNA for 48 hours prior to harvesting and plating on micro-patterned EGF surfaces (red channel). They were subsequently fixed and labeled with A488-phalloidin (green channel) or anti-phospho-tyrosine (4G-10) antibodies (blue channel). Scale bar: 20 μm.

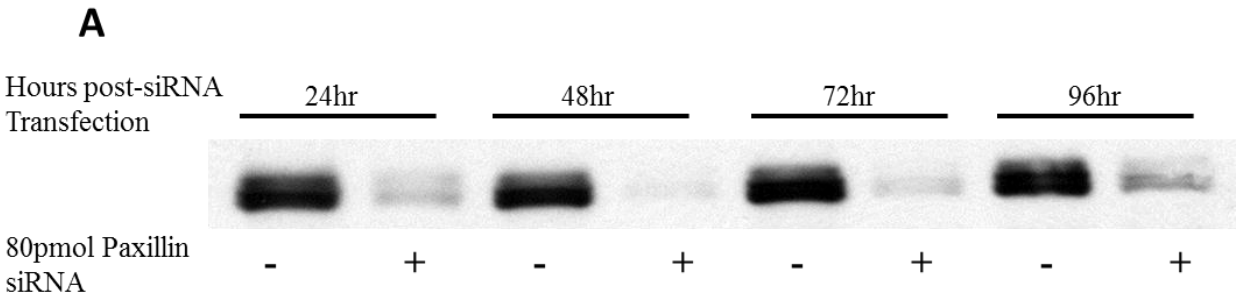
A
Hours post-siRNA Transfection
24hr
48hr
72hr
96hr
80pmol Paxillin siRNA
- + - + - + - +

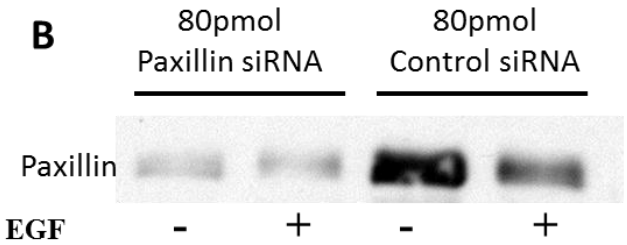
B
80pmol Paxillin siRNA
80pmol Control siRNA
Paxillin
EGF
- + - +

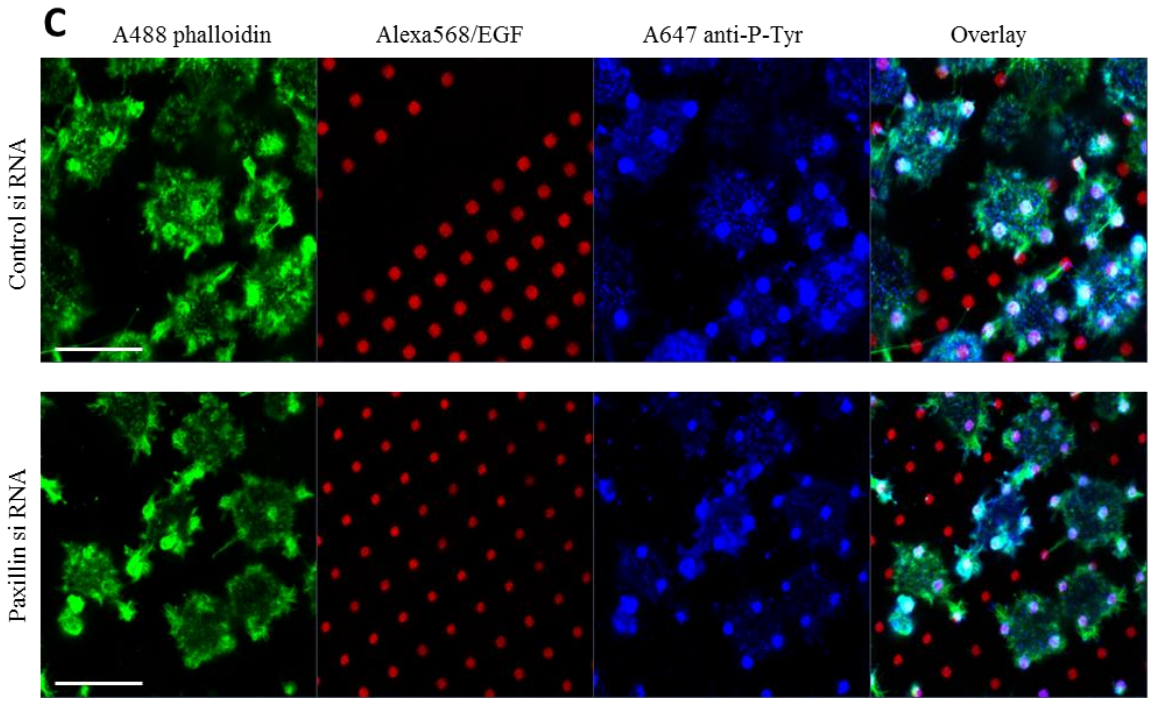
C
A488 phalloidin
Alexa568/EGF
A647 anti-P-Tyr
Overlay
Control si RNA
Paxillin si RNA

Figure 3.16: Recruitment of Erk to patterned EGF is affected by paxillin siRNA knockdown: A) NIH-3T3 (EGFR) cells were treated with paxillin siRNA or control siRNA for 48 hours prior to harvesting and plating on micro-patterned EGF surfaces (red channel). They were subsequently fixed and immunolabeled with phospho-Erk antibody (green channel), and anti-phospho-tyrosine (4G-10) antibodies (blue channel). B) Pearson's cross-correlation coefficients of green channel with red channel. N > 30 cells from 2 independent experiments (p value = 0.0298). C) Plated NIH-3T3 (EGFR) cells were transfected with 80 pmol paxillin siRNA or 80 pmol control siRNA and lysed after 48 hours to prepare samples for western blotting. Bands were labeled with anti-paxillin antibody (top lane), anti-phospho-Erk antibody (middle lane) or anti-Erk (bottom lane). Error bars represent SEM; * indicates $p \leq 0.05$. Scale bar: 20 μm.

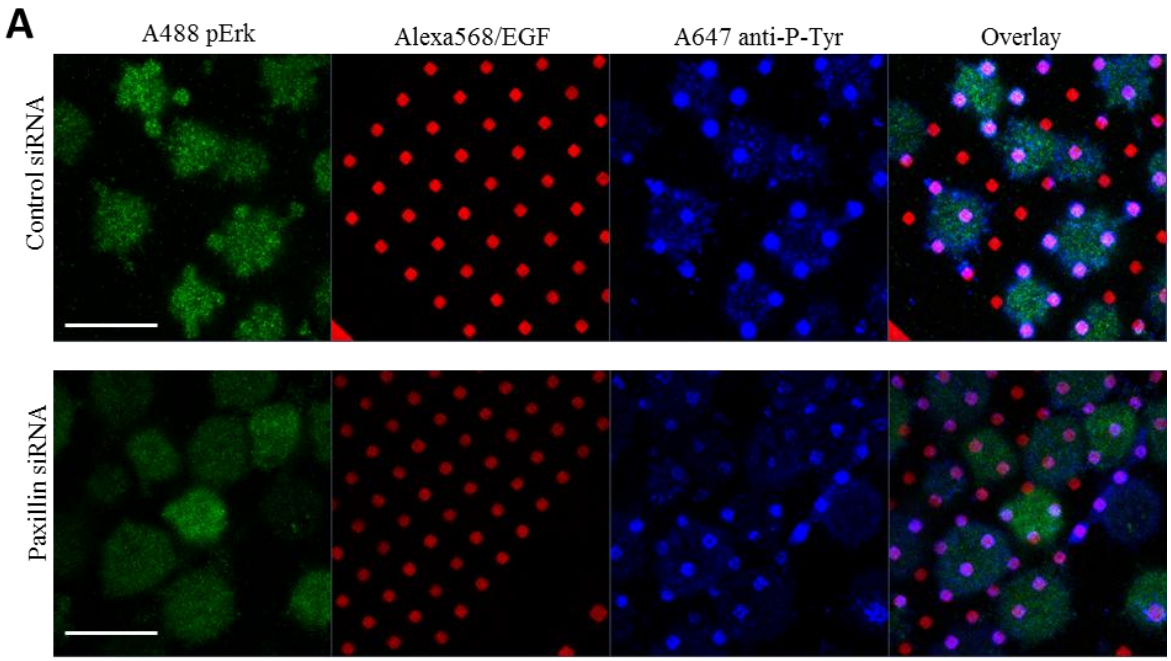
A
A488 pErk
Alexa568/EGF
A647 anti-P-Tyr
Overlay
Control siRNA
Paxillin siRNA

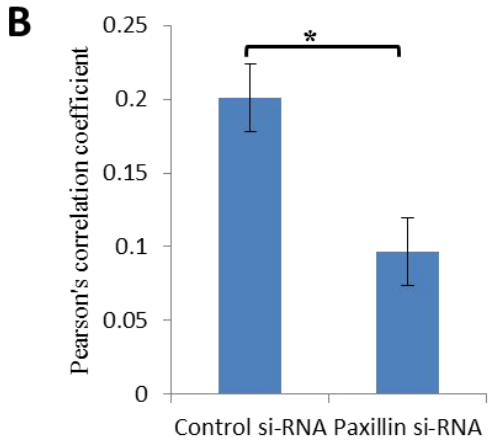
B
Pearson's correlation coefficient
0.25
0.2
0.15
0.1
0.05
0
*
Control si-RNA
Paxillin si-RNA

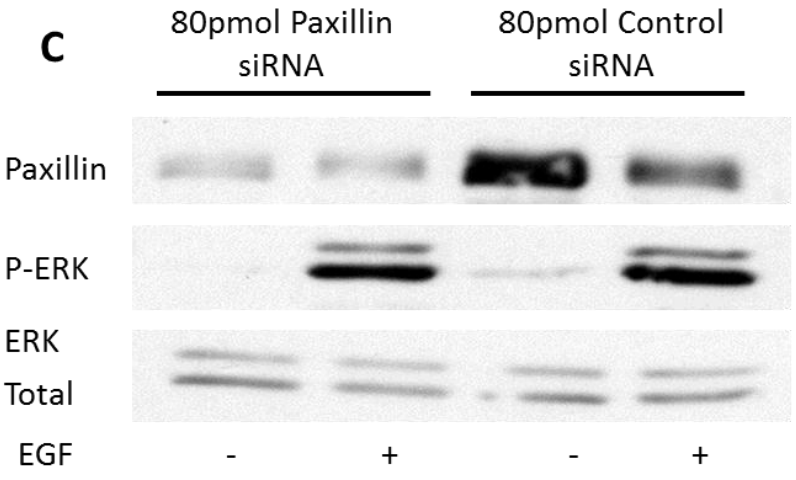
C
80pmol Paxillin siRNA
80pmol Control siRNA
Paxillin
P-ERK
ERK
Total
EGF
-
+
-
+

Figure 3.17: Recruitment of H-Ras is not inhibited by paxillin siRNA treatment: A) Plated NIH-3T3 (EGFR) cells were transfected with 80 pmol paxillin siRNA or control siRNA; they were transfected (or not) with GFP-H-Ras 24 hours after the initial siRNA treatement. The cells were then lysed after 48 hours after the siRNA treatment to prepare samples for western blotting. B) NIH-3T3 (EGFR) cells transfected with paxillin siRNA (bottom panel) or control siRNA (top panel) prior to transfection with GFP-H-Ras, and then harvested and plated on micro-patterned EGF surfaces (red channel). C) Pearson's cross-correlation coefficient of green channel with red channel. N > 30 cells from 2 independent experiments. Error bars represent SEM; n.s indicates non-significant statistical difference. Scale bar: 20 μm.

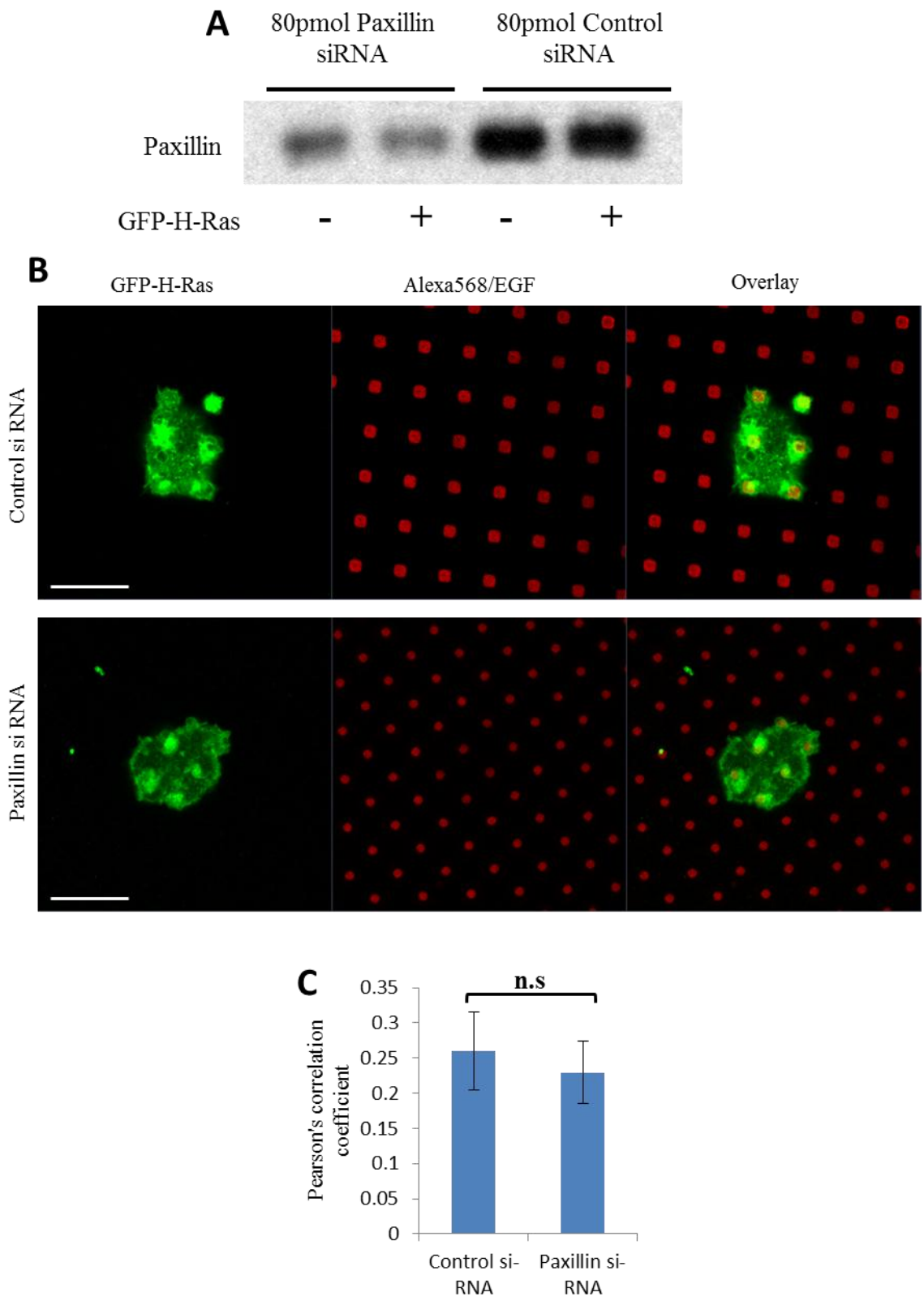
A
80pmol Paxillin siRNA
80pmol Control siRNA
Paxillin
GFP-H-Ras
-
+
-
+
B
GFP-H-Ras
Alexa568/EGF
Overlay
Control si RNA
Paxillin si RNA
C
n.s
Pearson's correlation coefficient
0.35
0.3
0.25
0.2
0.15
0.1
0.05
0
Control si-RNA
Paxillin si-RNA

(13, 46) and in breast cancer BT-20 cells (14). These previous studies utilized EGF micropatterned on surfaces with feature sizes of dimensions ~ 10 μm - 100 μm to investigate the activation of EGFR by tyrosine phosphorylation and found that cells cultured on surface-attached EGF show higher growth in comparison to the cells plated on surfaces without surface-attached EGF. Our experiments utilize patches of EGF-biotin, tightly bound to covalently attached A568-streptavidin, with the sub-cellular dimension of 1 μm – 2.5 μm to demonstrate that EGFR accumulates at these EGF patches, such that distinctly clustered EGFR is observed within individual cells (Figure 3.2). Initially, we found that RBL-2H3 cells transiently transfected with GFP tagged EGFR and incubated on substrates micro-patterned with non-covalent surface adsorbed rhodamine-EGF caused endocytic removal of rhodamine-EGF from the surface after binding to EGFR (data not shown). This demonstrates the importance of covalently attaching the ligand on micro-patterned surfaces to visualize robust recruitment of EGFR, and to form spatially resolved clusters (Figure 3.2). We also specifically observed that EGFR recruited to patterned EGF is tyrosine phosphorylated at Tyr 1068 residue (Figure 3.3), which is consistent with previous observations when EGFR is stimulated with soluble EGF (47). Upon binding to soluble EGF, EGFR is known to dimerize prior to transphosphorylation in its cytoplasmic domains (1). Our results indicate that the local concentration of EGF in micro-patterned surfaces is sufficiently high, such that EGFRs undergo transphosphorylation leading to initiation of downstream signaling. This stimulated tyrosine phosphorylation of EGFR depends on EGFR kinase activity and is inhibited by treatment with 10μM Iressa – a known inhibitor for EGFR kinase activity (Figure 3.3A). We note that pretreatment of cells with Iressa does not inhibit the interaction of EGF receptors with immobilized EGF patches (Figure 3.3B), and this implies that

EGFR kinase activity is not required for EGFR binding with micron-sized EGF patches, but it is required for its activation.

Activation of EGFR initiates a signaling cascade that leads to activation of Ras, which is known to be involved in the activation of Raf kinase (48, 49). Our results demonstrate recruitment of GFP-H-Ras to the clustered EGFR on the plasma membrane (Figure 3.9). This result makes it likely that Ras directly or indirectly associates with clustered EGFR at the plasma membrane. Ras activates Raf, which further activates MEK, which in turn phosphorylates Erk, to form a part of the MAP kinase cascade (50, 51). A previous study showed that, post activation, Erk and MEK are translocated as a complex into the nucleus to activate gene transcription, which lead to cell functions such as proliferation and cell division (52). Our experiments show that MEK and Erk interact with the EGFR at the plasma membrane of the cells that are clustered with micropatterned, immobilized EGF (Figure 3.9). Previously, these interactions have been hard to visualize due to limitations in optical resolution and to EGFR endocytosis after activation by EGF. To our knowledge, this is the first evidence of interaction of Erk with activated EGFR at the plasma membrane. This result demonstrates that macromolecular complexes of EGFR formed on the plasma membrane can activate Erk co-localized with these complexes, along with other members of this MAP kinase cascade, Ras and MEK.

Recent studies have pointed towards a role for paxillin in EGFR signaling (10, 53). We studied the involvement of paxillin, using micropatterned EGF surfaces and find that paxillin-GFP in NIH-3T3 cells interacts with the clustered EGFR at the plasma membrane in a process that depends on EGFR kinase activity (Figure 3.4). Paxillin is known be phosphorylated on Tyr 31 and 118 residues by Src kinase, and on Ser 83 and 126 residues by Erk (28). In agreement, we observe the phosphorylation of paxillin recruited to EGFR signaling complexes at plasma

membrane on Tyr 31 and Ser 126 residues by labeling with anti-phospho-paxillin antibodies (Figure 3.5). Consistent with the tyrosine phosphorylation of paxillin by Src (29), we observe recruitment of Lyn – a Src family kinase to the clustered EGFR at the plasma membrane (Figure 3.11). Treatment with PP2 inhibits the tyrosine phosphorylation of paxillin co-localized with these clusters, and this treatment causes a small increase in the recruitment of paxillin-GFP and phospho-Ser-paxillin as quantified by Pearson's correlation coefficients (Figure 3.6). This suggests enhanced association of paxillin with clustered EGFR in absence of Src kinase activity. However, the activity of Src kinase is not critical for the activation of Erk, as shown in experiments with patterned EGF as well as with soluble EGF (data not shown). In contrast, other studies demonstrated reduced Erk activation in presence of PP2 in prostate cancer cells (10). This difference in observation is possibly due to difference in the cell types and different contributions of other signaling pathways, such as formation of focal adhesions contributing to activation of Erk kinase.

To investigate further the role of paxillin in the formation these EGFR signaling complexes, we knocked down paxillin using siRNA. Our results show that paxillin knock down does not affect early steps in EGFR activation or the recruitment of Ras and F-actin to the EGFR signaling complexes (Figure 3.15, 3.17). However, it significantly ($p = 0.0049$) reduces the recruitment of Erk to these EGFR signaling complexes in 3T3 cells (Figure 3.16). In contrast, paxillin knock down does not inhibit phosphorylation of Erk upon stimulation with soluble EGF in NIH-3T3 cells (Figure 3.16). This result contrasts with previous observations, in which paxillin knock down in PC3 cells caused abrogation of activation of Erk upon treatment with soluble EGF (10). Again, this might also be due to differences between the cell types. Our results showing reduced recruitment of phosphorylated Erk to clustered, activated EGFR in cells due to

paxillin knock down indicate that paxillin contributes to stabilization of the EGFR signaling complexes.

Our previous experiments on the FcεRI receptor signaling system with micro-patterned ligands showed that F-actin is recruited to the clustered FcεRI complexes (11, 12). We also observed that Lyn, a Src family kinase, responsible for phosphorylation of FcεRI receptor, is recruited to clustered FcεRI. Large scale accumulation of Lyn over patterned ligands is inhibited by cytochalasin D. In contrast, in presence of cytochalasin D, tyrosine phosphorylation of FcεRI receptor upon stimulation with soluble antigen is enhanced (11). Based on these previous experiments we hypothesized that actin cytoskeleton stabilizes EGFR signaling complexes on the plasma membrane. Our results show recruitment of F-actin to the EGF-clustered EGFR (Figure 3.8), whereas the actin binding proteins ezrin and moesin do not visibly co-redistribute with EGF patterns. Consistent with our observations with FcεRI receptor complexes, we find that, in presence of cytochalasin D, there is no detectable recruitment of more downstream partners such as paxillin, H-Ras and Erk to the EGFR signaling complex at the plasma membrane (Figure 3.10 and data not shown). In contrast pretreatment with cytochalasin D did not inhibit the recruitment or tyrosine phosphorylation of EGFR or recruitment of dynamin 2 in a ligand-dependent manner. We found that stimulation with soluble EGF in presence of cytochalasin D caused ~50% decrease in Erk activation in NIH-3T3 (EGFR) cells (Figure 3.10 C and D), whereas a previous study showed no effect of cytochalasin D on EGFR-dependent activation of Erk in Rat 1a fibroblasts (38). These results indicate some cell type differences in the role of F-actin in stabilizing macromolecular signaling complexes formed with clustered EGFR at the plasma membrane.

Paxillin, F-actin and integrins are also known to participate in the formation of focal adhesion complexes, the macromolecular structures that are formed on the sites of cells interaction with extracellular matrix (33), and Erk is known to be activated via integrin-fibronectin mediated signaling through focal adhesions (44). We find that α-5 integrin-GFP, which is the most abundant integrin α chain in NIH-3T3 cells (34), is excluded from the EGFR signaling complexes at the plasma membrane. This indicates that the EGFR signaling complexes that are formed on the sites of micro-patterned EGF are independent of formation of focal adhesions at these sites.

Once EGFR is activated after binding EGF, it is normally endocytosed (5). In our experiments with micro-patterned EGF surfaces, we find that clathrin is visibly concentrated over EGF patterns in ~35% of the cells (data not shown). In contrast, we observe the recruitment of dynamin 2, a GTPase implicated for its role in both clathrin-dependent (54) and clathrin-independent endocytosis (55), to the clustered EGFR in >90% of cells. The actin cytoskeleton has also been implicated in endocytosis of EGFR (56). These two results suggest that proteins recruited to clustered EGFR may also be a part of the EGFR endocytic pathway, even though the endocytosis of EGFR is prevented, as EGF is covalently immobilized on the silicon substrate.

Phosphoinositides are known to play important roles in cell signaling in all cell types, as well as in receptor endocytosis (41). Our results indicate that recruitment of F-actin (Figure 3.12) and p-Erk (Figure 3.13) are inhibited by pretreatment with PAO or quercetin, which inhibit phosphoinositide synthesis in cells. Stimulation of Erk activation by soluble EGF was not inhibited by these compounds, as determined by western blotting experiments (data not shown). $PI(4,5)P_2$ has also been implicated in the reorganization of actin cytoskeleton (57), so our observed lack of recruitment of p-Erk to the clustered EGFR in presence of PAO or quercetin

might be an indirect consequence of inhibition of recruitment of F-actin. Our results also demonstrate that dynamin 2, which has a PH domain (43), is not recruited to the EGFR signaling complex in presence of PAO or quercetin (Figure 3.14), even though its recruitment is not affected by cytochalasin-D pretreatment (data not shown). This suggests that dynamin 2 recruitment to the EGFR signaling complex are driven by interactions with $PI(4,5)P_2$, independent of actin cytoskeleton. This is also consistent with some of our previous observations highlighting the role of dynamin 2 in the organization of actin cytoskeleton at the sites of activated FcεRI receptor in RBL-2H3 cells (Chapter 2). However, to test the role of dynamin 2 in the organization of F-actin at EGFR signaling complexes, dynamin 2 knock down experiments will need to be evaluated.

Our attempts to directly probe the concentration of $PI(4,5)P_2$ at the sites of EGF patterns by utilizing a GFP tagged PH domain-PLC-δ (58) did not reveal concentration of this marker co-localized with EGF patterns (data not shown). However, we note that the PH domain PLC-δ binds specifically but weakly to $PI(4,5)P_2$, and other, high avidity proteins will compete effectively for available $PI(4,5)P_2$. In addition, we observe recruitment of PLCγ1-GFP, which is known to interact with phosphorylated EGFR via its SH2 domains. PLCγ1-GFP mediates hydrolysis of $PI(4,5)P_2$ to IP_3 and DAG, which might further reduce the pool of accessible $PI(4,5)P_2$ for PH-domain-PLCδ at the EGFR signaling complexes. In combination, these results suggest that stimulated synthesis of $PI(4,5)P_2$ occurs at the micron sized EGFR signaling complexes at the plasma membrane to play a role in recruitment of other proteins such as F-actin-binding proteins and dynamin 2, directly or through regulation of adaptor proteins. However, directly assessing the local concentration of $PI(4,5)P_2$ at these micron sized EGFR signaling complexes on the plasma membrane may be difficult.

In conclusion, we have shown that micropatterned EGF surfaces are a useful tool to study the spatial aspects of the EGFR signaling that complements the biochemical tools such as immunoprecipitations and co-immunoprecipitations to detect the interactions of signaling partners with EGFR. Figure 3.18 schematically depicts the formation of the macro-molecular signaling complexes with clustered, EGF-bound EGFR on the plasma membrane of cells. Table 3.1 summarizes results from the different experiments described in this chapter to investigate EGFR signaling partners with clustered EGFR on the plasma membrane. Our experiments with immobilized EGF patterns show formation of macromolecular EGFR signaling complexes, including EGFR signaling partners PLCγ1, H- and N-Ras, MEK, and Erk, in addition to paxillin, F-actin, and dynamin-2. Our results provide strong evidence that phosphoinositide synthesis and the actin cytoskeleton play important roles in the stabilization of these EGFR signaling complexes. However, the structural basis of formation of these complexes is still incompletely understood. Formation of macro-molecular clusters of EGFR that are restricted from undergoing stimulated endocytosis, an important pathway for the down regulation of receptor activated signaling, may result in some non-physiological consequences. We note that capacity to detect signaling partners is limited by the sensitivity of fluorescent labeling of proteins and their concentration at the sites of clustered EGFR. Recruitment of some functionally relevant proteins may be difficult to detect.

Further experiments will be necessary to determine the sequence in which the signaling partners such as Ras, PI3-kinase, and PLCγ are recruited to the EGFR complex on the plasma membrane. These micro-patterned surfaces may also be utilized to understand the cross-talk between EGFR and other receptor signaling pathways such as integrin-mediated signaling. These

Proteins	**Control**	**PP2**	**Iressa**	**PAO/Querceti n**	**Cyto D (2μM)**
EGFR	**Yes**	**Yes**	**Yes**	**Yes**	**Yes**
P-EGFR	**Yes**	**Yes**	**None**	**Yes**	**Yes**
P-Tyr	**Yes**	**Yes**	**Very weak**	**Yes**	**Yes**
Paxillin-GFP	**Yes**	**Yes**	**None**	**None**	**None**
p-Tyr-Paxillin	**Yes**	**None**	**-**	**-**	**-**
p-Ser-Paxillin	**Yes**	**Yes**	**-**	**-**	**-**
F-actin	**Yes**	**Yes**	**None**	**None**	**None**
Ezrin	**None**	**-**	**-**	**-**	**-**
Moesin	**None**	**-**	**-**	**-**	**-**
H-Ras-GFP	**Yes**	**Yes**	**-**	**-**	**None**
MEK	**Yes**	-	-	-	**None**
P-Erk	**Yes**	-	-	**None**	**None**
PLCγ1-GFP	**Yes**	-	-	-	-
α5-Integrin-GFP	**Excluded**		-	-	-
Dynamin 2-GFP	**Yes**	-	-	**None**	**Yes**

Table 3.1 Observations from different experiments with NIH-3T3 (EGFR) cells: A 'Yes' indicates that proteins could be optically resolved as colocalized with micro-patterned EGF bound to EGFR, 'None' indicates no clustering was visually observed, and '-' indicates that the experiment was not performed.

Figure 3.18: Immobilized, micro-patterned EGF on silicon substrate forms actin cytoskeleton dependent EGFR signaling complexes: The schematic shows that the EGFR signaling complexes formed on the plasma membrane consists of phosphorylated EGFR, paxillin, MEK and pErk. Dynamin 2. PLCγ and F-actin are also recruited to these signaling complexes at the plasma membrane. Inhibitors of F-actin polymerization and phosphoinositide synthesis, do not affect the EGF dependent phosphorylation of Erk, but abolish any detectable recruitment of pErk to micro-patterned EGF surfaces.

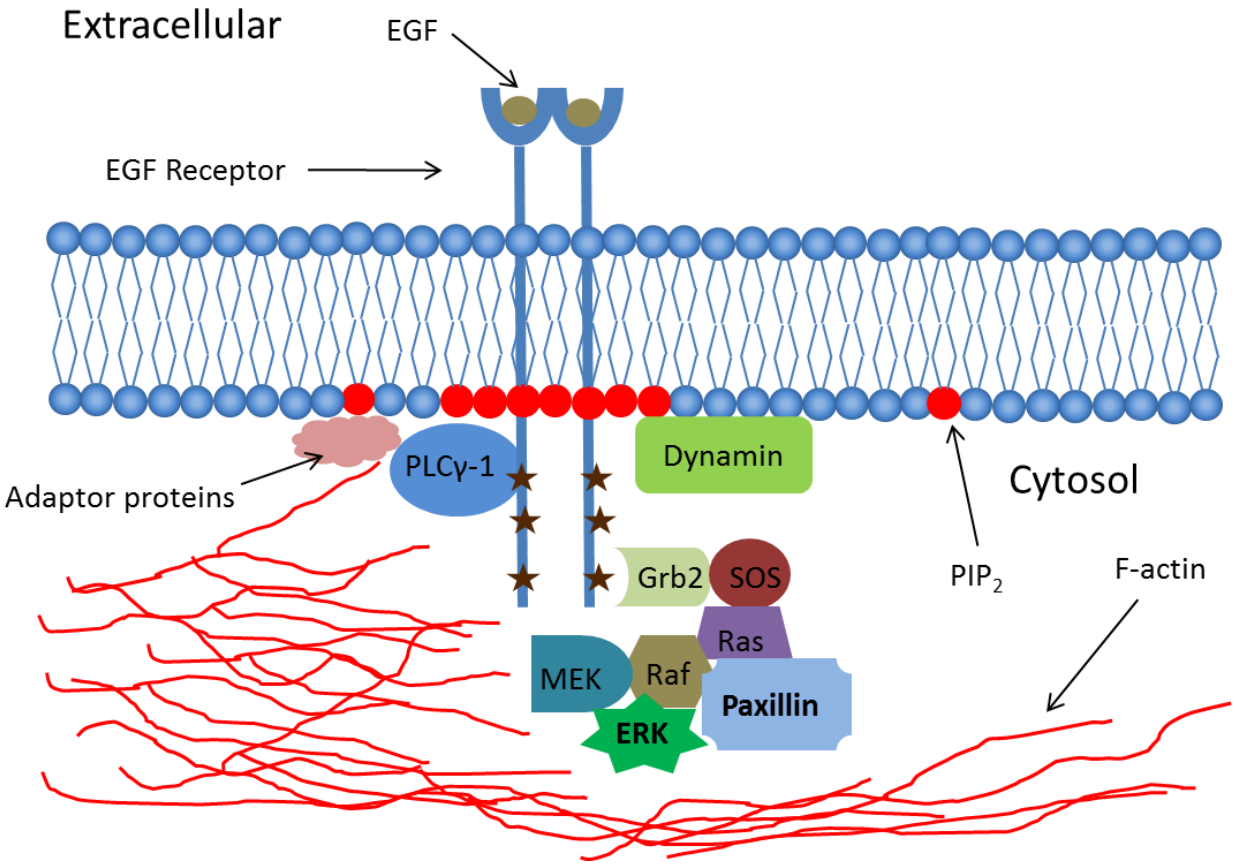
Extracellular
EGF
EGF Receptor
Adaptor proteins
PLCγ-1
Dynamin
Cytosol
PIP2
F-actin
Grb2
SOS
Ras
MEK
Raf
Paxillin
ERK

micro-patterned ligand surfaces open new avenues to explore spatiotemporal regulation of receptor mediated signaling.

REFERENCES

1. Lemmon MA, Schlessinger J. Cell signaling by receptor tyrosine kinases. Cell.2010;141:1117-1134.
2. Edwin F, et al. A historical perspective of the EGF receptor and related systems. METHODS IN MOLECULAR BIOLOGY-CLIFTON THEN TOTOWA-.2006;327:1.
3. Pines G, Köstler WJ, Yarden Y. Oncogenic mutant forms of EGFR: Lessons in signal transduction and targets for cancer therapy. FEBS letters.2010;584:2699-2706.
4. Gschwind A, Fischer OM, Ullrich A. The discovery of receptor tyrosine kinases: targets for cancer therapy. Nature Reviews Cancer.2004;4:361-370.
5. Sorkin A, Goh LK. Endocytosis and intracellular trafficking of ErbBs. Experimental cell research.2009;315:683-696.
6. Verveer PJ, Wouters FS, Reynolds AR, Bastiaens PIH. Quantitative imaging of lateral ErbB1 receptor signal propagation in the plasma membrane. Science's STKE.2000;290:1567.
7. Sigismund S, Argenzio E, Tosoni D, Cavallaro E, Polo S, Di Fiore PP. Clathrin-mediated internalization is essential for sustained EGFR signaling but dispensable for degradation. Developmental cell.2008;15:209-219.
8. Taub N, Teis D, Ebner H, Hess M, Huber L. Late endosomal traffic of the epidermal growth factor receptor ensures spatial and temporal fidelity of mitogen-activated protein kinase signaling. Molecular biology of the cell.2007;18:4698-4710.
9. Sousa LP, Lax I, Shen H, Ferguson SM, De Camilli P, Schlessinger J. Suppression of EGFR endocytosis by dynamin depletion reveals that EGFR signaling occurs primarily at the plasma membrane. Proceedings of the National Academy of Sciences.2012.
10. Sen A, O'Malley K, Wang Z, Raj GV, DeFranco DB, Hammes SR. Paxillin regulates androgen-and epidermal growth factor-induced MAPK signaling and cell proliferation in prostate cancer cells. Journal of Biological Chemistry.2010;285:28787-28795.
11. Wu M, Holowka D, Craighead HG, Baird B. Visualization of plasma membrane compartmentalization with patterned lipid bilayers. Proc Natl Acad Sci U S A.2004;101:13798-13803.
12. Torres AJ, Vasudevan L, Holowka D, Baird BA. Focal adhesion proteins connect IgE receptors to the cytoskeleton as revealed by micropatterned ligand arrays. Proc Natl Acad Sci U S A.2008;105:17238-17244.

13. Ito Y, Chen G, Imanishi Y. Micropatterned immobilization of epidermal growth factor to regulate cell function. Bioconjugate chemistry.1998;9:277-282.
14. Gonçalves R, Martins MCL, Oliveira MJ, Almeida-Porada G, Barbosa MA. Bioactivity of immobilized EGF on self-assembled monolayers: Optimization of the immobilization process. Journal of Biomedical Materials Research Part A.2010;94:576-585.
15. Cao H, Garcia F, McNiven MA. Differential distribution of dynamin isoforms in mammalian cells. Molecular biology of the cell.1998;9:2595-2609.
16. Monick MM, et al. Activation of the epidermal growth factor receptor by respiratory syncytial virus results in increased inflammation and delayed apoptosis. Journal of Biological Chemistry.2005;280:2147-2158.
17. Hammond S, Wagenknecht-Wiesner A, Veatch SL, Holowka D, Baird B. Roles for SH2 and SH3 domains in Lyn kinase association with activated FcεRI in RBL mast cells revealed by patterned surface analysis. Journal of structural biology.2009;168:161-167.
18. Wang XJ, Liao HJ, Chattopadhyay A, Carpenter G. EGF-Dependent Translocation of Green Fluorescent Protein-Tagged PLC-[gamma] 1 to the Plasma Membrane and Endosomes. Experimental cell research.2001;267:28-36.
19. Pierini L, Holowka D, Baird B. Fc epsilon RI-mediated association of 6-micron beads with RBL-2H3 mast cells results in exclusion of signaling proteins from the forming phagosome and abrogation of normal downstream signaling. J Cell Biol.1996;134:1427-1439.
20. Gosse JA, Wagenknecht-Wiesner A, Holowka D, Baird B. Transmembrane sequences are determinants of immunoreceptor signaling. The Journal of Immunology.2005;175:2123-2131.
21. Bryant K.L AM, Vasudevan L, Baird B, Holowka D, Cerione R. Ligand independent cell transformation by an ER-retained EGF Receptor Mutant. Manuscript in Preparation.2012.
22. Ilic B, Craighead HG. Topographical Patterning of Chemically Sensitive Biological Materials Using a Polymer-Based Dry Lift Off. Biomedical Microdevices.2000;2:317-322.
23. Orth RN, Wu M, Holowka DA, Craighead HG, Baird BA. Mast Cell Activation on Patterned Lipid Bilayers of Subcellular Dimensions. Langmuir.2003;19:1599-1605.
24. Torres AJ, Holowka D, Baird BA. Micropatterned Ligand Arrays to Study Spatial Regulation in Fc Receptor Signaling. Methods in molecular biology (Clifton, NJ).2011;748:195.
25. Wakeling AE, et al. ZD1839 (Iressa). Cancer Research.2002;62:5749.

26. Turner CE, Glenney Jr JR, Burridge K. Paxillin: a new vinculin-binding protein present in focal adhesions. The Journal of cell biology.1990;111:1059-1068.
27. Salgia R, et al. Molecular cloning of human paxillin, a focal adhesion protein phosphorylated by P210BCR/ABL. Journal of Biological Chemistry.1995;270:5039-5047.
28. Brown MC, Turner CE. Paxillin: adapting to change. Physiological reviews.2004;84:1315-1339.
29. Schaller MD, Schaefer EM. Multiple stimuli induce tyrosine phosphorylation of the Crk-binding sites of paxillin. Biochemical Journal.2001;360:57.
30. Huang C, Borchers CH, Schaller MD, Jacobson K. Phosphorylation of paxillin by p38MAPK is involved in the neurite extension of PC-12 cells. The Journal of cell biology.2004;164:593-602.
31. Woodrow MA, Woods D, Cherwinski HM, Stokoe D, McMahon M. Ras-induced serine phosphorylation of the focal adhesion protein paxillin is mediated by the Raf--> MEK--> ERK pathway. Experimental cell research.2003;287:325-338.
32. Bretscher A, Edwards K, Fehon RG. ERM proteins and merlin: integrators at the cell cortex. Nature Reviews Molecular Cell Biology.2002;3:586-599.
33. Turner CE. Paxillin and focal adhesion signalling. Nature cell biology.2000;2:E231-E236.
34. Dalton SL, Marcantonio E, Assoian R. Cell attachment controls fibronectin and alpha 5 beta 1 integrin levels in fibroblasts. Implications for anchorage-dependent and-independent growth. Journal of Biological Chemistry.1992;267:8186-8191.
35. Buday L, Downward J. Epidermal growth factor regulates p21ras through the formation of a complex of receptor, Grb2 adapter protein, and Sos nucleotide exchange factor. Cell.1993;73:611.
36. Morrison DK, Cutler RE. The complexity of Raf-1 regulation. Current opinion in cell biology.1997;9:174-179.
37. Gale NW, Kaplan S, Lowenstein EJ, Schlessinger J, Bar-Sagi D. Grb2 mediates the EGF-dependent activation of guanine nucleotide exchange on Ras.1993.
38. Luttrell LM, Daaka Y, Della Rocca GJ, Lefkowitz RJ. G protein-coupled receptors mediate two functionally distinct pathways of tyrosine phosphorylation in rat 1a fibroblasts. Journal of Biological Chemistry.1997;272:31648-31656.

39. Damke H, Binns DD, Ueda H, Schmid SL, Baba T. Dynamin GTPase domain mutants block endocytic vesicle formation at morphologically distinct stages. Mol Biol Cell.2001;12:2578-2589.
40. Margolis B, et al. The tyrosine phosphorylated carboxyterminus of the EGF receptor is a binding site for GAP and PLC-gamma. The EMBO journal.1990;9:4375.
41. Di Paolo G, De Camilli P. Phosphoinositides in cell regulation and membrane dynamics. Nature.2006;443:651-657.
42. Marcela de Souza Santos RMZGN, David Holowka and Barbara Baird. Inhibitors of PI(4,5)P2 Synthesis Reveal Dynamic Regulation of IgE Receptor Signaling by Phosphoinositides in Mast Cells. Journal of cell science.2012;Submitted.
43. Zheng J, Cahill SM, Lemmon MA, Fushman D, Schlessinger J, Cowburn D. Identification of the binding site for acidic phospholipids on the pH domain of dynamin: implications for stimulation of GTPase activity. Journal of molecular biology.1996;255:14-21.
44. Ishibe S, Joly D, Zhu X, Cantley LG. Phosphorylation-dependent paxillin-ERK association mediates hepatocyte growth factor-stimulated epithelial morphogenesis. Molecular cell.2003;12:1275-1285.
45. Ramos JW. The regulation of extracellular signal-regulated kinase (ERK) in mammalian cells. The international journal of biochemistry & cell biology.2008;40:2707-2719.
46. Chen G, Ito Y. Gradient micropattern immobilization of EGF to investigate the effect of artificial juxtacrine stimulation. Biomaterials.2001;22:2453-2457.
47. Ullrich A, Schlessinger J. Signal transduction by receptors with tyrosine kinase activity. Cell.1990;61:203-212.
48. Downward J. Control of ras activation. Cancer surveys.1996;27:87.
49. Leevers SJ, Paterson HF, Marshall CJ. Requirement for Ras in Raf activation is overcome by targeting Raf to the plasma membrane.1994.
50. Zheng CF, Guan KL. Activation of MEK family kinases requires phosphorylation of two conserved Ser/Thr residues. The EMBO journal.1994;13:1123.
51. McKay M, Morrison D. Integrating signals from RTKs to ERK/MAPK. Oncogene.2007;26:3113-3121.
52. Burack WR, Shaw AS. Live cell imaging of ERK and MEK. Journal of Biological Chemistry.2005;280:3832-3837.

53. Sen A, et al. Paxillin mediates extranuclear and intranuclear signaling in prostate cancer proliferation. The Journal of clinical investigation.2012.
54. Vieira AV, Lamaze C, Schmid SL. Control of EGF receptor signaling by clathrin-mediated endocytosis. Science.1996;274:2086-2089.
55. Mayor S, Pagano RE. Pathways of clathrin-independent endocytosis. Nat Rev Mol Cell Biol.2007;8:603-612.
56. Benesch S, et al. N-WASP deficiency impairs EGF internalization and actin assembly at clathrin-coated pits. Journal of cell science.2005;118:3103-3115.
57. Engqvist-Goldstein ÅEY, Drubin DG. Actin assembly and endocytosis: from yeast to mammals. Annual review of cell and developmental biology.2003;19:287-332.
58. Várnai P, Balla T. Visualization of phosphoinositides that bind pleckstrin homology domains: calcium-and agonist-induced dynamic changes and relationship to myo-[3H] inositol-labeled phosphoinositide pools. The Journal of cell biology.1998;143:501-510.

Chapter 4

Summary and Future Directions:

4.1 FcεRI internalization:

Endocytosis of ligand-bound, activated receptors is usually considered as a means to down regulate signaling cascades initiated by activation of the receptor. Recent studies have indicated that some receptors continue their signaling from inside the endosomes, and signals emanated from these endosomal receptors may be different from those activated by receptors at the plasma membrane (1). Elucidating mechanisms of receptor internalization will shed more light on understanding receptor mediated signaling events. Receptor endocytosis may occur via a variety of mechanisms, some of which are reviewed here (2). In the pathways utilized for receptor endocytosis, the roles of clathrin and dynamin 2 have been widely studied. Clathrin is a protein known to play a critical role in shaping the budding vesicles and sorting them to their destinations. Dynamin 2, a GTPase, is primarily responsible for scission of newly formed vesicles from the plasma membrane (3).

Previous studies have shown that IgE bound FcεRI is endocytosed rapidly at 37°C ($t_{1/2}$ ~ 5 minutes) in response to crosslinking with antigen (4, 5). Prior studies that FcεRI internalization is dependent on Lyn kinase in bone marrow-derived mast cells (BMMCs) (6),although others have reached a different conclusion in rat basophilic leukemia (RBL) cells (7). The roles of clathrin, dynamin 2, and actin cytoskeleton were not clearly understood. While most of the studies focused on FcεRI receptor internalization have utilized an acid-stripping method or flow cytometry to quantify internalization, we have implemented a several different approaches including fluorescence spectroscopy, confocal microscopy, and flow cytometry to assess FcεRI

internalization. Employing a combination of these methods, we demonstrate that, in certain circumstances, aggregated FcεRI receptors are located in membrane invaginations, but they are not pinched off from the plasma membrane. In these situations, the surface labeling antibodies that are used for detection in flow cytometry do not label the receptors in membrane invaginations that are not cleaved from the plasma membrane. This result indicates that flow cytometry alone may sometimes lead to misinterpretation of the fate of these receptors in membrane invaginations as internalized receptors, and thus may not be an adequate method for quantifying receptor internalization. These limitations may be overcome by a more comprehensive assessment of receptor internalization utilizing spectroscopic and microscopic approaches, in addition to flow cytometry measurements. Thus, a multifaceted approach using a combination of different methods will be helpful to better understand the endocytic state of the receptors.

Previously, our lab employed micro-patterned ligand surfaces in combination with confocal fluorescent microscopy to study the formation of IgE-FcεRI signaling complexes at the plasma membrane of RBL-2H3 cells (8). FcεRI is activated upon binding to its co-localized ligand in micro-patterned liganded bilayers, which leads to recruitment of downstream signaling partners including Lyn, a Src family kinase that is responsible for receptor phosphorylation. Experiments with these surfaces revealed that actin cytoskeleton-regulating proteins such as paxillin, vinculin, and talin are also recruited to these FcεRI signaling complexes in addition to accumulation of F-actin (9). Here, we demonstrate that activated dynamin 2 is recruited to FcεRI signaling complexes, and, furthermore, it regulates the organization of F-actin at these sites. In light of this result, two mechanisms are possible: 1) A direct connection between FcεRI signaling components and actin cytoskeleton regulating proteins and/or 2) Dynamin 2 operating as an

adapter protein that coordinates protein-protein interactions for signaling leading to degranulation and/or regulation and assembly of FcεRI endocytic machinery.

In our experiments to assess internalization, we have determined that FcεRI internalization is sensitive to cholesterol and the phosphoinositide content of the plasma membrane. In the presence of inhibitors of F-actin polymerization, a significant (~60%) fraction of aggregated FcεRI is in membrane invaginations that are not cleaved from the plasma membrane. This indicates that the actin cytoskeleton plays a role in cleaving budding endosomes from the plasma membrane. A plausible mechanism for cytoskeletal regulation of FcεRI internalization is depicted in Figure 4.1. After FcεRI activation, dynamin 2 is recruited to the FcεRI signaling complex, where it may regulate the selective accumulation of several actin binding proteins. This then leads to the formation of a cytoskeletal network, which may help in generating the contractile forces and membrane curvature in combination with BAR domain containing proteins, which induce and stabilize membrane curvature. In this model, the endocytic structure depicted in Figure 4.1 leads to internalization of vesicles containing clustered IgE-FcεRI complexes.

Further studies with selective knock down experiments will be required to determine the role of the other proteins such as BAR domain containing proteins and cytoskeletal adaptor proteins, such as actin related protein (Arp2/3) and Wiskott-Aldrich syndrome protein (WASP). Further biochemical characterization is needed to differentiate between the roles of dynamin-2 and actin cytoskeleton adapter proteins, both in FcεRI signaling and as regulators of FcεRI internalization. Co-immunoprecipitation studies may provide specific information about the proteins interacting with dynamin 2 and actin cytoskeletal adaptor proteins occurring after FcεRI activation. Further

Figure 4.1: A model for regulation of FcεRI endocytosis by dynamin 2: Dynamin 2 is recruited to FcεRI following aggregation of IgE bound receptors. Dynamin 2 then plays a role in recruitment of actin cytsokeletal regulating proteins and F-actin assembly at the IgE-FcεRI signaling complexes. Contractile forces induced by F-actin and dynamin, in colaboration with BAR domain proteins are responsible for the formation of endocytic vessicles containing the activated receptors. These vesicles are then cleaved via the fission mediated by GTPase activity of dynamin 2 (Reproduced from reference (5)).

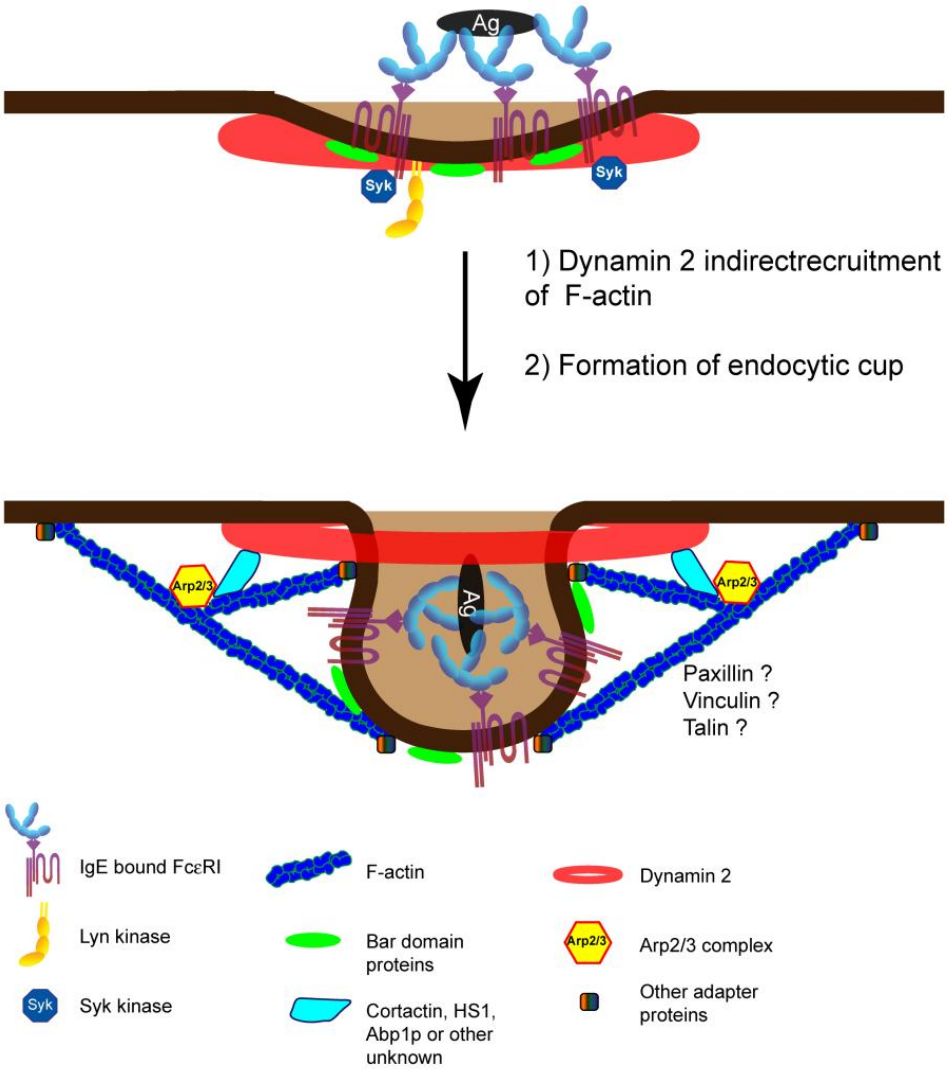
Ag
Syk
Syk
1) Dynamin 2 indirectrecruitment of F-actin
2) Formation of endocytic cup
Arp2/3
Arp2/3
Ag
Paxillin ?
Vinculin ?
Talin ?
IgE bound FcεRI
Lyn kinase
Syk
Syk kinase
F-actin
Bar domain proteins
Cortactin, HS1, Abp1p or other unknown
Dynamin 2
Arp2/3
Arp2/3 complex
Other adapter proteins

experiments will be required to understand the importance of FcεRI aggregation in ordered membrane domains and the role of phospholipids in its internalization. Utilization of micro-patterned surfaces in conjunction with cholesterol and phosphoinositide perturbations will be helpful in determining the role of plasma membrane composition in the recruitment of signaling partners and/or components of endocytic machinery to FcεRI signaling complexes.

Furthermore, it should be noted that micro-patterned ligand surfaces provide a useful way of stimulating cells, wherein the cell cannot internalize activated, ligand-bound FcεRI. Previous studies with Fc receptors have shown that particles < 1μm are endocytosed, whereas particles > 1μm are phagocytosed (10). Further experiments must be performed to characterize whether these liganded surfaces resemble a case of frustrated endocytosis or phagocytosis. It is conceivable that varying feature sizes on micro-patterned surfaces may show different cellular responses. For example, feature sizes < 500 nm could initiate a cellular response that will closely resemble endocytosis, which will be different from the responses seen in feature sizes ≥ 1 μm. With further advances in the nano/microfabriaction schemes utilized to synthesize these patterned substrates, lower feature sizes will be more available for experiments.

4.2 Spatial regulation of EGFR signaling with micro-patterned ligand surfaces

EGFR regulation of cell growth has been widely implicated in various cancers (11, 12). Here, we determined that micro-patterned surfaces of covalently immobilized EGF can activate the EGFR on the surface of cells. We observed the recruitment and phosphorylation of the adaptor protein paxillin to EGFR signaling complexes formed on the plasma membrane, which was previously implicated to play a role in EGFR signaling (13, 14). We demonstrated that, in addition to paxillin, F-actin is also recruited to the EGFR signaling complex, but integrin α-5 GFP is

excluded from these complexes. Our experiments demonstrated the recruitment of previously known signaling partners to the EGF-EGFR clusters: H-Ras, MEK, Erk and PLCγ. We also demonstrated that F-actin polymerization plays an important role in the stable recruitment of H-Ras and Erk to the EGFR signaling complex.

We also observed recruitment of dynamin 2 to the micro-patterned, immobilized EGF patches. Dynamin 2 is recruited to the EGF-containing surfaces, even in the presence of inhibitors of F-actin polymerization. This indicates that unlike H-Ras, pErk, and paxillin recruitment, dynamin-2 recruitment does not depend on the actin cytoskeleton. Since EGFR is also internalized upon activation by a dynamin 2 and an actin cytoskeleton-dependent mechanism (15), it is plausible that dynamin 2 might be playing a role in the recruitment of F-actin to the micro-patterned surfaces, which form the EGFR endocytic machinery. Recruitment of dynamin 2, F-actin, and Erk is diminished in presence of PAO or quercetin, inhibitors for phosphatidylinositol 4,5 bisphosphate ($PI(4,5)P_2$) synthesis, which indicates a role for phosphoinositides in the formation of EGFR signaling complexes. This raises two scenarios: 1) Phosphoinositides directly play a role in the recruitment of proteins such as dynamin 2 and actin adaptor proteins (N-WASP, radixin) by binding to their PH domains and/or 2) Phosphoinositides regulate the recruitment of the actin cytoskeleton to the EGFR signaling complexes at the plasma membrane, which in turn plays a role in the recruitment of signaling partners such as paxillin, H-Ras, and pErk.

It should be kept in mind that surface attached, immobilized ligands is possibly un-physiological method of stimulating the cells. The macromolecular receptor signaling complexes formed are not endocytosed and may continue signaling for longer time, in comparison to the case of stimulation with soluble ligands. In light of some recent evidence, which demonstrates that EGFR in endosomes is capable of signaling (1), more effort should be made to understand the

nature of receptor complexes at the plasma membrane. Furthermore, the structural basis of the formation of these signaling complexes on the plasma membrane of the cells is not well understood. Future experiments utilizing pharmacological inhibitors and specific protein knock downs will be required to determine the sequelae of interactions of proteins involved in the signaling complex and their effect on the formation of complex.

EGFR is known to be involved in cross-talk with other receptor mediated signaling pathways, which include G-protein coupled receptors (GPCR) (16) and integrins (17). Utilization of micro-patterned surfaces can help to elucidate the spatial interactions of the components of these signaling pathways. For example, we have demonstrated that integrin α-5 is excluded from the EGFR signaling complexes formed by stimulating with micro-patterned EGF. EGFR can be also activated by other EGF-like ligands, such as amphiregulin, transforming growth factor α (TGFα) and heparin-binding EGF-like growth factor (HB-EGF) (11), which adds another layer of signaling diversification in the regulation of EGFR activity. A recent investigation demonstrated that EGFR conformation change after binding with TGFα is different from the conformational changes it undergoes after binding with EGF (18). This may provide the structural basis for differential recruitment of signaling partners to increase the diversity in EGFR signaling responses after stimulation with different ligands. Substrates micro-patterned with these EGF-like ligands may be used to determine if EGFR activated by other ligands has a different recruitment of signaling partners as compared to stimulation with EGF.

4.3 Micro-patterned ligand surfaces to study receptor mediated signaling:

Cell biologists deal with a lot of complexities in their experimental systems, which makes it hard to interpret experimental results, and further necessitates combining multiple approaches to

establish a mechanism beyond reasonable doubt. In the past few years, tools developed by advances in physical sciences, such as fluorescent spectroscopy, genetically modified fluorescent tags, and confocal microscopy, have helped in expanding the tool set available to experimental cell biologists. Moreover, development of micro/nano-fabricated ligand patterns have provided an option of spatially controlling the stimuli provided to the cells (19). We previously utilized these surfaces to spatially control the stimulation of FcεRI receptor on mast cells to study the spatio-temporal aspects of FcεRI signaling leading to degranulation.

Here, we demonstrate that utilizing these micro-patterned surfaces, in combination with fluorescence spectroscopy and flow cytometery, provides new insights about the role of dynamin in assembly of FcεRI endocytic machinery. We also extended the use of micro-patterned ligand surfaces to study spatio-temporal aspects of EGFR signaling. With further advances in lithographic techniques to reduce the feature sizes and surface functionalization schemes for depositing functionally active biological substrates, we will be able to stimulate cells in a spatially controlled manner close to physiological conditions. Advances in sub-optical resolution fluorescence microscopy and other imaging techniques will allow us to obtain a detailed visualization of the spatial assembly signaling complexes. This understanding will be helpful to answer the basic questions of how cells respond to external stimuli.

References:

1. Sousa LP, Lax I, Shen H, Ferguson SM, De Camilli P, Schlessinger J. Suppression of EGFR endocytosis by dynamin depletion reveals that EGFR signaling occurs primarily at the plasma membrane. Proceedings of the National Academy of Sciences.2012.

2. Doherty GJ, McMahon HT. Mechanisms of endocytosis. Annual review of biochemistry.2009;78:857-902.

3. Hinshaw J. Dynamin and Its Role in Membrane Fission 1. Annual review of cell and developmental biology.2000;16:483-519.

4. Furuichi K, Rivera J, Isersky C. The fate of IgE bound to rat basophilic leukemia cells. III. Relationship between antigen-induced endocytosis and serotonin release. The Journal of Immunology.1984;133:1513-1520.

5. Torres AJ. Investigating cytoskeletal regulation of IgE receptor signaling by micropatterned ligand arrays [PhD thesis]. Ithaca, NY: Cornell University; 2011.

6. Kitaura J, Xiao W, Maeda-Yamamoto M, Kawakami Y, Lowell CA, Kawakami T. Early divergence of Fc epsilon receptor I signals for receptor up-regulation and internalization from degranulation, cytokine production, and survival. J Immunol.2004;173:4317-4323.

7. Andrews NL, et al. Small, mobile FcεRI receptor aggregates are signaling competent. Immunity.2009;31:469-479.

8. Wu M, Holowka D, Craighead HG, Baird B. Visualization of plasma membrane compartmentalization with patterned lipid bilayers. Proc Natl Acad Sci U S A.2004;101:13798-13803.

9. Torres AJ, Vasudevan L, Holowka D, Baird BA. Focal adhesion proteins connect IgE receptors to the cytoskeleton as revealed by micropatterned ligand arrays. Proc Natl Acad Sci U S A.2008;105:17238-17244.

10. Rejman J, Oberle V, Zuhorn IS, Hoekstra D. Size-dependent internalization of particles via the pathways of clathrin-and caveolae-mediated endocytosis. Biochemical Journal.2004;377:159.

11. Gschwind A, Fischer OM, Ullrich A. The discovery of receptor tyrosine kinases: targets for cancer therapy. Nature Reviews Cancer.2004;4:361-370.

12. Lemmon MA, Schlessinger J. Cell signaling by receptor tyrosine kinases. Cell.2010;141:1117-1134.

13. Sen A, O'Malley K, Wang Z, Raj GV, DeFranco DB, Hammes SR. Paxillin regulates androgen-and epidermal growth factor-induced MAPK signaling and cell proliferation in prostate cancer cells. Journal of Biological Chemistry.2010;285:28787-28795.

14. Sen A, et al. Paxillin mediates extranuclear and intranuclear signaling in prostate cancer proliferation. The Journal of clinical investigation.2012.

15. Sorkin A, Goh LK. Endocytosis and intracellular trafficking of ErbBs. Experimental cell research.2009;315:683-696.

16. Daub H, Weiss FU, Wallasch C, Ullrich A. Role of transactivation of the EGF receptor in signalling by G-protein-coupled receptors. Nature.1996;379:557-560.

17. Moro L, et al. Integrins induce activation of EGF receptor: role in MAP kinase induction and adhesion-dependent cell survival. The EMBO journal.1998;17:6622-6632.

18. Scheck RA, Lowder MA, Appelbaum JS, Schepartz A. Bipartite Tetracysteine Display Reveals Allosteric Control of Ligand-Specific EGFR Activation. ACS chemical biology.2012.

19. Torres AJ, Wu M, Holowka D, Baird B. Nanobiotechnology and cell biology: micro- and nanofabricated surfaces to investigate receptor-mediated signaling. Annu Rev Biophys.2008;37:265-288.